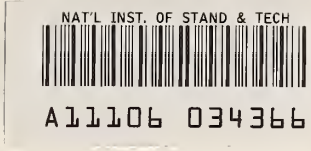


NBSIR 85-3203

# Response Behavior of Hot-Wires and Films to Flows of Different Gases

William M. Pitts
Bernard J. McCaffrey

U.S. DEPARTMENT OF COMMERCE
National Bureau of Standards
National Engineering Laboratory
Center for Fire Research
Gaithersburg, MD 20899

July 1985

Supported in part by:
orce Office of Scientific Research
orce Systems Command, USAF
ington, DC

NBSIR 85-3203

# RESPONSE BEHAVIOR OF HOT-WIRES AND FILMS TO FLOWS OF DIFFERENT GASES

William M. Pitts
Bernard J. McCaffrey

U.S. DEPARTMENT OF COMMERCE
National Bureau of Standards
National Engineering Laboratory
Center for Fire Research
Gaithersburg, MD 20899

July 1985

Supported in part by:
Air Force Office of Scientific Research
Air Force Systems Command, USAF
Washington, DC

U.S. DEPARTMENT OF COMMERCE, Malcolm Baldrige, *Secretary*
NATIONAL BUREAU OF STANDARDS, Ernest Ambler, *Director*

TABLE OF CONTENTS

LIST OF TABLES

LIST OF FIGURES

ABSTRACT

Measurements of the voltage output for hot-wire and film anemometers placed in flows of nine different gases have been made as a function of flow velocity. It has been possible to correlate the measurements quite accurately by treating the data in terms of suitably defined Reynolds and Nusselt numbers. In order to obtain these correlations it has been necessary to consider and correct for the effects of probe end conduction losses, temperature dependencies of gas molecular properties, flow slip at the probe surfaces, and gas accommodation. With the exception of the results for helium (for which accommodation effects are strong), the most important correction is shown to be that for the different temperature dependencies of the gas molecular properties. This finding is contrasted with previous studies which have assumed that the largest effect among different gases was due to variations in the Prandtl number. The importance of the nature of the flow over the cylindrical devices to the heat transfer behavior is described. A previously unreported hysteresis in the heat transfer behavior for Re ~ 44 has been characterized and attributed to the presence or absence of eddy shedding from the heated cylinder.

## 1. INTRODUCTION

The simultaneous measurement of concentration and velocity in turbulent flows of gas mixtures has traditionally been very difficult. Such measurements are necessary before comprehensive models of turbulent mixing in variable density flows can be developed. Recently, we have demonstrated that the techniques of Rayleigh light scattering for concentration measurement

[1,2] and hot-wire or film anemometry can be combined in order to make such measurements in isothermal flows [3,4]. This new technique is capable of simultaneous, spatially-resolved, real-time measurements of concentration and velocity in turbulent flows of two gases.

In order to apply this diagnostic technique, it is first necessary to calibrate the response of the hot-wire or film as functions of concentration and velocity. This may be done by monitoring the response of the heated filament as a function of velocity for several different mixtures of gases covering the concentration range of interest. However, this procedure is tedious and time consuming. A second method would be to have suitable empirical laws so that a calibration of wire response for a single gas would be sufficient to allow the prediction of the wire response for other gases and mixtures.

With the hope of generating such empirical laws we have measured the response of hot-wires and films for a variety of gases and binary gas mixtures. In this paper we will describe the behavior of the wire and film in pure gases. (Note that air is included as a pure gas.) A second paper [5] will describe similar measurements for binary gas mixtures.

Since we are primarily interested in calibrating the anemometers for use in our flow system, we have limited our study to one overheat ratio for the film and one for the wire and to the velocity range of interest in our experiments ($\approx$ 50 to $\approx$ 1000 cm/s).

As will be shown, we have been able to generate empirical relationships for predicting hot-wire and film response variations as a function of changes in gas composition. In the process we have developed a much better understanding of the behavior of hot-wires and films. Such an understanding is necessary in order to be able to assess the accuracy of velocity measurements in flows of varying composition. These new results also allow a more critical examination of past experiments reported in the literature. In particular, the effects of thermal conduction along the probes, rarefied gas effects, thermal accommodation on the probe surface, temperature dependence of gas properties, and flow transitions on heat transfer behavior are described.

In the following section (2) we will describe past studies which are relevant to this work. This will be followed by sections describing our experimental techniques (3) and the results of our measurements (4). Efforts to develop empirical heat transfer laws which correlate these measurements will be reported in section 5. In section 6 we will discuss possible explanations for and implications of our observations concerning the behavior of the hot-wire and film. Finally, section 7 contains a summary of important results and conclusions.

## 2. PAST WORK

### 2.1 Results for Air

Hot-wire and film anemometry are the most widely used techniques for velocity measurements in fluid flows. Many books and monographs contain extensive discussions of the use and applications of these devices (e.g.,

[6-12]). When such anemometers are employed carefully, they are highly precise and accurate.

As might be expected, the vast majority of gas velocity measurements using heated filament anemometers have been made for air. There are very few reports of their use in other gases and still fewer regarding their application in measurements where the gas composition is fluctuating. Here we will describe the relevant findings for air flows and then describe past studies of hot-wire and film responses in different gases.

The principle underlying the use of hot-wire or film anemometry is that heat transfer from an electrically heated surface depends on the velocity of fluid passing over the surface. If the heated element also has a temperature dependent resistivity, the heat loss from the surface due to forced convection and changes in the probe temperature are coupled. By proper choice of operating parameters it is possible to relate velocity to the measured power dissipation of the filament.

Most of the hot-wire and film anemometers in use today employ cylindrical conducting wires or conducting films applied to nonconducting substrates. These probes are usually operated in the "constant temperature" mode. Since the resistivity of the probe depends on temperature, in practice this means the resistance of the probe is held constant and the amount of current flowing through the probe is measured to obtain the power dissipation within the probe. If it is assumed that the only heat loss mechanism is due to convection, the power loss of the probe can be related to velocity.

Heat transfer laws for infinitely long cylinders are often used to predict the behavior of heated wires and films in gas flows. These laws are usually expressed in nondimensional form by giving the Nusselt number (Nu) as a function of Reynolds number (Re). Symbols are defined in the nomenclature table. One of the first heat transfer laws was due to and bears the name of King [13]. It can be written as

$$Nu = \frac{1}{\pi} + \left(\frac{2Pe}{\pi}\right)^{1/2} \tag{1}$$

where Pe is the Peclet number which is equal to the product of Re and the Prandtl number (Pr). King's derivation was based on the assumption of potential flow which has been shown to provide a poor approximation of real flows. However, relations based on eq. (1) are often used in the form

$$Nu = C_1(Pr) + C_2(Pr)Re^{1/2}, \tag{2}$$

as a basis for empirical heat transfer laws for hot-wires and films. $C_1$ and $C_2$ are parameters which depend on Pr.

For air or other gases this relation can be rewritten as

$$Nu = A + BRe^{n}, \tag{3}$$

where the exponent, n, is now treated as a parameter to accommodate the experimental observation that n may vary. Andrews et al. [14] have compiled a list of many of the correlations found in the literature which have been used to predict Nu behavior as a function of Re.

The nondimensional correlation which is used most often is due to Collis and Williams [15]. It can be written as

$$Nu_a \left(T_m/T_\infty\right)^a = A_a + B_a Re^n, \tag{4}$$

where the values of the powers a and n, as well as $A_a$, and $B_a$ have the values listed in table 1. These measurements were made for overheat ratios (defined as $\left(T_s - T_\infty\right)/T_\infty$) in the range of 0.1 to 1. The fluid properties necessary for eq. (4) are evaluated at the mean temperature of the sensor surface and the ambient gas, $T_m$. A modification of heat transfer behavior at Re $\approx$ 44 was found. It was abrupt and attributed to the onset of vortex shedding from the cylinder. A similar observation of this flow transition had been reported earlier by Hilpert [16].

The subscript a in $Nu_a$ refers to a continuum Nusselt number which has also been corrected for accommodation effects. Collis and Williams [15] showed that rarefied gas effects are important for small diameter wires. They derived an approximate correction for these effects which for air can be written as

$$\frac{1}{Nu_\infty} - \frac{1}{Nu_a} = 2Kn \tag{5}$$

where Kn is the Knudsen number, $\lambda/D$. The subscript $\infty$ indicates a Nusselt number for a wire of infinite length, i.e., no end losses. These authors also found that buoyancy effects become important in the heat transfer at very low Re. They concluded that buoyancy effects are negligible when

$$Re > Gr^{1/3}, \tag{6}$$

where both Re and the Grashof number (Gr) are evaluated for air at ambient conditions. For the above overheat ratios, velocities ought to be larger than about 2 to 5 cm/s to insure that buoyancy effects can be neglected.

Bradbury and Castro [17] verified the results of Collis and Williams [15] for overheat ratios of 0.07 to 2.1. These authors reported some temperature decay measurements for wires heated by current pulses which also supported the findings of Collis and Williams.

Andrews et al. [14] have also investigated the responses of hot-wires in air. They have given an excellent discussion of the corrections necessary for rarefied gas and accommodation effects.

Accommodation effects [18] are treated using the accommodation coefficient ($\alpha$), defined as

$$\alpha = \frac{\varepsilon_i - \varepsilon_r}{\varepsilon_i - \varepsilon_s} \tag{7}$$

which can be thought of as the ratio of the average increase in energy of the gas molecules after striking the surface and the increase in energy they would have if they remained near the surface long enough to come into equilibrium at the surface temperature. $\alpha = 0$ if the gas "accommodates" no energy from the surface and $\alpha = 1$ if gas molecules striking the surface come into thermal equilibrium at the surface temperature.

Heat transfer to a rarefied gas from a heated surface is treated using the concept of a temperature jump at the surface [18]. For a heated cylinder, the temperature jump is defined as

$$T_s - T_s' = \Delta \frac{\partial T}{\partial r} \tag{8}$$

where $T_s'$ is the temperature the surface would have if the temperature jump did not occur and $\Delta$ is the temperature jump distance. Kennard [18] showed that for a rarefied gas with gas accommodation effects, $\Delta$ can be expressed as

$$\Delta = \left(\frac{2 - \alpha}{\alpha}\right) \left(\frac{2\gamma}{\gamma + 1}\right) \left(\frac{\lambda}{Pr}\right) \tag{9}$$

A slip parameter which relates $\Delta$ to the diameter of the cylinder is often defined as

$$\beta = \frac{\Delta}{D} = \theta' Kn, \tag{10}$$

where $\theta' = \Delta/\lambda$.

Andrews et al. [14] showed that for an ideal gas the Nu for the gas in the absence of rarefied effects and with $\alpha = 1$ could be related to $Nu_a$ by

$$Nu_a = \frac{Nu_\infty}{1 - \phi \, KnNu_\infty} \tag{11}$$

where,

$$\phi = \theta' \left( \frac{2T_s/T_\infty}{1 + T_s/T_\infty} \right)^{0.5+x+y} \tag{12}$$

x and y are the exponents which are found by assuming $\mu \approx T^x$, $k \approx T^y$ and $\theta'$ is evaluated at $T_s$. While not exact, these two expressions do provide a good approximation for the temperature dependencies of these gas properties. For eq. (11), Kn is evaluated at $T_m$. Eq. (12) is derived by assuming $T_s'$ is nearly equal to $T_s$. This is generally a good assumption.

Andrews et al. found that $2.23 < \phi < 2.67$ for air at their experimental conditions. Substituting $\phi$ in eq. (11) shows that there is rough agreement between their more exact theoretical treatment and the simplier model of Collis and Williams [15] as given by eq. (5). In fact, for reasons of simplicity, Andrews et al. treated their data using eq. (5).

Unlike the work of Collis and Williams [15], Andrews et al. [14] found that a correction for temperature loading was not required when eq. (5) was used to correct $Nu_\infty$ for rarefied gas and accommodation effects. For large aspect ratios ($\ell/D$) they found that the equation

$$Nu_a = 0.34 + 0.65Re^{0.45} \qquad (13)$$

could be used for $0.02 < Re < 20$, $0.02 < (T_s - T_\infty)/T_\infty$ and $0.052 < Kn < 0.1$. Since Collis and Williams [15] also included Kn effects in their study it is difficult to understand why the results of Andrews et al. [14] differ from this earlier work, the answer may lie in the different molecular properties used by the two groups (see the discussion in section 6.1.3).

The work described above is for heated wires of sufficient aspect ratio that heat transfer from the ends of the wires to the supports can be ignored.

In practice, this is often not the case. Andrews et al. [14] found that the aspect ratio was important for $\ell/D < 400$. These workers investigated wires having aspect ratios in the range $24 < \ell/D < 1300$. They employed an effective $Nu_m$ based on observed wire heat loss and did not correct for end losses. Eq. (3) was used to treat their data. They concluded that the value of n remained constant, but that the parameters $A_m$ and $B_m$ increased as $\ell/D$ decreased. These observations are consistent with earlier experiments reported by Collis [19] and Champagne and Lundberg [20]. The increase of $B_m$ was shown to be much less rapid with decreases in $\ell/D$ than the $A_m$ value. This is not unexpected since the $A_m$ value is generally associated with free convection and conduction losses while $B_m$ is believed to be primarily dependent on forced convection.

Several authors (e.g., [6,7,11,12,21,22]) have discussed the effects of probe end conduction on measured heat loss and have provided methods for calculating the predicted heat loss in the absense of conduction. Most of these derivations are based on a simplified heat transfer differential equation which can be written as the sum of conductive heat losses,

$$Q_c = - A_s k_s \frac{d^2\theta}{dx^2} \tag{14}$$

convective heat losses,

$$Q_h = \pi D h \theta \tag{15}$$

and joulean heating,

$$Q_j = I^2 \rho_r(\theta) \tag{16}$$

The above expressions assume no radial temperature gradiants, no temperature dependence of probe thermal conductivity ($k_s$), the probe diameter is constant, and radiative heat losses are negligible.

For thermal equilibrium,

$$Q_c + Q_h - Q_j = 0 \tag{17}$$

The local resistance of the probe is usually written as,

$$\rho_r(\theta) = \rho_r(0)\left(1 + \alpha_\rho \theta\right), \tag{18}$$

where higher order terms in $\theta$ are disregarded.

By substituting eqs. (14), (15), (16), and (18) into eq. (17) and rearranging, the following equation is obtained,

$$\frac{d^2\theta}{dx^2} - C_o\theta + D_o = 0 \tag{19}$$

where

$$C_o = \frac{\pi D h}{A_s k_s} - \frac{I^2 \rho_r(0)\alpha_\rho}{A_s k_s} \tag{20}$$

and

$$D_o = \frac{I^2 \rho_r(0)}{A_s k_s} \tag{21}$$

Clearly $D_o$ is > 0. For practical flows, $C_o$ is also found to be greater than zero.

In solving eq. (19) for a heated probe oriented perpendicularly to the flow it is usually assumed that the temperature distribution is symmetrical about the center of the probe (x = 0) which requires that $d\vartheta/dx = 0$ at x = 0. The probe is also assumed to be attached to massive prongs having an infinite heat capacity and a temperature equal to the ambient flow temperature. This condition can be written as $\theta = 0$ at $x = \pm \ell/2$. The solution of eq. (19) for these boundary conditions is

$$\theta/\theta_o = 1 - \frac{\cosh\left(\sqrt{C_o}\, x\right)}{\cosh\left(\ell\, \sqrt{C_o}/2\right)} \tag{22}$$

where $\theta_o = D_o/C_o$ is the overheat which would exist in the absence of end heat losses due to conduction.

By integrating along the probe, an expression can be obtained for the average overheat, $\bar{\theta}$,

$$\bar{\theta}/\theta_o = 1 - \frac{2}{\ell\, \sqrt{C_o}} \tanh\left(\frac{\ell}{2}\, \sqrt{C_o}\right) \tag{23}$$

In the hot-wire literature the effects of end conduction are often discussed in terms of the "cold length", $\ell_c$, introduced originally by Betchov [23]. The cold length is related to the above equations by $\ell_c = 1/\sqrt{C_o}$.

The above description of probe thermal conduction effects is related most closely to the development given by Corrsin [6]. We will use these results in

section 3.7 to develop a method for correcting our experimental results for end conduction losses.

Collis and Williams [15] found that for large aspect ratio wires it was necessary to multiply $Nu_a$ by $(T_m/T_\infty)^{-0.17}$ to correlate their results (see eq. (4)). Koch and Gartshore [24] reported a study for 5 μm wires having aspect ratios of 230. Even though these workers did not correct their results for end conduction losses or accommodation effects, they fit their data to an equation of the same form as eq. (4). Nusselt numbers based only on experimentally observed heat losses are denoted $Nu_m$. In agreement with Collis and Williams [15], it was found that plots of $Nu_m$ versus Re were fit best for $n = 0.45$. As expected, based on the discussion above, their measured values of $A_m = 0.72$ and $B_m = 0.80$ are larger than found by Collis and Williams (see table 1) and $A_m$ is increased proportionally more than $B_m$. The major surprise of this work is the measured value of $a = 0.67$. This value of a has a different sign and much larger magnitude than found by Collis and Williams [15]. This difference was attributed by Koch and Gartshore [24] to aspect ratio effects.

Bruun [25] also reported a study of the effect of overheat ratio on the response of hot-wires when operated in the constant temperature mode. The hot-wires used in this study had aspect ratios varying from 360 to 420. The results of this study were not treated in terms of eq. (4), but rather in terms of the observed voltage drop across the hot-wire,

$$\frac{E_s^2}{R_s(T_s - T_\infty)} = A' + B'U^n, \tag{24}$$

which is proportional to $Nu_m$.

Bruun found that a value of $n = 0.45$ fit his results well for velocity ranges corresponding to $Re < 44$. Even though his measurements were not analyzed in the form of eq. (4), he was able to show that the value of a in this equation depended quite strongly on velocity. His measured values of a differed markedly from those of Collis and Williams [15] or Koch and Gartshore [24].

In treating his data, Bruun mentioned potential problems in obtaining accurate values of $E_s$ which can arise when utilizing standard constant temperature anemometry circuitry. Such circuits consist of a Wheatstone bridge, for which one leg is formed by the probe, and a feedback amplifier which responds to variations in probe resistance in such a way as to maintain a constant resistance. Usually, these amplifiers also include a small offset voltage which is designed to force the bridge slightly out of balance in order to obtain a minimum damping of the amplifier outlet. In this manner the frequency response of the device is maximized. Due to this offset voltage, a measurement of the voltage drop across the bridge does not provide a true measure of the voltage drop across the probe. Bruun overcame this problem by measuring the voltage drop across different legs of the bridge.

The effects of offset voltage on constant temperature anemometry was discussed in much greater detail by Morrison [26]. He provided a theoretical analysis which showed that the offset voltage setting can modify the observed voltage drop across the bridge and lead to what appears to be a probe overheat dependence which is in reality an artifact due to the electronics.

Experiments were reported which supported the theoretical conclusions. Morrison notes how this artifact can result in errors in measured heat transfer laws and proposed this effect as the source of disagreement between the measured value of a for the work of Collis and Williams [15] and Koch and Gartshore [24].

It seems clear from these papers that differences in observed heat transfer laws for hot-wire anemometers should be expected unless great care is taken to account for end conduction losses and response behaviors of the electronics used.

## 2.2 Results in Different Gases

Most of the relevant studies on hot-wire behavior in different gases have resulted from efforts to use two hot-wires (and/or films) to make simultaneous concentration and velocity measurements. As first noted by Corrsin [27], such measurements are possible when the heat loss of the two heated filaments is different for a given velocity and concentration. By simultaneously monitoring the heat loss of each wire, the concentration and velocity can be determined from suitable calibration curves.

Even though there had been previous efforts to use the ideas of Corrsin [27] to extend hot-wire anemometry to variable composition flows [28-30], the first literature reports appear to have been due to Kassoy [31] and Aihara et. al. [32] who investigated the response of hot-wires in mixtures of helium and nitrogen as a first step in calibrating hot-wires for making simultaneous concentration and velocity measurements. They attempted to use a modified King's law written in the form

$$E^2 = k_\infty \left(A + BPe^{1/2}\right) \qquad (25)$$

to predict the response of the wire when placed in different gases. By using measurements in nitrogen as a reference, eq. (25) was used to predict the voltage required by the hot-wire to maintain a constant temperature in flows of helium and mixtures of nitrogen and helium for Re ≈ 10. To their surprise, they found that the calculated heat loss, which is proportional to $E^2$, was much less than predicted. For this reason, they performed an extensive theoretical [31] and experimental [32] study for Re < 0.1. These studies indicated that the observed discrepancies were due to temperature slip effects at the surface of the wire. Even though the Kn were in a range (≈ 0.01) where such effects are generally considered to be small, the extremely low thermal accommodation coefficient ($\alpha$) of helium on tungsten greatly increases the importance of slip effects. A theory was developed by Kassoy [31] which predicted the behavior of $Nu_a$ in terms of the flow parameters, gas properties, and the slip parameter ($\beta$) as defined by eq. (10).

The above studies were performed for a Re range which is much lower than generally used in hot-wire studies. Furthermore, the theoretical study [31] considered infinite cylinders and the experimental work [32] used wires having large $\ell/D$ ratios and guard heaters to minimize heat transfer to the prongs. For these reasons, this early work is not directly applicable to the hot-wires generally used in practice. However, they do contain several findings which are necessary to understand the response of practical hot-wires and films in variable composition flows. As already discussed, the importance of thermal slip effects was noted. These effects were shown to be much less important for nitrogen than for helium. In fact, the heat transfer of the tungsten wire

in nitrogen could be predicted without including the effects of thermal slip as shown by the agreement between the predictions of Kassoy's theory [31] and experiment. Both the measurements and theory were in excellent agreement with the empirical correlation of Collis and Williams [15]. These papers emphasized the problems in predicting the effects of thermal accommodation behavior and the lack of theories for predicting $\alpha$ in mixtures.

A third paper from this same group reported measurements similar to those discussed above for nitrogen-neon mixtures as well as further measurements of nitrogen-helium mixtures [33]. It was shown that the thermal accommodation coefficient of neon on tungsten must be considered in using Kassoy's theory [31] to predict the $Nu_\infty$ for a given flow velocity. A simple gas kinetic theory argument was used to predict the behavior of $\alpha$ as a function of neon concentration.

Wu and Libby [34] later reported $Nu_\infty$ measurements versus Re for a Re range of 0.03 to 10 for air, helium, and mixtures of the two gases. In this way they were able to compare the results at lower Re with earlier work from the same group [31-33] and at the same time obtain measurements over a Re range of more interest for practical hot-wire measurements. These experiments were done using a platinum wire instead of tungsten. In analyzing their data these workers introduced a modified version of eq. (4) using the values of A, B, and n listed in table 1 for Re < 44,

$$Nu_\infty = \left(\frac{T_m}{T_\infty}\right)^{0.17} \left[0.24 \left(\frac{Pr_x}{Pr_{air}}\right)^{0.20} + 0.56 \left(\frac{Pr_x}{Pr_{air}}\right)^{0.33} Re^{0.45}\right] \qquad (26)$$

where x refers to the gas under investigation. The Pr dependence in eq. (26)

is taken from the work of Kramers [35]. Kramers deduced his correlation for heated cylinders (which differs slightly from that of Collis and Williams [15]) by using data for air, water, and several viscous oils. It is somewhat alarming that in deducing this relation he dismissed the existence of a flow transition at Re ≈ 50. This is the same flow transition which is clearly shown in the work of Collis and Williams [15].

Wu and Libby found measurements of $Nu_\infty$ as a function of Re for air to be in excellent agreement with predictions using Collis and Williams' relationship [eq. (4)]. However, when they investigated pure helium and mixtures of helium and air, the observed $Nu_\infty$ for a given Re was lower than predicted by eq. (26). Differences between the predictions and experiment were attributed to thermal slip. These workers used the parameter $\beta'$ to characterize the effects of thermal slip by an equation which is very similar to eq. (5),

$$1/Nu_\infty - 1/Nu_a = \beta'/2, \tag{27}$$

where $\beta'$ is treated here as an empirical parameter. Based on experimental results, they estimated $\beta'$ to be 0.274 which gives $\alpha = 0.11$ from eqs. (9) and (10). An empirical relationship which assumed that $\beta'$ for helium-air mixtures was a linear function of helium mole fraction gave limited agreement with experimental results.

Another early study which considered the effects of variable composition on hot-wire response was done by Wasan et al. [36]. These authors modified a heat transfer correlation due to Van der Hegge Zijnen [37] to obtain an equation that predicted $Nu_\infty$ behavior as a function of Re, Pr, and Gr and which was

shown to be valid in Re regions where mixed natural and forced convection were occurring. Measurements were reported for a constant temperature platinum wire which showed that this expression gave reasonably good predictions of the heat loss for a low velocity air flow [37].

These authors also studied flows of air and water vapor. As expected, the response of the wire was modified when water vapor was added to the air flow. Using their correlation, they were able to predict the modifications of the wire behavior quite well. Despite this success, this type of correlation has not come into widespread use and apparently has not been tested for other gases. Furthermore, at higher Re this correlation predicts a $Nu_\infty$ dependence similar to eq. (3) with n = 0.5. Since n is believed to be 0.45 for Re < 44, this correlation might be questioned over the Re range of 0.01 to 44.

Later, Wasan and Baid [38] published a study of the response of hot-wires and films to flows of air, carbon dioxide, and mixtures of these two gases. These authors chose to try and fit their results to Collis and Williams' correlation [15] (eq. (4) with the constants of table 1 for 0.02 < Re < 44). Using their results they were unable to distinguish between 0.45 and 0.5 as the best value of n to use in eq. (4). By using measurements in air as a reference, they attempted to predict the heat loss for carbon dioxide as a function of velocity using eq. (4). They calculated a considerably smaller $Nu_m$ for $CO_2$ than was actually observed. Analysis showed that most of the error was in the parameter $A_m$ and that $B_m$ was nearly equal for the two gases. Note that no dependence on Pr is included in eq. (4) such as that in eq. (26). However, the Pr numbers of air and $CO_2$ are so similar that any effect of their difference will be small.

Wasan and Baid were able to predict hot-wire and film responses in air, $CO_2$, and mixtures of the two by using experimental values of the parameters A and B of eq. (4) for gases of two different compositions and performing a linear extrapolation of the values as a function of gas thermal conductivity. They concluded, based on this result, that this procedure could be used for any suitable pair of gases.

Andrews et al. [14] have also investigated the effects of molecular composition on hot-wire response. Their study included results for measurements of methane/nitrogen mixtures as well as the air measurements already discussed above. Based on their findings they concluded that eq. (13) can be used to fit their mixture results as well as those for air and suggested it would be of value for other gases and mixtures.

McQuaid and Wright [39] have reported a study of hot-wire response in different gases. Instead of treating the instantaneous response of the wire, they chose to derive relationships in terms of average values and intensities of concentration and velocity fluctuations on two different sensors. They showed that these values could be related to the time-average and root mean square of the voltage drops across the two hot-wires. For carbon dioxide-air and argon-air mixtures it was found that the function

$$\psi\,(Y_x) = \frac{\bar{E}^2 - \bar{E}_1^2}{\bar{E}_2^2 - \bar{E}_1^2}\,, \tag{28}$$

where all of the voltage values are recorded for a constant velocity, is independent of velocity. The overbars indicate time-averages and subscripts 1 and 2 refer to results for pure gases. The lack of a velocity dependence in eq. (28) requires that calibration equations written in the form

$$E^2 = A' + B'U^n \qquad (29)$$

have a common intersection point for all concentrations of the given gas pair. Note that A' and B' are concentration dependent and that for constant temperature operation eq. (29) can be reduced to the form of eq. (3) by using the relationships between $E^2$ and $Nu_\infty$ and $U^n$ and $Re^n$, respectively. For cases where heat loss to the prongs is important, $Nu_\infty$ should be replaced by $Nu_m$. These authors found that hot-wire voltage behavior as a function of velocity could be fit well using n = 0.45. This is in agreement with the findings of Collis and Williams [15].

For $CO_2$-air mixtures, McQuaid and Wright [39] found that $\psi(Y_{CO_2})$ was linearly dependent on $Y_{CO_2}$. There was a great deal of scatter in the measurements due to the small difference in heat loss of the hot-wire to air and $CO_2$ which resulted in large uncertainties when the differences in eq. (28) were taken. In fact, when calibration results for air and $CO_2$ were fit to eq. (29), the two lines crossed at a velocity of ≈ 8m/s for an overheat ratio of 0.8. Argon-air mixtures also gave results for $\psi(Y_{Ar})$ which were independent of velocity, but in this case the dependence of $\psi$ on $Y_{Ar}$ was nonlinear. Due to the large differences in the heat loss of the wire in air and argon, the uncertainties in $\psi(Y_{Ar})$ were considerably less than found for $\psi(Y_{CO_2})$.

These authors also gave criteria to serve as a basis for choosing suitable gas pairs for simultaneous concentration and velocity measurement. A heat transfer law of the form of eq. (26) was used as the basis for these criteria. However, it was emphasized that this relation is expected to be only crudely correct and to only be suitable for the prediction of gross effects.

Simpson and Wyatt [40] have investigated the heat loss of various hot-films in air, helium, and argon and in helium-air and argon-air mixtures. Both cylindrical and parabolic sensors were considered. These authors used the modified Collis and Williams' heat transfer law given in eq. (26) as a basis for analysis of their results. Since cylindrical hot-films have very small aspect ratios, it was necessary to allow the numerical constants (0.24 and 0.56) in eq. (26) to be parameters and determine them experimentally. Using the resulting equation, they were able to obtain an excellent correlation of their experimental results for argon, air, and mixtures of these two gases.

However, when they considered helium and helium-air mixtures they found that the modified Collis and Williams' equation overpredicted the convective heat transfer from the film to the gas. This observation is similar to those found by Libby and coworkers [32-34] for helium-air and helium-nitrogen mixtures. In this earlier work, the decrease in $Nu_\infty$ from that expected was attributed to thermal accommodation effects on the surface of the platinum and tungsten wires. However, Simpson and Wyatt [40] noted that $\alpha$ for helium on quartz (the overcoating used on the film sensor) is expected to be larger than on the metals used for construction of the wires. The result is that thermal accommodation effects should be much less important for films than for wires. For this reason, these authors attribute the decrease in $Nu_m$ to thermal diffusion effects. Thermal diffusion refers to concentration gradients which are formed when gas mixtures are placed in temperature gradients such as exist around a heated filament. These concentration gradients result in variations in fluid properties of the mixture near the heat source and modify the heat transfer from that expected in the absence of thermal diffusion. There is

apparently no theory which allows the prediction of such effects on hot-wire behavior. It should be noted that Khalifa et al. [41] have considered the effects of thermal diffusion in the context of hot-wire thermal conductivity measurements. We shall discuss the effects of thermal diffusion and develop an approximate theory to describe these effects in the paper dealing with hot-wire behavior in mixtures [5].

Some work has been reported on the heat transfer from hot surrounding gases to cooled-films [42]. These experiments are obviously related to the hot-wire studies, but Fingerson and Ahmed [42] argue that the same heat transfer laws should not hold because of differences in the dynamical dissimilarity with temperature loading between heating and cooling of rods. Measurements were reported in heated flows of $N_2$, He, $CO_2$, and various mixtures of these gases [42]. Their studies covered a range of ambient temperatures from 800 to 1600 K and film surface temperatures from 350 to 525 K. For $5 < Re < 44$ they found that their results could be well correlated by

$$Nu_m = (0.21 + 0.50\ Re^{0.45})\ (\nu_\infty/\nu_m)^{-0.15} \qquad (30)$$

This equation is clearly similar to eq. (4) when the parameters of table 1 for $Re < 44$ are used. However, the temperature loading factors lead to different calculated Nu based on the two expressions.

It is interesting that Fingerson and Ahmed [42] have been able to correlate their measurements of He, $CO_2$, $N_2$, and mixtures of these gases. This implies that for their experimental conditions such effects as thermal

slip and thermal diffusion are absent. This observation is consistent with the large Kn for the film and the large accommodation coefficient for helium on quartz as pointed out by Simpson and Wyatt [40].

Brown and Rebollo [43] have given a general discussion of the response of a hot-wire to variations in the concentration of a constant velocity flow in connection with their development of an analytical probe for concentration measurements in binary gas mixtures. This device was designed to operate as a sonically choked aspirating probe in such a way that flow past the internally mounted hot-wire would be at a constant velocity as long as the external pressure was constant. As a part of this study these workers attempted to predict the wire response to different gases using heat transfer laws similar to those previously discussed. For a platinum wire they concluded that it is necessary to consider accommodation effects when helium and argon are used.

Tombach [30,44] has also briefly described the importance of thermal slip effects on hot-wire measurements and noted a memory effect for hot-wires placed in helium and then used to measure air flow velocities. These difficulties led Tombach to investigate the alternate diagnostic technique of heat pulse anemometry for velocity measurements in inhomogeneous flows.

# 3. EXPERIMENTAL SYSTEM AND DATA TREATMENT

## 3.1 Flow System

The response of the hot-wire and film were investigated as a function of velocity using a TSI model 1125 flow calibrator*. This device consists of a flow regulator, baffles and flow straighteners, and carefully machined nozzles of decreasing size which are designed to provide uniform velocity profiles. The velocity probe is aligned perpendicularly to the flow direction at a small distance above the exit of the nozzle.

We have investigated flows of relatively low velocity (≈ 50 cm/s to ≈ 1000 cm/s). For these velocities the gases can be considered to be incompressible to a very high degree of accuracy. In this case, the pressure drop across the nozzle is related to velocity by the Bernoulli equation which can be written as

$$U = \left(\frac{2\Delta P}{\rho}\right)^{1/2} \tag{31}$$

where $\Delta P$ is the pressure drop across the nozzle and $\rho$ is the density of the gas which is determined by the molecular weight of the gas, the atmospheric pressure, and gas temperature.

---

*Certain commerical equipment, instruments, or materials are identified in this paper in order to adequately specify the experimental procedure. Such identification does not imply recommendation or endorsement by the National Bureau of Standards, nor does it imply the materials or equipment are necessarily the best available for the purpose.

The difference in pressure on either side of the nozzle was determined using a Datametrics electronic manometer (type 1014A) equipped with a 1 torr differential head which could be used for pressure measurements to 1.3 torr. The pressure reading of the instrument is available as a voltage which was read by a 3-1/2 digit digital volt meter. The performance of the electronic manometer was checked against a Serta Systems electronic manometer. The two instruments gave identical readings.

### 3.2 Sources of Gases

Experiments have been performed for a wide variety of gases. Table 2 lists the sources of the gases and stated purities.

### 3.3 Gas Properties

A knowledge of the physical properties as a function of temperature is required for the gases used in this study. Densities have been obtained from known values at given temperatures and extrapolated to the temperature of interest assuming ideal gas behavior. In recent years reliable values of $\mu$, k, and $C_p$ have become available for most of the gases we have investigated. Where possible, we have chosen to use the values listed in the Thermophysical Properties of Matter, The TPRC Data Series [45-47] which is published by the Thermophysical Property Research Center of Purdue University. The only exception is the thermal conductivity of propane which is taken from a more recent measurement [48]. The values found in these tables are based on extensive reviews of the existing literature (up to the early seventies) and critical analysis of these results. Uncertainties are quoted for the values over various temperature ranges.

Physical properties for gases not listed in the TPRC Data Series are taken from various sources. Table 3 lists references to property data for all the gases studied here.

During the course of this work it was necessary to calculate mean free paths for some of the gases investigated. We have chosen to do this using the relationship between viscosity and the mean free path:

$$\lambda = 2\mu/\rho\bar{c}, \tag{32}$$

where $\bar{c}$ is the average velocity of the molecule which for an ideal gas is equal to

$$\bar{c} = \left(\frac{8RT}{\pi M}\right)^{1/2} \tag{33}$$

This same relation was used by Collis and Williams in their classic study [15].

## 3.4 Anemometer Electronics

A standard commercial anemometer system was used in this study. This system consists of several modules. A TSI model 1051-2 monitor and power supply generates the necessary voltages for the anemometer system and also outputs a voltage equal to that necessary to maintain the sensor bridge circuit in a balanced condition. This voltage is measured with a 4 digit voltmeter having a 0.1 second time constant.

The constant resistance of the sensors is maintained by a balanced 5:1 Wheatstone bridge. This bridge is contained in a TSI model 1054B linearized anemometer module. Note that the linearizing circuits were not utilized in this investigation and that the recorded output is the bridge voltage necessary to maintain the balance of the bridge. We have not made corrections for the voltage offset of the high gain amplifier used in the feedback circuit to maintain a constant resistance. This value was set as recommended in the operating manual for the anemometer. Checks showed that the measured bridge voltage was very insensitive to the setting of the offset voltage for the present situation of a single temperature setting.

The resistance of the probe leg of the bridge is determined by the external application of a known control resistance to the model 1054B. A variable decade resistor (TSI model 1056) is used for this purpose. The actual resistance of the heated filament ($R_s$ in table 4) is obtained by subtracting the internal probe and connecting cable resistances from the total resistance of the sensor leg of the bridge $(R_s')$.

The power dissipated in the wire or film is calculated from a knowledge of the resistance and current flow of the heated filament using $P_s = i^2 R_s$. The current through the sensor is equal to $V/R_T$ where $R_T$ is the total of the standard resistance in series with the probe leg $(R_o)$ and $R_s'$. These resistance values are all available and the total power dissipation within the heated filament can be written as

$$P_s = \frac{E^2 R_s}{(R_s' + R_o)^2} \tag{34}$$

## 3.5 Probes

All of the measurements reported in this work were made for one wire and one film. The wire measurements employed a TSI 1210-T1.5 tungsten wire which is coated with a very thin layer of platinum to minimize surface oxidation. Table 4 summarizes the dimensional data, operating resistance, the operating temperature of the wire ($T_s$) assuming a uniform temperature along the entire length of the wire, overheat ratio $((T_s - T_\infty)/T_\infty)$, and $T_m$ defined as the average of $T_\infty$ and $T_s$. The active length of the wire is determined by gold plating placed on the prong ends of the wire. These wire parameters have been calculated using data supplied by TSI. The operating temperature is calculated using the relation

$$\theta = \frac{1}{\alpha_\rho} \frac{R_s - R_\infty}{R_\infty} \tag{35}$$

$R_s$ and $R_\infty$ are the resistances of the wire at the operating and ambient gas temperatures, respectively. $\alpha_\rho$ is calculated from TSI calibrations of the wire resistance at the ice and steam points of water.

The film element is a TSI 1205-20. These probes are manufactured by depositing a thin film of platinum onto a cylindrical quartz substrate. The active length of the sensor is then defined by plating a layer of gold ($\approx$ 6.4 μm thick) at both ends which are attached to the probe mount. The layer of gold provides a low resistance path to the platinum as well as a means for holding the ends of the active area at a temperature very nearly equal to that of the prongs $(T_\infty)$. Finally, the entire probe is overcoated with a protective layer of alumina. The exact thicknesses of the substrate

and coatings of these devices are difficult to measure and are expected to vary from probe to probe. After consultation with TSI, we have assumed the following dimensions for our calculations: substrate diameter = 50 μ, $t_{Pt}$ = 0.1 μ, and $t_{Al}$ = .8 μ. The film parameters listed in table 4 are obtained in the same manner as those for the wire.

### 3.6. Experimental Procedure

The following experimental procedure was used for measuring the responses of the hot-wire and film to varying velocities of the different gases. A cylinder of the pure gas was connected to the calibrator. The gas was allowed to flow for a period of time sufficient to flush the entire flow system. The electronic manometer was then zeroed for a zero flow velocity. Pairs of measurements of pressure drop across the nozzle ($\Delta P$) and voltage drop across the bridge (E) were then recorded for velocities spanning the range of interest. Generally, 20 to 35 measurements were taken. The readings were taken from high to low velocities and back to high velocity to insure the absence of systematic or time dependent effects. The zero velocity calibration of the manometer was checked often.

### 3.7 Data Analysis

The results of our measurements on the hot-wire and film have been analyzed in several different ways. First the data are fit using eq. (29). The value of E used is the experimentally observed voltage drop across the bridge and the velocity (U) is calculated from the observed pressure drop using eq. (31).

The exponent n is treated as a variable. Linear least squares fits of the data are obtained using a range of different n values (steps of 0.01). The goodness of fit for these lines can be quantified by using the parameter

$$\chi^2 = \Sigma(E_m^2 - E_{com}^2)^2 \tag{36}$$

where the subscripts m and com refer to measured and computed values of $E^2$. For a given n the linear least squares fitting procedure generates a minimum value of $\chi^2$. $\chi^2$ varies as a function of n and we have defined the optimum value of n (denoted as $n_o$) as that which gives the smallest $\chi^2$.

A crude estimate of the uncertainty in a single point for the fitting of $E^2$ is obtained by taking the square root of $\chi^2$ and dividing by the total number of measurements. The relative error is estimated by dividing this value by the median value of $E^2$.

The measured Nusselt and Reynolds numbers are then calculated for each point and the results fit to eq. (3). $Nu_m$ is calculated as

$$Nu_m = P_s/(\pi k \ell (T_s - T_\infty)) \tag{37}$$

where $P_s$ is given by eq. (34). All of the properties of the gas under study used to calculate $Nu_m$ and Re are taken at the appropriate $T_m$ listed in table 4 for the wire or film. Note that for any one gas, $Nu_m$ is related to $E^2$ and Re is related to U by constants. For this reason, the $n_o$ for use in eqs. (3) and (29) are identical.

We have also corrected $Nu_m$ for end conduction effects to obtain $Nu_\infty$. Eqs. (20), (21), and (23) are used for this purpose. Eq. (23) can be rewritten as

$$\frac{\bar{\theta}}{D_o} = \frac{1}{C_o} - \frac{2 \tanh \left(\ell \sqrt{C_o}/2\right)}{\ell \, C_o^{3/2}} \tag{38}$$

Eq. (21) shows that $D_o$ is a function of I, $\rho_r(0)$, $A_s$ and $k_s$. All of these values can be measured or estimated for each experimental data point and a value of $D_o$ calculated. The values of $k_s$ used for the hot-wire and film are included in table 4. For the wire this is a literature value [53] of tungsten at 293 K. The hot-film value is obtained by summing together values of $A_{qt}k_{qt}$, $A_{Pt}k_{Pt}$, and $A_{Al}k_{Al}$ and dividing by $A_s$ to give a $k_{eff}$ for the probe. Necessary values for thermal conductivities are taken from [53,54]. This procedure must be considered a crude approximation since it ignores the effects of radial temperature gradiants on the heat transfer process.

Since the value of $\bar{\theta} = T_s - T_\infty$ is also known, eq. (38) can be solved for a value of $C_o$. In practice we do this by comparing a table of $C_o$ values as a function of $\bar{\theta}/D_o$ with the $\bar{\theta}/D_o$ value determined using $\theta$ from table 4 and $D_o$ calculated from eq (21).

Once a value of $C_o$ is obtained, it is substituted in eq. (20) along with values of $A_s$, $k_s$, $I^2$, $\rho_r(0)$ and $\alpha_\rho$ to yield a value for $\pi Dh$ where h is the heat transfer coefficient for the wire or film when end losses are zero. $Nu_\infty$ is obtained from $\pi Dh$ by dividing by $\pi$ and $k_{T_m}$ for the gas.

Once values of $Nu_\infty$ and Re are available for the entire data set, a least squares analysis which is identical to that described above is used to fit the results to the form of eq. (3).

Values of $Nu_\infty$ are then corrected for thermal slip effects. This is first done assuming that the thermal accommodation of the gas on the probe surface is perfect (i.e., $\alpha = 1$). With this assumption, values of $Nu_c$ are calculated from $Nu_\infty$ using eq. (11) with $\phi$ given by eq. (12) and $\theta'_{T_s}$ calculated using eqs. (9) and (10). The results of these calculations are then fit to eq. (3) and values of $n_o$, $A_c$, and $B_c$ are determined. For gases for which it is necessary to consider accommodation effects, the above calculations are repeated using a suitable value of $\alpha$ in eq. (9). The Nu which results from this calculation is denoted $Nu_a$ and the parameters which result from fits to eq. (3) are denoted as $n_o$, $A_a$, and $B_a$.

The above calculations have been programmed on a minicomputer. In order to obtain values of A, B, and n it is only necessary to input experimental values of E and $\Delta P$ along with the physical properties of the gas under study.

## 4. RESULTS

### 4.1 Hot-wire

Figure 1 shows a plot of E versus U for the response of the hot-wire in a flow of air. This data has been fit to eq. (29) using the procedure described in section 3.7. Equation (29) was found to fit the data quite well. A plot of $\chi^2$ (defined by eq. (36)) versus n is shown in fig. 2. It is clear from

this figure that the value of n which gives the best fit of eq.(29) (denoted by $n_o$) lies between 0.42 and 0.43. The sharpness of the minimum in the plot of $\chi^2$ versus n has been found to depend strongly on the quality of the experimental data. Smaller uncertainties in the data result in much more clearly defined values of $n_o$. The results shown in fig. 2 are typical of those we have found for all of our measurements using the hot-wire.

For the data shown in fig. 1 we find that the best parameters for use in eq. (29) are $n_o = 0.43$, $A' = 3.618 \pm .0004\ V^2$, and $B' = 0.3649 \pm .0003\ V^2(s/cm)^{0.43}$. The error limits given refer solely to those arising from the impreciseness of the linear least squares fit to the data and are not intended to be an estimate of the actual experimental uncertainty in the paramters A' and B'. The A', B', and $n_o$ values have been used to generate the solid line shown in fig. 1 which is in excellent agreement with the experimental results. Using the definition given in section 3.7, the relative uncertainty for a single point compared to the calculated line is estimated to be 0.0016. An uncertainty of this magnitude is consistent with the numbers of significant figures available in the measurements of E and U.

The response of the hot-wire to changes in velocity has been calibrated for ten different pure gases. These gases include nitrogen and air. The results for nitrogen and air were so similar that we have only reported the results for air. Figure 3 shows examples of $E^2$ versus $U^{0.43}$ for eight of these gases. The strong dependence of the hot-wire heat loss at a given velocity for different gases is clear from this figure. The results for helium are not included in this figure since these measurements were made over a wider range of velocity and the bridge voltage is considerably larger than for the other gases.

Table 5 summarizes the results for all of the hot-wire calibration runs that have been made. Values of $n_o$ are listed in the first column. These measurements show that all of the experimental data, with the exception of that for helium, can be fit accurately to eq. (29) using n = 0.43. For this reason, the values of A' and B' reported in Table 5 are fits of eq. (29) with n = 0.43.

The measurement results summarized in Table 5 were obtained over a period of several months. In general, both A' and B' values for a given gas were found to be reproducible to within ≈ 0.5%. While small, these variations are considerably larger than the uncertainty in the fit of a set of data recorded during a single calibration. Comparison of data recorded at different times show that there are slight systematic variations in the measurements. We attribute these variations to minor modifications on the surface of the wire (e.g., due to dust or oxidation) and environmental influences such as small temperature changes.

We have also fit our calibration results to eq. (3) in terms of $Nu_m$ using the calculational procedures described in section 3.7. Figure 4 shows examples of $Nu_m$ plotted as a function of $Re^{0.43}$ for all of the gases investigated. Note that helium has been included on the plot despite the fact that the value of $n_o$ for this gas is less than 0.30. Values of $A_m$ and $B_m$ for fits of eq. (3) using n = 0.43 are included in Table 5. These values refer to the particular data sets which are displayed in fig. 4. The approximate Re range of the measurements is also included in this table.

Equations (20)-(23) and (38) have been used to calculate $Nu_\infty$ for each bridge voltage reading recorded during a given pure gas calibration. Examples of the results of these calculations for each gas are shown in fig. 5 where $Nu_\infty$ is shown plotted against $Re^{0.43}$. The data for each gas have been fit to eq. (3). Table 5 lists the resulting values of $A_\infty$ and $B_\infty$.

The following observations concerning the effects of end conduction corrections on the calculated Nu behavior are obtained by comparing $Nu_m$ and $Nu_\infty$:

1) $Nu_\infty$ is always less than $Nu_m$. For this reason, $A_\infty < A_m$ and $B_\infty < B_m$.

2) The fractional decrease of $B_\infty$ compared to $B_m$ is much less than the corresponding decrease of $A_\infty$ compared to $A_m$.

3) The value of $n_o$ is increased slightly by the correction, but, in general, $\Delta n_o < 0.01$.

4) The larger the k value for the gas, the smaller is the relative reduction of $Nu_\infty$ from the value of $Nu_m$.

5) The relative decrease of $Nu_m$ at higher velocities is slightly reduced from that found at lower velocities.

It should be noted that the calculational result that $n_o$ remains essentially constant while $A_m$ and $B_m$ both increase with end conduction losses

is consistent with the experimental conclusions of Andrews et al. [14] and others [19,20]. The relative changes in the magnitudes of $A_m$ and $B_m$ after these corrections are also consistent with these past experimental results.

$Nu_\infty$ data shown in fig. 5 have been corrected for thermal slip effects assuming $\alpha = 1$ as described in section 3.7. Values of $n_o$ along with $A_c$ and $B_c$ for $n = 0.45$ which result from fits of eq. (3) are listed in table 6. In general, $n_o$ values for these fits are slightly lower than 0.45. However, we have chosen to treat our data in this form to be consistent with Collis and Williams [15] as well as a large number of other workers. Differences in the quality of fits using actual values of $n_o$ or $n = 0.45$ will be very small for every gas except helium. Figure 6 shows plots of $Nu_c$ versus $Re^{0.45}$ for the nine gases studied.

For some gases it has been necessary to consider accommodation effects. Calculations made for $\alpha \neq 1$ will be discussed in section 5.

By comparing fig. 3 with figs. 4, 5, and 6 and the numerical results listed in tables 5 and 6, it is clear that the use of eq. (3) in terms of either $Nu_m$, $Nu_a$, or $Nu_c$ gives a rough correlation of the hot-wire data for different gases. It is also clear that this correlation is not complete and that other factors must be considered. This point will be discussed further in section 5.

Note that the highest Re value reached for the hot wire measurements ($Re = 6.2$) was well below that required for the onset of vortex shedding ($Re \approx 44$).

## 4.2 Hot-Film

Calibrations for the hot-film have been performed using procedures identical to those described for the hot-wire. We have investigated the hot-film response for eight pure gases. Figure 7 shows examples of the hot-film data for different gases plotted as $E^2$ versus $U^{0.45}$. Data for helium has been omitted from the figure for the same reasons as described above. Comparison of figs. 3 and 7 shows that there are similarities in relative voltage magnitudes and slopes for the same gas on the hot-wire and film. Further inspection reveals some striking differences. All of the hot-wire data was fitted quite accurately by using eq. (29) with n = 0.43. A velocity exponent of 0.45 gives an accurate fit for some of the hot-film results (e.g., air and Ar), but there is a clear curvature in the plots of some of the other gases (e.g., $C_3H_8$ and $SF_6$) which indicates that other values of n would give an improved fit of the data to eq. (29).

The data for all of the different gases investigated have been fit to eq. (29). Table 7 summarizes values of $n_o$, A', and B' for all of the hot-film measurements we have made. A' and B' are the parameters for least squares fits taken with n = 0.45. Note that there is excellent agreement between the results of measurements for the same gas made over a period of several weeks. Comparison of $n_o$ values shows that the curvature observed in the data for different gases in fig. 7 is related to variations in this parameter. For the hot-wire results, only helium gave an $n_o$ value which differed significantly from 0.43. However, for the hot-film, values of $n_o$ vary from 0.37 to 0.45. This variation in $n_o$ complicates the comparison of the hot-film response in different gases.

Values of $Nu_m$ as a function of Re have been calculated for the hot-film results using eq. (37). Examples of the results for different gases are shown in fig. 8 plotted as $Nu_m$ versus $Re^{0.45}$.

Table 7 includes the values of $A_m$ and $B_m$ which give the best fit of eq. (3) with n = 0.45 for selected data sets. Table 7 also includes the approximate Re ranges over which the measurements for different gases have been made. A comparison of these ranges with the observed values of $n_o$ indicates that those gases for which the data extend to higher Re have smaller values of $n_o$. As will be discussed in section 6.3, we attribute this behavior to transitions in the flow behavior of the gas as it passes over the heated cylindrical film.

A dramatic demonstration of the importance of these transitions can be found by making the hot-film measurements for $C_3H_8$, $CF_3Br$, and $SF_6$ at slightly higher velocities than employed for the data reported above. Figure 9 shows results of measurements made over the Re regime where the flow transition occurs. A clear change in heat transfer behavior can be seen. Least squares fits generated from the lower velocity data clearly give poor fits to the data recorded at flow velocities corresponding to Re which lie above the flow transition region. In a Re range extending from ≈ 36 to ≈ 55 a distinct hysteresis is observed which depends on whether the flow velocity is increased or decreased to the measurement value. Figure 10 shows plots of such measurements for the three gases. The source of this hysteresis will be discussed in section 6.3, however, it is worthwhile to point out here that it occurs over a Re regime where a flow transition (Re ≈ 44) was observed by Collis and Williams [15] and attributed by these authors to the onset of vortex shedding.

The hot-film results have also been corrected for end conduction losses and rarefied gas effects using the calculational procedures given in section 3.7. It has been assumed that $\alpha = 1$. The corrections due to slip effects are very small. Figure 11 shows examples of $Nu_c$ plotted as a function of $Re^{0.45}$. Values of $A_c$ and $B_c$ from least squares fits of the data to eq. (3) are included in table 7.

As is the case for the hot-wire results, it is found that eq. (3) alone is not sufficient to correlate the hot-film results. The similarities between figs. 4 and 8 and figs. 6 and 11 are encouraging in that they indicate the major source of variation in Nu behavior between different gases is due to gas properties and not to such variables as device response (two different devices were used), $T_s$ (the wire and film were operated at different $T_s$), or Re regimes (due to the different diameters of the wire and film the Re ranges of the measurements vary widely).

## 5. CORRELATION OF EXPERIMENTAL RESULTS

The experimental results shown in figs. 6 and 11 and summarized in tables 6 and 7 show that the hot-wire and film responses in different gases are not correlated by simply plotting $Nu_c$ versus $Re^n$. We have tried many schemes for collapsing our data for different gases to single curves.

Two different philosophies have been employed in the literature to correlate heat transfer data such as that generated in this study. The first assumes that an expression in the form of eq. (3) can be used to fit all of the data if the proper corrections can be found for the coefficients A and

B. The modification of A and B in eq. (26) to allow for Pr dependencies is an example of this approach. The second philosophy assumes that a simple correction should be applied to the Nu in order to collapse the experimental data to a single curve. The temperature correction included in eq. (4) and the $\nu$ correction included in eq. (30) are typical examples of this approach. Both philosophies have been tried in this work as described below.

The first attempt to correlate the hot-wire experimental data assumed an equation of the form of eq. (26), i.e., a Prandtl number correction. This equation has been suggested as a means of correlating hot-wire results for different gases by several authors [34,39,40]. Figure 12 shows log-log plots of $A_c$ and $B_c$ as functions of the Pr for the various gases. If eq. (26) provided a means of correlating the measurements, these sets of data would form two straight lines. It is clear from fig. 12 that this is not the case. Apparently, the use of eq. (26) alone is not sufficient to correlate our experimental results. Note that we are omitting helium from consideration at this point due to the large accommodation effects expected in heat transfer from the hot-wire to this gas.

We next considered other means for reducing $A_c$ and $B_c$ values for the different gases to universal coefficients. The approach used is demonstrated in figs. 13 and 14 which show log-log plots of $A_c$ and $B_c$ as functions of $\mu_m$ and $\nu_m/\nu_\infty$, respectively. Note that the $B_c$ value of helium ($B_c = 0.410$) has been omitted from these plots. If the coefficient data fall on straight lines, then the dependent variable provides a means to correlate the coefficients. Many different expressions for the dependent variable were tried. These included $k_m$, $\nu_m$, and $\lambda_f$ as well as those shown in figs. 12-14. Most of

these plots indicated $A_c$ and $B_c$ had little or no dependence on these variables. However, as shown in fig. 14, values of $B_c$ were fit quite well by assuming a power law dependence of $B_c$ on values of $\nu_m/\nu_\infty$ for the different gases. Only methane seems to be in disagreement with this conclusion. It will be shown that this disagreement is most likely due to a small accommodation effect. $B_c$ was also found to be roughly correlated with $k_m/k_\infty$, but the correlation with $\nu_m/\nu_\infty$ was slightly better. As shown in fig. 13, values of $A_c$ were found to be dependent on $\mu_m$. Values of $A_c$ for all nine gases seem to be reasonably well correlated using this parameter.

Since the molecular properties of air, Ar, $CO_2$, and $C_3H_8$ are believed to be more accurately known than those for the other gases, the results for measurements in these four gases have been used to calculate expressions for $A_c$ and $B_c$ in terms of the suitable dependent variable. The results are

$$(B_c)_x = 0.2606\ (\nu_m/\nu_\infty)_x^{1.355}, \tag{39}$$

and

$$(A_c)_x = 0.0431/(\mu_m)_x^{0.222}, \tag{40}$$

for gas x. Equations (39) and (40) are taken from linear least squares fits of the logs of the independent and dependent variables. The lines corresponding to these fits are included in figs. 13 and 14.

Equations (39) and (40) have been used to develop a correlation of the experimental results for the different gases. Instead of using these equa-

tions directly, we have normalized the results to those of air by plotting $Nu_c - (K_A)_x$ versus $Re^{0.45}(K_B)_x$ for $(K_A)_x$ defined as

$$(K_A)_x = (A_c)_{air} - [(\mu_m)_{air}/(\mu_m)_x]^{0.222} (A_c)_{air} \tag{41}$$

and $(K_B)_x$ as

$$(K_B)_x = [(\nu_m/\nu_\infty)_x/(\nu_m/\nu_\infty)_{air}]^{1.355}. \tag{42}$$

Figure 15 shows the data plotted in this manner. Its clear that this calculational procedure provides a good correlation for all of the data except that for helium and methane.

In the past, deviations in the heat transfer behavior of heated cylinders in flows of helium have been attributed to the lack of "accommodation" of this light gas on the surface. This effect can be treated using eqs. (9)-(12) and allowing $\alpha$ to be a parameter. Eq. (11) is then used to generate new values of $Nu_a$ from $Nu_c$ where $\phi$ is now a function of $\alpha$. Values of $Nu_a$ are then fit to eq. (3). In order to determine the best value of $\phi$ for use in eq. (11), it has been assumed that $B_a$ equals the $B_c$ predicted for helium using eq. (39). For helium, this was found to be true for $\alpha = 0.48$.

Significantly, $n_o$ is found to be 0.45 when $Nu_a$ values for helium are fit to eq. (3) by the linear least squares fitting procedure. This result is in excellent agreement with the values of $n_o$ found for measurements in the other gases. Contrast this value of $n_o$ with that of $n_o = 0.35$ which results from a plot of the helium results as $Nu_c$ versus $Re^n$.

Values of $A_a$ and $B_a$ for helium with $\alpha = 0.48$ are plotted as solid symbols in figs. 13 and 14. As required by the calculational procedure, $B_a$ lies on the line corresponding to eq. (39) which is included in fig. 14. There is also good agreement between the value of $A_a$ and that predicted by eq. (40) as can be seen in fig. 13.

As noted earlier, the value of $B_c$ (see fig. 14) for methane is slightly lower than predicted by eq. (39). We have assumed that this observation is due to a slight accommodation effect for methane on the probe surface and have treated the data in the same manner as for helium. In this case, $B_a$ is found to equal the predicted $B_c$ for $\alpha = 0.61$. The value of $n_o = 0.47$ found for the plot of $Nu_a$ versus $Re^n$ is a little higher than expected, but is not unreasonably larger than the values of 0.44 and 0.45 found for the other gases. Values of $A_a$ and $B_a$ for methane are included in figs. 13 and 14 as solid symbols. As for helium, there is good agreement between these values and those predicted using eqs. (39) and (40).

Figure 16 shows the effects of correcting $Nu_c$ for accommodation effects on the collapse of the experimental data to a single curve. Values of $Nu_a - (K_A)_x$ with $\alpha = 0.48$ for helium, $\alpha = 0.61$ for methane, and $\alpha = 1$ for the remaining seven gases are plotted as a function of $Re^{0.45}(K_B)_x$. Collapse of the experimental data to a single curve is excellent. Corrected values of $A_a$ and $B_a$ for the nine gases are listed in the last two columns of table 6. The calculational procedure has clearly correlated the heat loss data for the nine different gases to a high degree.

Correlations similar to eq. (30) have also been tried. Ratios of $(\nu_m/\nu_\infty)$ and $(k_m/k_\infty)$ have been used as fitting parameters. The exponents necessary to generate the best fits have been treated as variables. They have been generated by making log-log plots of calculated values of $Nu_c$ at Re = 1 against $(\nu_m/\nu_\infty)_x$ for x equal air, $C_3H_8$, $CF_4$, $CF_3Br$, $CO_2$, Ar, and $SF_6$. A linear least squares fitting procedure gives the exponent from the slope of the line. For $\nu_m/\nu_\infty$ the exponent was found to 1.48. This value is considerably larger than the value of 0.15 given by Ahmed and Fingerson [42] for a cooled film. The exponent for use with $(k_m/k_\infty)$ is calculated to be 0.274.

Figure 17 shows $Nu_c\,(K_\nu)_x$, where

$$(K_\nu)_x = [(\nu_m/\nu_\infty)_{air}/(\nu_m/\nu_\infty)_x]^{1.48}, \tag{43}$$

plotted against $(Re)^{0.45}$. As above, the data for the different gases have been normalized to the results for air. This procedure does give a fairly good correlation for all of the gases except helium, for which the fit could be improved using an $\alpha \neq 1$ as was done above. By comparing figs. 16 and 17, it is clear that the calculational procedure which modifies the parameters $A_c$ and $B_c$ as given by eqs. (39) and (40) provides a much better correlation of the experimental results.

Figure 18 shows $Nu_c(K_k)_x$ plotted as a function of $Re^{0.45}$. $(K_k)_x$ is defined analogously to $(K_\nu)_x$, namely

$$(K_k)_x = [(k_m/k_\infty)_{air}/(k_m/k_\infty)_x]^{0.274}. \tag{44}$$

Plotting the experimental data in this way also gives an improved correlation of the data for the different gases as compared to using $Nu_c$ alone. However, the degree of correlation can be seen to be slightly less than shown in fig. 17, while fig. 16 still seems to provide the best collapse of the data.

Attempts to correlate the results for the hot-film response in different gases is complicated by the variation of $n_o$ when the experimental data are fit to eq. (3). For this reason, it was decided to treat the hot-film data in the same way as described above for the hot-wire data. The hope was that such a treatment would collapse the hot-film data for different gases to a single curve. Figure 19 shows $Nu_c - (K_A)_x$ versus $Re^{0.45}(K_B)_x$ for the eight gases for which hot-film response measurements have been made. Here $(K_A)_x$ and $(K_B)_x$ are given by eqs. (41) and (42) with $T_m$ taken as 472 K. The data plotted in this figure show that the hot-film response for different gases is correlated well by treating the data in this manner. However, the collapse of the data to a single curve is not as complete as found for the hot-wire data. Note that it is not necessary, as is the case for the hot-wire, to modify calculated values of $Nu_c$ of He and $CH_4$ for effects due to a lack of gas accommodation on the surface of the hot-film.

The fact that the same correlation procedure works for the hot-wire and hot-film results implies that the procedure is independent of probe surface temperature effects, aspect ratio, and probe diameter since these parameters are very different for the two probes investigated here. The implications of this finding will be discussed further in the next section.

# 6. DISCUSSION

## 6.1 Correlation of Hot-wire and Hot-film Responses in Different Gases

### 6.1.1 Precision of Correlations

Figures 16, 17, and 18 show that it is possible to collapse the experimental data for the response of a hot-wire in different gases to a single line with a high degree of accuracy. For each of these plots, the data for different gases are normalized by suitable correction procedures to the results for air plotted as $Nu_c$ (or $Nu_a$) against $Re^{0.45}$. Note that $K_A$, $K_B$, $K_\nu$, and $K_k$ are all equal to one for air. The line which results from fitting the air results to eq. (3) with n = 0.45 is

$$Nu_c = 0.272 + 0.650\ Re^{0.45}. \tag{45}$$

Analysis of the data shown in fig. 16 indicates that the largest deviations from this line for the data of other gases is + 2.0% and - 2.7%. As can be seen in fig. 16, it is the data for $CF_4$, $CF_3Br$, and $SF_6$ which are in poorest agreement with eq. (45). On the other hand, the data for $C_3H_8$, $CH_4$, Ar, and $CO_2$ all fall within 1% of the values predicted by eq. (45).

A similar analysis shows that the method of correlation used for the data displayed in fig. 17 gives results which all lie within + 3.6% and - 4.5% of the line given by eq. (45). Clearly the deviations of the data from eq. (45) are greater for data calculated by multiplying $(Nu_c)_x$ by $(K_\nu)_x$ than using the two parameter correction employed for the results shown in fig. 16. Note that as drawn in fig. 17, the $Nu_c$ values for helium and methane have not been corrected for accommodation effects. The error limits reported here refer to

data corrected for these effects. The correction employed for the data shown in fig. 17 corresponds to multiplying $(A_c)_x$ and $(B_c)_x$ by $(K_\nu)_x$. Comparison of eqs. (42) and (43) shows that there is very little difference between values of $(K_A)_x$ and $(K_\nu)_x$. For this reason, the increased scatter of the one parameter correction is due primarily to improper correction of the intercepts $(A_c)_x$.

In fig. 18 the maximum deviations found from the line given by eq. (45) are + 2.9% and - 7.3%. As already noted in section 5, the calculational procedure used for the data displayed in this figure yields the poorest correlation of the three used.

In discussing the precision of the various correlations for the hot-wire results, it must be kept in mind that there are uncertainties in the values of molecular properties used in the various calculations. Unfortunately, the largest uncertainties are found in the thermal conductivities for the different gases. These values are very important since they play a dominant role in end conduction loss calculations as well as appearing to the first power in the Nu. The parameters A and B given in eq. (3) are directly proportional to this variable.

For two of the gases, namely $CF_3Br$ and $C_3H_8$, widely different values of k are available in the literature. We have chosen to use the literature values of k which yield values of $Nu_c$ consistent with those found for the other gases investigated. In the case of propane, this is a value taken from work [48] published after the TPRC tables [45] had appeared. The later value of k is 5.6% times larger than the TPRC value. Interestingly, an uncertainty estimate

of 5% is given in the TPRC for $k_{C_3H_8}$ at the temperature of interest to this study. In the case of $CF_3Br$ we have used a value of k taken from an earlier handbook [49] and have ignored a later measurement [55] of $k_{CF_3Br}$ which gives a value which is 4.7% greater.

Given such uncertainties in k values, we conclude that our calculational procedures yield correlations of hot-wire response data which are as precise as possible within the limits of our knowledge of gas properties. In fact, such uncertainties may explain the small variations of the data plotted in fig. 16 from eq. (45). It is the data for $CF_3Br$, $SF_6$, and $CF_4$ which deviate to the largest degree. These gases are also those for which the largest uncertainties in k values are expected.

Comparison of the hot-film results plotted in fig. 19 with those for the hot-wire shown in fig. 16 indicates clearly that the hot-film results are not correlated quite as well. There are several possible explanations for this observation. Perhaps the most likely lies in the simplifying assumptions used to treat end heat conduction losses for the hot-film. This device has a very complicated physical structure and the assumption of a one-dimensional heat transfer is certainly naive. Furthermore, as pointed out in section 3.7, $k_s$ must be considered as an approximation of the true one-dimensional heat transfer conductivity. Since $\ell/D$ is much smaller for the hot-film than for the hot-wire, end loss corrections are expected to be more important in the case of the hot-film.

We have assumed that the hot-film results can be corrected for gas property temperature dependencies using the same procedures as for the hot-

wire (see eqs. (41) and (42)). Even though this assumption should be approximately correct, it is possible that the same correction may not apply if the hot-film surface has a different surface temperature distribution or heat loss behavior. Uncertainties in the values of molecular properties may also be playing a role.

We conclude that correlating our hot-film results in the same manner as for the hot-wire yields a collapse of the data that is precise to within the limits defined by our lack of detailed knowledge of heat conduction within the probe and uncertainties in the values of molecular properties for the different gases investigated.

### 6.1.2 Physical Reasonability of the Correlation

In developing the correlations of heat transfer behavior given in section 5 we have made a variety of assumptions and approximations. It seems pertinent to try and understand the physical basis of these assumptions and also to relate them to past engineering practice.

The first choice we have made is to treat our experimental results in terms of nondimensional variables. Reduction of experimental data in this way is standard engineering practice and has its basis in dimensional analysis [56]. Problems of heat transfer to and from flows of gases are usually treated by experimentally determining variations of Nusselt number as a function of flow Reynolds number and other possible nondimensionalized numbers such as the Prandtl number. One of the major limitations of this approach is that there are no definitive recipes for deciding how such nondimensional

variables should be formed. For instance, in this study there were standard and physically based expressions for generating the appropriate Nu and Re (i.e., in terms of probe diameter), but there was no standard method for deciding at which temperature to evaluate the molecular properties which are used to form the nondimensional variables. A wide variety of different temperatures have been used in the literature. We finally settled on an evaluation of properties at $T_m$ not only because this temperature is widely used in the literature, but also because it seems reasonable from a physical point of view. The choice of a median temperature for molecular properties should minimize the effects of property variation with temperature.

We first attempted to correlate our results in terms of $Nu_m$. These attempts failed due to the neglect of heat losses at the end of the probe. These conduction heat losses not only vary with the flow parameters, but are also dependent on the thermal conductivity of the gas. End heat loss corrections are discussed further in section 6.2 where we conclude that the mathematical procedure used is physically realistic for the hot-wire and is only approximately correct for the hot-film.

Comparison of figs. 4 and 5 shows that not only are values of $Nu_\infty$ for the different gases greatly reduced from $Nu_m$ by this correction, but the relative spacings and orderings of the data for different gases are changed. This is particularly true in the case of helium which has an unusually large value of $k_m$. For this reason, values of $Nu_m$ for this gas are reduced proportionally less by this correction than found for the other gases. Similarly, $CF_3Br$ has an extremely small $k_m$ value and the reductions of its $Nu_m$ values following end loss corrections are proportionally greater than found for the other gases.

Correction of $Nu_m$ for end conduction losses leads to a Nusselt number ($Nu_\infty$) which corresponds to the Nu for convective heat transfer from an infinite cylinder. It is not surprising that the use of $Nu_\infty$ yields a better correlation of experimental results than $Nu_m$.

Values of $Nu_\infty$ are next corrected for what might be called "classical" thermal slip. By this we mean noncontinuum effects on heat transfer, but assuming perfect accommodation of the gas on the surface of the probe. Equations (9-12) with $\alpha$ set to 1 are used for this purpose. Figure 6 shows plots of the data for the nine gases plotted as $Nu_c$ versus $Re^{0.45}$. Comparing values of $Nu_c$ shown in fig. 6 with the corresponding values of $Nu_\infty$ shown in fig. 5 indicates that the correction for noncontinuum effects has very little effect on the relative ordering or spacing of the results for different gases. Note that there is a significant increase in value of $n_o$ following the correction for thermal slip. As might be expected, the largest effect is for helium (Kn = 0.075) which has the largest Kn of any of the gases investigated here. Even for this gas, correction of our measurements for "classical" thermal slip only increases values of $Nu_c$ by $\approx$ 10% as compared to $Nu_\infty$.

As figs. 6 and 11 show, plots of $Nu_c$ as functions of $Re^{0.45}$ for the different gases do not lead to a complete correlation of the results. Clearly, some additional correction must be made. As discussed in section 5, multiplying $Nu_c$ by either $(k_m/k_\infty)_x$ or $(\nu_m/\nu_\infty)_x$ raised to suitable powers increases the degree of correlation of the results (see figs. 17 and 18). Is this physically reasonable? The answer is yes. By multiplying $Nu_c$ by either of these ratios, we are partially correcting values of $Nu_c$ for variations in the temperature dependencies of the molecular properties of the gases. Heat

transfer from a heated cylinder actually occurs along a temperature gradiant, therefore, it is not surprising that the temperature dependence of the molecular properties is important in the heat transfer. Since variations in k and $\nu$ for different gases are roughly related, it is expected that correlations in terms of either $k_m/k_\infty$ or $\nu_m/\nu_\infty$ will give nearly the same collapse of the data. This is found to be the case.

The necessity of providing corrections for physical property temperature dependencies is well known. The method used here is consistent with approaches which have been employed in past engineering studies [57].

Modification of $(Nu_c)_x$ by multiplying by either $(K_k)_x$ or $(K_\nu)_x$ gives a much better collapse of the data than is found for data simply plotted as $(Nu_c)_x$. However, by using equations of the same form as eq. (3) and looking for ways to correlate the values of $A_c$ and $B_c$ individually, it has been possible to obtain an improved correlation of the results.

The parameter $B_c$ was found to be dependent on $(\nu_m/\nu_\infty)_x$ raised to a power (see fig. 14 and eq. (39)). This dependence is similar to that described above for the corrections of $Nu_c$ for the temperature dependence of gas properties. Since the parameter B in eq. (3) is generally thought to be determined by forced convection, it is reasonable to expect this parameter to show a similar dependence on molecular property temperature variation.

On the other hand, the parameter $(A_c)_x$ has been shown to be primarily dependent on values of $(\mu_m)_x$ raised to a power (see fig. 13 and eq. (40)). While not exactly correct, this parameter is expected to be determined

primarily by buoyant and conductive heat transfer processes. It has not been possible to relate such heat loss mechanisms to a dependence on $\mu_m$. At this time the physical basis of the observed dependence of $(A_c)_x$ on $(\mu_m)_x$ must be considered as unknown and perhaps coincidental.

It has been necessary to make one further correction of the data in order to obtain a satisfactory correlation of the experimental results for all of the gases. This final correction allows for accommodation effects [18]. This effect will be discussed in greater detail in section 6.4. Eqs. (9), (11), and (12) which have been used here to correct $Nu_c$ for the effects of accommodation provide a good approximation of the dependence of heat transfer on Kn and $\alpha$ which are found in more detailed theories of this effect.

In general, it is found that lighter gases show more pronounced accommodation effects than heavier gases [58]. This is due to their smaller sizes and higher average molecular speeds. In this study we have only found it necessary to modify the hot-wire values of $Nu_c$ measured in helium and methane in order to account for changes in transfer behavior due to small values of $\alpha$. This finding does not imply that small accommodation effects are not present for the other gases investigated, but only that such corrections are similar for measurements made in the other gases. See the discussion in section 6.4.

In the case of helium it is highly significant that the correction for accommodation effects also changes the observed value of $n_o$ from 0.35 for the data in terms of $Nu_c$ to the value of 0.45 found for the data treated as $Nu_a$. This is a clear indication that the correction of $Nu_c$ for accommodation is

behaving properly since the new value of $n_o$ is in complete agreement with those found for the other gases when plotted in terms of $Nu_c$. Further verification of this conclusion is provided by the results of the hot-film measurements in helium. For this case, no accommodation effects are required in order to correlate the helium data with that found for the other gases (see fig. 19). This observation is in accord with the expectation that helium will be accommodated much better on a heated alumina surface (film) than on a heated platinum surface (wire) [58]. The reduction in accommodation effects in the heat transfer of helium for a hot-film as compared to a hot-wire has been discussed by Simpson and Wyatt [40].

When developing the types of corrections for heat transfer data we have used here it must be remembered that very simple equations are being used to approximate very complicated processes involving complex boundary layers and heat transfer at surfaces. Despite this, after correction of the experimental data for physically realistic heat loss processes and known molecular effects a very good correlation of the heat transfer data from heated filaments is found for a wide range of gases. This finding is the best justification for the various approximations and simplifications which have been employed.

### 6.1.3 Comparison of Results for Air With Literature Correlations

Most of the past work on correlations of heat transfer from anemometric probes has been reported for measurements made in air. Figure 20 shows the line corresponding to our results for air plotted as $Nu_c$ versus $Re^{0.45}$. Note that the actual value of $n_o$ in this work was determined to be 0.44. This small change in $n_o$ has very little effect on the fit of the data to the equa-

tion. On the same plot the corresponding curves are drawn for results taken from Collis and Williams [15] (eq. (4)), Andrews et al. [14] (eq. (13)), and Fingerson and Ahmed [42] (eq. (30)). For eq. (4) values of $T_m$ and $T_\infty$ correspond to those used in this study. Similarly, values of $\nu_m$ and $\nu_\infty$ used in eq. (30) are taken for the conditions of the hot-wire in our study. The two literature hot-wire studies employed probes having large aspect ratios while the cooled-film used by Fingerson and Ahmed had a small aspect ratio. Apparently, the latter results have not been corrected for end heat conduction effects.

Figure 20 shows that the present experimental results for $Nu_c$ as a function of $Re^{0.45}$ lie very close to the curve given by Collis and Williams. There is a difference of ≈ 9% in slope and ≈ 6% in intercept. Given the various corrections applied to our finite aspect ratio hot-wire measurements, this agreement must be considered excellent. As discussed in section 2.1, variations in heat transfer laws might also be expected due to the use of a feedback amplifier in our electronic circuitry [25,26].

The correlation reported by Andrews et al. [14] is in poor agreement with our results (≈ the same slope and ≈ 25% higher in intercept) as well as that given by Collis and Williams [15]. A possible explanation for this discrepancy can be found by comparing the thermal conductivity values for air used in the two earlier papers. Andrews et al. report that their k and μ values were taken from the International Critical Tables [59] published in 1928 while Collis and Williams have used a formula for k given by Kannuluik and Carman [60] and have taken their ν values from the tables of Goldstein [61]. The values of kinematic viscosity employed in these two earlier studies

are nearly identical to those used in this study. However, the values of k for air at $T_m$ obtained from the literature sources for the three studies are $7.51 \times 10^{-5}$, $8.34 \times 10^{-5}$, and $8.38 \times 10^{-5}$ cal/cm • K • s for Andrews et al., Collis and Williams, and this work, respectively. The value of k used by Andrews et al. is 10% smaller than that used in this study or the work of Collis and Williams. The effect of using the more recent value of k on the results of Andrews et al. is shown in fig. 20 where their results have been redrawn (dotted line) using our value of $(k_m)_{air}$. It can be seen that the results for all three studies of heat transfer from hot-wires in flowing air now lie relatively close together. On this basis, we conclude that our measurements of $Nu_c$ in air are consistent with past literature measurements.

The correlation of cooled-film results reported by Fingerson and Ahmed [42] lies considerably below those measured for the hot-wires. This apparent difference between the most suitable correlations for the hot-wire and cooled-film results has already been noted by Fingerson and Ahmed and attributed to a dynamical dissimilarity between heating and cooling of cylinders.

Figure 21 shows the line corresponding to our hot-film results in air plotted as $Nu_c$ versus $Re^{0.45}$. Lines corresponding to the results of Collis and Williams [15] and Andrews et al. [14] (both as given by the authors and corrected for k values as described above) are shown on the same plot. It is clear that there is relatively poor agreement between the hot-film results and the two earlier correlations obtained for hot-wires. Both the slope and intercept for our data are higher. Using a larger value of $k_s$ for the thermal conductivity of the film would result in decreased values of $Nu_c$ when $Nu_m$ is corrected for end conduction losses and noncontinuum effects. Such a

modification would give better agreement with the hot-wire correlations. However, as already noted in section 4.1, the primary effects of the end conduction corrections are to generate a relatively large decrease in $A_c$ and a much smaller decrease in $B_c$. Test calculations indicate that while reducing $k_s$ does indeed increase the agreement of our hot-film results with those of Collis and Williams and Andrews et al., this correction alone is not sufficient to give agreement for both $A_c$ and $B_c$. We attribute this observation to the simplifications which have been made by assuming a one-dimensional heat conduction along the film. Improved agreement between heat transfer laws for hot-films and hot-wires will require a better theoretical treatment of heat conduction losses for the hot-film.

### 6.1.4 Comparison of Results for Different Gases with Available Literature Correlations

There are several studies available which have investigated the responses of hot-wires and films to changes in gas composition [14,27-40]. Most of these studies have involved no more than three different gases and usually one of these was air.

The most common correlation suggested for the treatment of hot-wire and film measurements in different gases is the combination of Collis and Williams' [15] relationship for air with Kramers' [35] results for heat transfer from cylinders placed in different fluids to give eq. (26). This equation has been used or suggested by at least three groups of workers [34,39,40]. Figure 12 shows that there is very little relationship between values of $A_c$ or $B_c$ for the various gases and the corresponding Pr. Perhaps more importantly, given the small variations in Pr among different gases, the

exponents required on the Pr ratios in eq. (26) would have to be many times larger than the values of 0.20 and 0.33 in order to reduce the data for the gases investigated here to a common curve. We conclude, based on these observations, that while it is possible that forced convective heat transfer from cylinders to gases may have a weak dependence on gas Pr, this dependence is hidden by the much stronger effect of molecular property temperature variations on the heat transfer.

Fingerson and Ahmed [42] are the only other workers of which we are aware who have used a temperature dependent property ratio to correlate heat transfer results for anemometers placed in different gases. Their correlation for cooled-films is given by eq. (30). The ratio of $\nu_m/\nu_\infty$ used in this correlation is similar to one of the corrections we have used to modify $Nu_c$ (see eq. (43)). As already noted, the exponent for the property ratios are very different for the two studies, but it is significant that both of these studies have required such a ratio to correlate heat loss results in different gases. Interestingly, these authors have reached the same conclusion as given above concerning the inability to discern an effect of Pr on the heat transfer behavior.

It is also of interest to compare our results with the conclusions of Andrews et al. [14] who reported measurements of hot-wire response in air and mixtures of methane and nitrogen. These workers correlated their results for pure gases and mixtures in terms of $Nu_a$ by correcting large aspect wire results for thermal slip effects. The agreement was quite good, but in light of the results given in this paper must be considered fortuitous. As fig. 6 shows, values of $Nu_c$ for methane and air plotted as functions of $Re^{0.45}$ do not

lie on the same curve. The discrepancy in the findings of these two studies may be due to differences in the values of thermal conductivity used.

## 6.2 End Conduction Corrections

In section 3.7 we have given a recipe for the correction of measured Nu made for finite aspect ratio probes. This correction compensates for heat losses to the prongs supporting the probe due to heat conduction along the probe. The resulting Nu corresponds to that for heat transfer from an infinite probe at the same average probe temperature. In making these calculations we have made several assumptions and approximations as discussed in section 2.1. Additionally, a literature value of thermal conductivity of tungsten was used for $k_s$ despite the fact that the probe is known to have a layer of platinum deposited on its surface. Despite these approximations, we have obtained results for air which are in excellent agreement with measurements of hot-wire response where end conduction effects are known to be absent [14,15,17,34]. Barring the accidental cancellation of errors, this finding validates the procedure used to correct for heat losses by conduction along the hot-wire.

It is extremely encouraging that the correction procedure leads to conclusions 1-5 listed in section 4.1. These calculated effects of changes in heat loss behavior with aspect ratio are in complete agreement with experimental findings. This agreement lends further support to the model used here to make the end loss corrections. The importance of making such corrections is clear from the finding that no correlation of our results in terms of $Nu_m$ could be found.

In the case of the hot-film measurements, it is clear that our correction procedure only provides an approximate physical picture for end conduction heat losses. It is not surprising that our approximations fail in this case since heat transfer along the hot-film is not expected to be one-dimensional. A more highly developed heat transfer expression for conduction heat losses along the heated film needs to be developed in order to allow more exact correlations of our hot-film data in different gases.

## 6.3 Reynolds Number Dependence of Heat Transfer

It has been shown that the hot-wire results for different gases can all be fit extremely well in terms of $Nu_a$ using a value of $n = 0.45$ as the exponent for the Re. Table 5 lists the Re ranges over which these measurements have been made. All of the measurements taken together cover a Re range from $\approx 0.1$ to $\approx 6.2$. Note that the results for some of the gases fall at the lower end of the range while those for others fall at the upper end. The fact that observed values of $n_o$ are so similar for all of the different gases requires that there be very little change in heat transfer behavior over this limited Re range.

The situation for the hot-film is very different. In this case, the Re range covered is $\approx 1.0$ to $\approx 43$. Gases which fall in the lower portion of this range (e.g., air, Ar, and $CH_4$) have $n_o$ values of $\approx 0.45$. These values are consistent with those found for the hot-wire. On the other hand, the three gases for which results lie at the high end of the Re range ($C_3H_8$, $SF_6$, and $CF_3Br$) give $n_o$ values in the 0.36 to 0.39 range. Significantly, the measurements for $CO_2$, which lie in an intermediate Re range, give a $n_o$ value of 0.42

which is between the $n_o$ values found for the measurements made at the extremes of the Re range. Note that all of the measurements are made for velocities low enough to insure that the sharp flow transition at Re ≈ 44 has not occurred.

The results of measurements made over the transition region mentioned in the last paragraph have been described in section 4.2. Figures 9 and 10 show clearly that there is an abrupt transition in heat transfer behavior for this Re range as described by Collis and Williams [15] and much earlier by Hilpert [16]. Collis and Williams used hot-wire anemometry in the wake of the hot-wire to show conclusively that the Re for which the transition occurs is identical to that for which eddy shedding commences from the heated probe.

The sharpness of this flow transition is demonstrated by the data plotted in fig. 10. A clear hysteresis is observed in the heat transfer behavior depending on whether the velocity of the gas is increased or decreased to the measurement value. This observation implies that there is a narrow bistable Re regime which lies between the flow velocities where eddies are not shed from the cylinder and those where such shedding always occurs. Closer inspection reveals that for the three cases investigated, the transition from no eddy shedding to the onset of shedding is extremely abrupt and occurs within a Re change of ≈ 0.6. The results for propane also show a sharp transition from flow with eddy shedding to flow without eddy shedding. Interestingly, the results for $SF_6$ and $CF_3Br$ indicate that flows of these gases have a smooth transition in heat transfer behavior on going from the eddy shedding to no eddy shedding flow conditions. The differences in transition behavior for $SF_6$ and $CF_3Br$ as compared to $C_3H_8$ result in the bistable region of the former two

gases extending over a wider range of Re. At the present time we can offer no firm explanation for the differences in transition behavior between $C_3H_8$ and the heavier molecular weight gases. It is intriguing to speculate that there may be a molecular weight effect on this flow transition behavior.

There are some additional points which should be made concerning the onset of vortex shedding. First, note that the Re range covered by the transition regions extend from Re ≈ 36 to ≈ 55 which is nearly centered on the value of Re ≈ 44 quoted by Collis and Williams [15] as the Re for the onset of eddy shedding flow behavior. In their study of cooled-films, Fingerson and Ahmed [42] also report a flow transition between Re = 40 and 55. These three studies have been made for a wide range of temperatures varying from room temperature to 1700 K. The fact that the onset of eddy shedding is found at Re ≈ 44 in all of these studies is a strong recommendation for the use of $T_m$ in determining gas properties for use in the nondimensional variables. If values of $\nu$ at different temperatures (e.g., $T_s$ or $T_\infty$) were used, the observed values of Re for the transition would vary widely. Minor variations are observed in the exact Re ranges over which the hysteresis occurs for the different gases as can be seen in fig. 10. We attribute these to uncertainties in the values of $\nu$ used to calculate Re and to differences in the temperature dependencies of $\nu$. In analogy with the discussion given in 6.1.2, such variations are expected when $T_m$ is used to determine values of $\nu$ for use in calculating Re.

The behavior of heat transfer from heated cylinders as a function of Re are related to the values of $n_o$ required to fit eq. (3) for $Nu_c$ (or $Nu_a$) as a function of $Re^n$. The findings of this study can be broken down into the following four Re regimes:

I. Re ≈ 0.1 to ≈ 5: $n_o$ remains essentially constant at ≈ 0.45 for measurements falling into this Re range,

II. Re ≈ 5 to ≈ 35: $n_o$ decreases as the Re increases,

III. Re ≈ 35 to ≈ 55: This is the bistable region determined by the presence or absence of eddy shedding from the heated cylinder. Very low values of $n_o$ (< 0.35) are associated with gas flows for which no eddies are being shed. Large values of $n_o$ (> 0.50) result when eddies are present behind the cylinder, and

IV. Re > 55: Values of $n_o$ which fit the data in this Re regime are $\geq$ to 0.50. We have not made extensive measurements in this Re regime.

It is interesting to discover that Hilpert [16] divided his heat transfer results for heated cylinders in air into three regimes roughly corresponding to I, II, and IV above with a break between II and IV at Re ≈ 40. This author fit his experimental results to an equation of the form

$$Nu_\infty = C[Re(T_s/T_\infty)^{1/4}]^{n'} \qquad (46)$$

where values of C and n' appropriate for the given Re ranges are listed in table 8. If Hilpert's results for $Nu_\infty$ as a function of Re are fit to an equation of the form of eq. (3) for Re = 4 to 40, $n_o$ is found to be 0.39 which is in good agreement with our experimental results for gases falling in this

Re range. Unfortunately, a similar calculation for the 1 to 4 Re range gives a still smaller value of $n_o$ which is the opposite of our experimental finding.

In general, Collis and Williams [15] found good agreement with Hilpert's results [16], but argued that the transition at Re ≈ 4 does not actually exist but is an artifact of the small number of experimental measurements used by Hilpert to deduce its existence. As shown by eq. (4) and table 1, Collis and Williams only required two Re flow regimes to fit their experimental measurements which extended from Re ≈ 0.02 to ≈ 140. A careful examination of the data given in their paper shows that the slow variation in $n_o$ we find just before the flow transition at Re ≈ 44 may not have been large enough to be discerned by these authors.

It is possible to speculate on the physical basis for a modification of heat transfer behavior on going from Re regime I to II. This can be done by looking at the flow patterns which exist around an infinite cylinder in a gas flow [62,63]. At Re < 4 the flow past a cylinder does not display a wake and the flow moves over the cylinder as a nonseparating flow. At Re ≈ 4 the flow separates from the cylinder, a stagnation region develops behind the cylinder, and a wake appears. As the Re is increased, the stagnation point moves slowly forward on the cylinder and recirculation eddies develop in the rear of the cylinder. These eddies grow and intensify until Re ≈ 44 at which point alternate shedding of vortices occurs from the sides of the cylinder.

The effects of these transitions can be seen in a plot of the drag coefficient ($C_D$) as a function of Re [64]. The modification of $C_D$ due to the change in flow behavior at Re ≈ 4 appears larger than that due to the transition at Re ≈ 44 for the data plotted on a log-log plot.

It seems clear that the variations in $n_o$ observed over Re ranging from $\approx 5$ to $\approx 50$ and for which vortex shedding is absent are due to the formation of stagnation points and the growth of recirculation zones behind the heated cylinder. For heat transfer from the cylinder this is a gradual and continuous change as reflected in the slowly decreasing values of $n_o$ as the Re range of the measurements is increased. For $Re < 5$ the fluid flow corresponds to nonseparated flow and no variation of $n_o$ with Re is expected. This conclusion is in agreement with experimental findings.

The above discussion indicates that the existence of Re regimes 1, 2, and 4 can be identified with the known flow behavior of gases over a cylinder. Apparently, the hysteresis in heat transfer behavior which is the distinguishing characteristic of regime III has not been reported previously in the heat transfer or hot-wire literature. However, such bistable regions are not uncommon in fluid mechanics and the existence of a hysteresis for vortex shedding from a cylinder should not be a surprise.

## 6.4 Accommodation Effects

In section 5 we argued that it is necessary to consider accommodation effects in correlating our hot-wire measurements in flows of helium and methane. For the remaining seven gases investigated $\alpha$ was assumed equal to 1. It seems advisable to question these assumptions as well as the plausibility of the values of $\alpha$ ($\alpha = 0.48$ for helium and $\alpha = 0.64$ for methane) determined.

Thermal accommodation behavior is poorly understood, but is thought to arise on a molecular level due to the incomplete transfer of heat from a heated surface to a molecule or atom striking the surface. The species colliding with the surface only "accommodates" a fraction of the energy available from the surface with the result that the Boltzmann temperature of the gas phase species near the surface is lower than expected based on the surface temperature. Theories which treat this effect are usually based on the temperature jump which exists at the boundary of the solid and gas. The result of this temperature jump is that heat transfer is reduced from the value which would be found if it did not exist.

The primary impression which results from a review of the literature on thermal accommodation is the degree of complexity of the effect. In particular, a great deal of variability in measured values of accommodation coefficients is observed unless extremely clean and well-characterized surfaces are employed [65]. This variability has severely limited attempts to understand and predict values of $\alpha$. The effects of such important system parameters as surface temperature, gas pressure, and gas molecular weight on thermal accommodation are poorly characterized and understood.

Despite the confusing and sometimes contradictory experimental findings concerning the characteristics of thermal accommodation, the following general observations are believed to be correct [58]. The degree of surface "cleanness" is critical to measured values of $\alpha$. Cleaner surfaces result in lower values of $\alpha$. Values of $\alpha$ for polycrystalline or ordinary industrial matrices "which are macroscopically clean but contaminated with miscellaneous physically and chemically absorbed materials" [66] are expected to be substantially

larger than those found for carefully prepared surfaces. Increasing molecular weight and complexity are associated with increasing values of $\alpha$. There is an apparent effect of surface temperature on the degree of thermal accommodation, but the experimental results are contradictory and no definitive trends are discernible [58]. The effect of pressure on observed values of $\alpha$ is believed to be small except for cases where the pressure determines whether or not gas layers are present on the surface.

The extreme sensitivity of thermal accommodation to so many system parameters makes prediction of values of $\alpha$ nearly impossible except for experiments made under highly controlled conditions. Measurements with hot-wires and films certainly do not fall into this class. The surface structures of these probes are not characterized well and are expected to contain very uneven and variable surfaces due to the manufacturing processes used in their construction. Furthermore, these probes are usually operated in environments which are expected to continuously contaminate and modify the probe surface. In this study involving the use of several different gases, the nature of gases absorbed on the surface of the probe might also be expected to vary from experiment to experiment.

The above discussion makes it clear that one cannot expect to use a theoretical development to predict values of $\alpha$ for use in hot-wire anemometry. The best one can hope to do is determine values of $\alpha$ phenomenologically and compare the experimental results with the general characteristics of thermal accommodation.

In the case of the work reported here, the first assumption which should be questioned is the use of $\alpha = 1$ for all of the gas flows over the hot-wire and film with the exception of the wire results for helium and methane. Andrews et al. [14] have listed selected values of $\alpha$ for a wide range of surfaces and gases. The variability of results found in measurements of $\alpha$ is quite clear from this table. Despite this, it is possible by using the reported values of $\alpha$ along with the expected modifications due to the hot-wire probe surface conditions to estimate that the value of $\alpha$ will lie between 0.9 and 1 for air on the hot-wire. Based on the molecular and complexity arguments described above, the same estimate will apply to all of the higher molecular weight gases investigated (i.e., all of the gases investigated except helium and methane). Values of $\alpha$ should be very nearly equal to one for all of these gases on the alumina surface of the hot-film.

These estimates of $\alpha$ can be used to evaluate the effect of thermal accommodation on the correlations of our hot-wire and film results. $\alpha$ enters our calculations of $Nu_a$ in eq. (9) as a factor in the thermal slip parameter ($\Delta$). In calculating $\Delta$ the value of what we have referred to as the "classical" slip parameter is multiplied by $(2-\alpha)/\alpha$. For an $\alpha$ value of 0.9 this corresponds to an increase of 22% in the value of $\Delta$ over that expected in the absense of thermal accommodation effects. Since values of $\Delta$ enter directly into eq. (12) the parameter $\phi$ will also increase by 22%. $\phi$ is used in eq. (11) to correct $Nu_a$ for noncontinuum effects. For air the value of $\phi$ is calculated to be 1.85 if $\alpha = 1$. By substituting this value of $\phi$ into eq. (11) along with the Kn for air one finds that a value of $Nu_c = 1.050$ is calculated assuming a value of $Nu_\infty = 1.00$. The corresponding value of $\phi$ is 2.260 for $\alpha = 0.9$ which gives a value of $Nu_a = 1.062$ when $Nu_\infty$ is corrected for non-

continuum effects. The value of $Nu_a$ is only 1% larger than $Nu_c$. This result shows that the use of $\alpha = 1$ gives results for $Nu_c$ which differ only slightly from values of $Nu_a$ which would be calculated if the actual values of $\alpha$ for air were known. This conclusion will be true for the hot-wire measurements made in air, Ar, $CO_2$, $C_3H_8$, $CF_4$, $SF_6$, and $CF_3Br$. It justifies our conclusion that it is possible to correlate the results for these gases (see figs. 16-18) in terms of $Nu_c$. The errors introduced in the correlation by the use of $Nu_c$ instead of $Nu_a$ are considerably smaller than those arising from other sources such as uncertainty in molecular property values. This approximation will be even more correct for the hot-film for which values of $\alpha$ should be even closer to one than for the hot-wire.

The effect of accommodation on hot-wire anemometry measurements has been investigated primarily for helium. Libby and coworkers [32-34] were the first researchers to note the importance of the small accommodation coefficients for this gas on the metal surfaces of hot-wire probes. For tungsten wires, values of $\alpha = 0.030$ [32] and $\alpha = 0.040$ [33] were reported. A later study [34] of the heat transfer from a platinum hot-wire gave $\alpha = 0.11$. In all three cases the values of $\alpha$ were shown to fall within the ranges reported in literature measurements of helium on the appropriate surfaces. For the results on tungsten, Baccaglini et al. [33] indicate that researchers in the area of gas-surface interactions had questioned the very small values of $\alpha$ determined due to the contaminated nature of the hot-wire surfaces. These workers [33] went on to state that they "have sufficient confidence in our technique to take the view that reasons for the low values of $\alpha$ require further study by researchers concerned with gas-surface interactions".

Our experimental determination of $\alpha$ for helium on the platinum surface of the hot-wire gave $\alpha = 0.48$. We feel that this result is an accurate estimate of $\alpha$ not only because it yields values of $Nu_a$ for helium which are well correlated with our results for seven other gases, but also because it gives a value of $n_o$ for data plotted as $Nu_a$ versus $Re^n$ which is in excellent agreement with those found for measurements in other gases. The value of $n_o$ is highly dependent on the magnitude of $\alpha$ as it changes from 0.35 for $\alpha = 1$ to 0.45 for $\alpha = 0.48$.

Our value of $\alpha$ for helium on the platinum hot-wire surface is consistent with values found in the literature. Devienne [58] lists an average value of $\alpha = 0.54$. However, as noted above, the reader is cautioned that the experimental results quoted by Devienne covered an extensive range of values.

It is difficult to suggest a reason as to why our value of $\alpha$ for helium is so much larger than those found by Libby and coworkers [32-34]. The most obvious possibility is that the surfaces of the probes are really different enough to account for the variations. Even though the earlier works were not corrected for the temperature variations of fluid properties, these variations are so similar for helium and air that they can account for only a small fraction of the differences observed.

Our results indicate that there is also a small accommodation effect ($\alpha = 0.61$) for methane. This is reasonable since methane is lighter than air and has high energy vibrational modes. For these reasons, this molecule is expected to have a value of $\alpha$ which is intermediate between that of helium and air as observed.

One other study has reported accommodation effects on hot-wire measurements. Brown and Rebollo [43] considered such effects in their development of a concentration probe which incorporated a hot-wire. These workers indicate that it is necessary to account for accommodation effects for Ar on platinum in correlating their experimental results. This disagrees with our findings. However, these workers did not correct their measurements for end heat loss effects or the temperature dependence of gas properties. The neglect of such effects can lead to erroneous conclusions concerning the importance of accommodation effects on heat transfer behavior.

Based on the above discussion, we feel that, while neither justified by past practice or a strong theoretical basis, our procedures for treating accommodation effects are sufficiently accurate for correlation purposes. Our general findings concerning this effect are in good agreement with the trends expected (e.g., with regards to the effect of molecular weight).

## 6.5 Some Comments on Hot-Wire and Film Calibrations

There are a number of opinions in the literature concerning procedures to be used in calibrating the response of hot-wire anemometers [8]. Disagreements concern such general questions as whether universal correlation laws should be used at all and more specific questions such as which exponent to use in fitting calibration data to equations of the form of eqs. (29) or (3). While we do not wish to join this ongoing controversy, a few comments based on the findings of this work are relevant. Perhaps the major finding is that hot-wire and film responses to flows of different gases can be correlated. If accommodation effects are expected to be absent and molecular property data

are available, it should be possible to predict the response of the probe in a second gas following calibration in another gas. This finding could provide a considerable savings of time and effort for experiments in which the flow velocity of several gases are to be investigated. In generating these correlations it is necessary to correct the measurements for end heat loss effects, temperature variation of properties, and "classical" noncontinuum effects. The question of whether to use an equation of the form of eq. (3) often arises in calibrating hot-wires. Variations of the value of $n_o$ with Re are often discussed [7]. Our work indicates that these variations are due primarily to changes in the flow behavior with Re and to noncontinuum effects for small probes and light molecular weight gases. The choice of an equation to fit experimental calibration data should be based on the Re at which the probe will be operated. Our findings indicate that either eq. (3) or eq. (29) will be appropriate if the probe Re falls in the 0.5 to 6 range. The best value of n to use will depend on exactly how the data is treated. For instance, all of our hot-wire data, with the exception of helium, can be fit quite accurately by assuming a value of n = 0.43 and using either eq. (29) or eq. (3) in terms of $Nu_m$. Note that these forms will not allow a correlation of data for different gases. On the other hand a value on n = 0.45 is more suitable for data treated as $Nu_c$ or $Nu_a$. In making such assessments, care must be taken to identify noncontinuum flow effects. If measurements are made in the Re regime from 6 to 40 the use of eq. (3) becomes questionable as we have shown that $n_o$ values vary over this range. Measurements in the bistable range of Re from $\approx$ 35 to 55 should be avoided if at all possible.

## 6.6 Heat Transfer Studies Using Hot-Wires or Films

The hot-wire and film investigated here are employed primarily as velocity measurement devices and this study is designed to investigate this use of these devices. However, it is worthwhile to point out that these devices are quite sensitive to changes in convective heat transfer and are therefore able to provide quite detailed measurements of heat transfer from cylinders.

This study has generated information on the behavior of heat transfer in the Re range from 0.5 to 55. The results have allowed us to reach conclusions concerning the effects of flow transitions on heat transfer behavior. A very clear hysteresis in heat loss behavior has been observed and associated with the presence or absence of eddy shedding from the cylinder. Use of a large number of different gases have allowed us to identify the importance of fluid property temperature dependence when the nondimensional parameters are calculated in terms of gas properties evaluated at $T_m$. All of these effects were poorly characterized in the literature. Clearly, our investigation of heated velocity probes has generated a great deal of new information of interest to workers in the area of heat transfer.

It is also of interest to note that with further development measurements of the type reported here might yield values of gas thermal conductivity or viscosity. For instance, if the types of correlations we have used here are shown to be reproducible and universal, it would be relatively simple to determine a value of k for a gas if the corresponding value of $\nu$ was available. Since accurate values of $\nu$ are easier to measure experimentally, it

will often be true that such values will be available when k values are not. Measurements of this type should be possible which have a precision, and perhaps accuracy, of ≈ 1%.

Measurements of this type also seem to offer the promise of a method for measuring accommodation coefficients for gases on surfaces in a relatively straightforward and rapid manner. It may be possible to develop a technique based on hot-wire anemometry for studying this complex and poorly understood phenomenon.

## 7. FINAL REMARKS

This paper has described hot-wire and film calibrations which have been made for a wide variety of gases. The use of gases having a broad range of gas molecular properties has allowed us to isolate the corrections which must be made in order to correlate the data in the usual form of a Nu as a function of flow Re. These corrections include end heat losses due to conduction along the probe, a very strong effect due to the temperature dependence of gas molecular properties, "classical" noncontinuum effects, and accommodation effects on heat transfer from the probe surfaces to the gases. All of these effects are known and each has been used separately in the literature in attempts to correlate hot-wire or film responses. This is the only study of which we are aware that has investigated the effects of each correction on heat transfer behavior and has been able to develop a systematic procedure which allows the correlation of such a wide range of experimental data.

In the case of the hot-wire the resulting Nu ($Nu_c$ or $Nu_a$ depending on whether or not accommodation effects are important) has a dependence on Re in air which is very close to that found for previous hot-wire measurements where end heat losses are absent and noncontinuum effects have been accounted for. This observation offers the possibility that universal calibration laws may be possible to describe the response of a hot-wire. The agreement for the hot-film results is not nearly as complete. We have attributed this to the approximation of a one-dimensional heat loss used to treat the heat losses at the end of the probe. It should be possible to develop better models to treat this process.

The finding that the heat loss behavior of these devices (as reflected in the value of $n_o$ for fitting data to the form of eq. (3)) is strongly dependent on the nature of the flow around the probe should also allow a much better prediction of probe response for a given Re range. These results should be considered when choosing a probe for a particular application.

Only one overheat ratio has been used for the hot-wire. A slightly larger value has been used for the hot-film. For this reason, this study offers no conclusions regarding the effect of overheat ratio on heat transfer behavior. It is impossible to conclude whether the probe temperature dependence noted in past experiments is due to property temperature dependencies or to other possible effects such as buoyancy, etc. The role of offset voltage setting on constant temperature hot-wire anemometry may also be important. Further studies should be done to clarify this point.

Our major goal for this work was to be able to understand and perhaps predict the response of a heated cylindrical probe to convective flows of different gases. The experiments reported here have discussed our findings for pure gases. For these gases great strides have been made toward our goal. A second paper [5] will describe the results for mixtures of different gases.

## 8. ACKNOWLEDGEMENTS

This research has been partially sponsored by the Air Force Office of Scientific Research, Air Force Systems Command, USAF, under Grant Number AFOSR-ISSA-00005. The U.S. Government is authorized to reproduce and distribute reprints for Governmental purposes notwithstanding any copyright notation thereon. The authors would like to thank Dr. Howard Baum of the Center for Fire Research, NBS for many helpful discussions and Dr. Roger Simpson of Virginia Polytechnic Institute and State University for sending us a copy of unpublished work. Thanks are also due to Dr. John Rockett for a thorough review of this rather long manuscript.

## REFERENCES

[1] Pitts, W.M. and Kashiwagi, T., The Application of Laser-Induced Rayleigh Light Scattering to the Study of Turbulent Mixing, National Bureau of Standards Internal Report, NBSIR 83-2641 (1983).

[2] Pitts, W.M. and Kashiwagi, T., The Application of Laser-Induced Rayleigh Light Scattering to the Study of Turbulent Mixing, J. Fluid Mech. 141, 391-429 (1984).

[3] Pitts, W.M., McCaffrey, B.J. and Kashiwagi, T., A New Diagnostic for Simultaneous, Time-Resolved Measurements of Concentration and Velocity in Simple Turbulent Flow Systems, presented at the Fourth Symposium on Turbulent Shear Flows, Karlsruhe, W. Germany (Sept. 12-14, 1983).

[4] Pitts, W.M., McCaffrey, B.J. and Kashiwagi, T., to be published.

[5] McCaffrey, B.J., Pitts, W.M. and Baum, H.R., manuscript in preparation.

[6] Corrsin, S., Turbulence: Experimental Methods, in Handbuch der Physik, Vol. 8/2, Flugge, S. and Truesdell, C., eds., 523-590, Springer Verlag, Berlin (1963).

[7] Hinze, J.O., Turbulence, 2nd Ed., McGraw-Hill, New York (1975).

[8] Bradshaw, P., An Introduction to Turbulence and Its Measurement, Pergamon Press, Oxford (1971).

[9] Comte-Bellot, G., Hot-Wire Anemometry, Ann. Rev. Fluid Mech. 8, 209-231 (1976).

[10] Comte-Bellot, G., Hot-Wire and Hot-Film Anemometry, in Measurement of Unsteady Fluid Dynamic Phenomena, Richards, B.E., ed., 123-162, Hemisphere Publishing, Washington (1977).

[11] Fingerson, L.M. and Freymuth, P., Thermal Anemometers, in Fluid Mechanics Measurements, Goldstein, R.J., ed., 99-154, Hemisphere Publishing, Washington (1983).

[12] Perry, A.E., Hot-Wire Anemometry, Oxford University Press, New York (1982).

[13] King, L.V., On the Convection of Heat from Small Cylinders in a Stream of Fluid: Determination of the Convection Constants of Small Platinum Wires with Applications to Hot-Wire Anemometry, Trans. Royal Soc. 214A, 373-432 (1914).

[14] Andrews, G.E., Bradley, D. and Hundy, G.F., Hot Wire Anemometry Calibrations for Measurements of Small Gas Velocities, Int. J. Heat Mass Trans. 15, 1765-1786 (1972).

[15] Collis, D.C. and Williams, M.J., Two-Dimensional Convection from Heated Wires at Low Reynolds Numbers, J. Fluid Mech. 6, 357-384 (1959).

[16] Hilpert, R., Warmeabgabe von geheizten Drahten und Rohren im Luftstrom, Forsch. Gebiet. Ingen. 4, 215-224 (1933).

[17] Bradbury, L.J.S. and Castro, I.P., Some Comments on Heat-Transfer Laws for Fine Wires, J. Fluid Mech. 51, 487-495 (1972).

[18] Kennard, E.H., Kinetic Theory of Gases, McGraw-Hill, New York (1938).

[19] Collis, D.C., Forced Convection of Heat from Cylinders at Low Reynolds Numbers, J. Aero. Sciences 23, 697-698 (1956).

[20] Champagne, F.H. and Lundberg, J.L., Linearizer for Constant Temperature Hot Wire Anemometry, Rev. Sci. Ins. 37, 838-843 (1966).

[21] Lowell, H.H., Design and Applications of Hot-Wire Anemometers for Steady-State Measurements at Transonic and Supersonic Airspeeds, National Advisory Committee for Aeronautics Technical Note NACA-TN2117 (1950).

[22] Davies, P.O.A.L. and Fisher, M.J., Heat Transfer from Electrically Heated Cylinders, Proc. Royal Soc. 280A, 486-527 (1964).

[23] Betchov, R., L'influence de la conduction thermique sur les anemometres a fils chauds, Proc. Kom. Ned. Akad. Wetenscha. 51, 721-730 (1948). See also Betchov, R., Theorie non-lineaire de l'anemometre a fil chaud, Proc. Kom. Ned. Akad. Wetenscha. 52, 195-207 (1949), translated in Nonlinear Theory of a Hot-Wire Anemometer, National Advisory Committee for Aeronautics Technical Memorandum NACA-TM1346 (1952).

[24] Koch, F.A. and Gartshore, I.S., Temperature Effects on Hot Wire Anemometer Calibrations, J. Phys. E. Sci. Ins. 5, 58-61, (1972).

[25] Bruun, H.H., On the Temperature Dependence of Constant Temperature Hot-Wire Probes with Small Wire Aspect Ratio, J. Phys. E. Sci. Ins. 8, 942-951 (1975).

[26] Morrison, G.L., Errors in Heat Transfer Laws for Constant Temperature Hot Wire Anemometers, J. Phys. E. Sci. Ins. 9, 50-52 (1976).

[27] Corrsin, S., Extended Applications of the Hot-Wire Anemometer, National Advisory Committee for Aeronautics Technical Note NACA-TA1864 (1949).

[28] Conger, W.M., The Measurement of Concentration Fluctuations in the Mixing of Two Gases by Hot-Wire Anemometry Techniques, Ph.D. Thesis, University of Pennsylvania (1965).

[29] Baid, K.M., Measurement of Velocity in Gas Mixtures, M.S. Thesis, Illinois Institute of Technology (1967).

[30] Tombach, I.H., Velocity Measurements with a New Probe in Inhomogeneous Turbulent Jets, Ph.D. Thesis, California Institute of Technology (1969).

[31] Kassoy, D.R., Heat Transfer from Cylinders at Low Reynolds Numbers. I. Theory for Variable Property Flow, Phys. Fluids 10, 938-946 (1967).

[32] Aihara, Y., Kassoy, D.R. and Libby, P.A., Heat Transfer from Cylinders at Low Reynolds Numbers. II. Experimental Results and Comparison with Theory, Phys. Fluids 10, 947-952 (1967).

[33] Baccaglini, G., Kassoy, D.R. and Libby, P.A., Heat Transfer to Cylinders in Nitrogen-Helium and Nitrogen-Neon Mixtures, Phys. Fluids 12, 1378-1381 (1969).

[34] Wu, P. and Libby, P.A., Heat Transfer to Cylinders in Helium and Helium-Air Mixtures, Int. J. Heat Mass Trans. 14, 1071-1077 (1971).

[35] Kramers, H., Heat Transfer from Spheres to Flowing Media, Physica 12, 61-80 (1946).

[36] Wasan, D.T., Davis, R.M. and Wilke, C.R., Measurement of the Velocity of Gases with Variable Fluid Properties, AIChE J. 14, 227-234 (1968).

[37] Van der Hegge Zijnen, B.G., Modified Correlation Formulae for the Heat Transfer by Natural and by Forced Convection from Horizontal Cylinders, Appl. Sci. Res. 6A, 129-140 (1956).

[38] Wasan, D.T. and Baid, K.M., Measurement of Velocity in Gas Mixtures: Hot-Wire and Hot-Film Anemometry, AIChE J. 17, 729-731 (1971).

[39] McQuaid, J. and Wright, W., The Response of a Hot-Wire Anemometer in Flows of Gas Mixtures, Int. J. Heat Mass Trans. 16, 819-828 (1973).

[40] Simpson, R.L. and Wyatt, W.G., The Behavior of Hot-Film Anemometers in Gas Mixtures, J. Phys. E. Sci. Ins. 6, 981-987 (1973).

[41] Khalifa, H.E., Kestin, J. and Wakeham, W.A., The Theory of the Transient Hot-Wire Cell for Measuring the Thermal Conductivity of Gaseous Mixtures, Physica 97a, 273-286 (1979).

[42] Fingerson, L.M. and Ahmed, A.M., Operation and Application of Cooled Film Sensors for Measurements in High-Temperature Gases, in Measurements in Heat Transfer, Eckert, E.R. and Goldstein, R.J., eds., 579-596, McGraw-Hill, New York, 579-596 (1976).

[43] Brown, G.L. and Rebollo, M.R., A Small, Fast-Response Probe to Measure Composition of a Binary Gas Mixture, AIAA J. 10, 649-652 (1972).

[44] Tombach, I.H., An Evaluation of the Heat Pulse Anemometer for Velocity Measurement in Inhomogeneous Turbulent Flow, Rev. Sci. Ins. 44, 141-148 (1973).

[45] Touloukian, Y.S., Liley, P.E. and Saxena, S.C., Thermophysical Properties of Matter, The TPRC Data Series, Vol. 3, Thermal Conductivity--Nonmetallic Liquids and Gases, IFI/Plenum, New York (1970).

[46] Touloukian, Y.S., Saxena, S.C. and Hestermans, P., The Thermophysical Properties of Matter, The TPRC Data Series, Vol. 11, Viscosity, IFI/Plenum, New York (1975).

[47] Touloukian, Y.S. and Makitas, T., Thermophyiscal Properties of Matter, The TPRC Data Series, Vol. 6, Specific Heat--Nonmetallic Liquids and Gases, IFI/Plenum, New York (1970).

[48] Ehya, H., Faubert, F.M. and Springer, G.S., Thermal-Conductivity Measurements of Propane and N-Butane in the Range 300 to 1000 Deg K, J. Heat Trans. 94C., 262-265 (1972).

[49] Thermophysical Properties of Refrigerants, American Society of Heating, Refrigeration, and Air Conditioning Engineers, New York (1976).

[50] Hellemans, J.M., Kestin, J. and Ro, S.T., The Viscosity of $CH_4$, $CF_4$ and $SF_6$ Over a Range of Temperatures, Physica 65, 376-380 (1973).

[51] Bakulin, S.S. and Ulybin, S.A., Thermal Conductivity of Sulfur Hexafluoride at Temperatures of 230-350°K and Pressures Up to 50 MPa, High Temper. 16, 46-52 (1978), Translation of Tep. Vys. Temper. 16, 59-66 (1978).

[52] Adler, L.S. and Yaws, C.L., Physical and Thermodynamic Properties of Sulfur Hexafluoride, Sol. State Tech. 18(1), 35-38 (1975).

[53] Touloukian, Y.S., Powell, R.W., Ho, C.Y. and Klemens, P.G., Thermophysical Properties of Matter, The TPRC Data Series, Vol. 1, Thermal Conductivity--Metallic Elements and Alloys, IFI/Plenum, New York (1970).

[54] Touloukian, Y.S., Powell, R.W., Ho, C.Y. and Klemens, P.G., Thermophysical Properties of Matter, The TPRC Data Series, Vol. 2, Thermal Conductivity--Nonmetallic Solids, IFI/Plenum, New York (1970).

[55] Geller, V.Z., Gorykin, S.F., Zaporozhan, G.V. and Voitenko, A.K., Study of Thermal Conductivity of Freon-13B1 and Freon-23 Over a Wide Range of State Parameters (in Russian), J. Eng. Phys. 24, 581-588 (1975).

[56] Kreith, F., Principles of Heat Transfer, 3rd Ed., Harper & Row, New York (1973).

[57] Kays, W.M. and Crawford, M.E., Convective Heat and Mass Transfer, 2nd Ed., McGraw-Hill, New York (1980).

[58] Devienne, F.M., Accommodation Coefficients and the Solid-Gas Interface, in The Solid-Gas Interface, Vol. 2, Flood, E.A., Ed., 815-828, Marcel-Dekker, New York (1967).

[59] International Critical Tables of Numerical Data--Physics, Chemistry and Technology, Vol. 5, McGraw-Hill, New York (1929).

[60] Kannuluik, W.G. and Carman, E.H., The Temperature Dependence of the Thermal Conductivity of Air, Aust. J. Sci. Res. 4, 305-314 (1951).

[61] Goldstein, S. (Ed.), Modern Developments in Fluid Dynamics, Vol. I, Oxford, London (1938).

[62] Whitaker, S., Fundamental Principles of Heat Transfer, Pergamon Press, New York (1977).

[63] Whitaker, S., Introduction to Fluid Mechanics, Prentice-Hall, Englewood Cliffs (1968).

[64] Schlichting, H., Boundary Layer Theory, 4th Ed., Translated by Kestin, J., McGraw-Hill, New York (1960).

[65] Thomas, L.B., Thermal Accommodation of Gases on Solids, in Fundamentals of Gas-Surface Interactions, Saltsburg, H., Smith, J.N., and Rogers, M., Eds., 346-369, Academic Press (1967).

[66] Flood, E.A. and Hobson, J.P., Simple Kinetic Theory and Accommodation, Reflection and Adsorption of Molecules, in The Solid-Gas Interface, Vol. 2, Flood, E.A., Ed., 829-846, Marcel-Dekker, New York (1967).

## NOMENCLATURE

| | |
|---|---|
| $a$ | exponent of temperature loading factor or temperature dependence of transport property in Nusselt expression, see eq. (4) |
| $A$ | intercept in linear Nu vs. Re expression, see eq. (3) |
| $A_s$ | cross sectional area of sensor |
| $B$ | slope in linear Nu vs. Re expression, see eq. (3) |
| $\bar{c}$ | molecular speed, see eq. (33) |
| $C$ | parameter used in eq. (46) |
| $C_D$ | drag coefficient for flow around a cylinder |
| $C_i$ | i - 1,2 symbolic constants (replaced by more specific A and B), see eq. (2) |
| $C_p$ | specific heat at constant pressure |
| $C_v$ | specific heat at constant volume |
| $C_o$ | coefficient in heat loss equation, see eq. (19) |
| $D$ | sensor diameter |
| $D_o$ | coefficient in heat loss equation, see eq. (19) |
| $E$ | voltage drop across wheatstone bridge of anemometer system |
| $g$ | acceleration due to gravity |
| $Gr$ | Grashof number, defined as $\frac{g(T_s - T_\infty)}{\nu^2 T_\infty} D^3$ |
| $h$ | convective heat transfer coefficient |
| $I$ | current through probe leg of anemometer circuit |
| $k$ | thermal conductivity |
| $K_A$ | see eq. (41) |
| $K_B$ | see eq. (42) |
| $K_\nu$ | see eq. (43) |
| $K_k$ | see eq. (44) |
| $Kn$ | Knudsen number, defined as $\lambda/D$ |

| | |
|---|---|
| $\ell$ | active length of wire or film |
| $\ell_c$ | cold length parameter used in calculating end loss, equal to $1/\sqrt{C_o}$ |
| M | molecular weight of gas |
| n | exponent of Reynolds number in expression for Nusselt number |
| n' | exponent for use in eq. (46) |
| $n_o$ | optimized value of n which gives a minimum $\chi^2$ |
| Nu | Nusselt number, defined as $\frac{hD}{k}$ |
| $\Delta P$ | pressure drop used for velocity measurement, see eq. (31) |
| P | electrical power dissipation |
| Pe | Peclet number equal to Re x Pr |
| Pr | Prandtl number, defined as $C_p\mu/k$ |
| Q | heat |
| R | gas constant |
| $R_o$ | resistance of standard resistance placed in series with the sensor |
| $R_s$ | electrical resistance of sensor |
| $R_s'$ | total electrical resistance of sensor log |
| Re | Reynolds number, defined as $\frac{\rho VD}{\mu}$ |
| t | thickness |
| T | temperature |
| U | gas velocity |
| x | axial distance along probe from center and exponent of temperature dependence of viscosity, see eq. (12) |
| y | exponent of temperature dependence of thermal conductivity, see eq. (12) |
| $\alpha$ | accommodation coefficient, see eq. (7) |
| $\alpha_\rho$ | thermal coefficient of probe electrical resistance |
| $\beta$ | slip parameter, see eq. (10) |

| | |
|---|---|
| $\beta'$ | parameter associated with thermal slip, see eq. (27) |
| $\gamma$ | $C_p/C_v$ |
| $\Delta$ | temperature jump distance, see eq. (8) |
| $\varepsilon$ | total thermal energy of molecule, see eq. (7) |
| $\theta$ | temperature difference, $T - T_\infty$ |
| $\theta_o$ | overheat for sensor with infinite $\ell/D$, see eq. (22) |
| $\theta'$ | temperature jump, $\Delta/\lambda$ |
| $\lambda$ | mean free path of gas molecule |
| $\mu$ | dynamic viscosity |
| $\nu$ | kinematic viscosity |
| $\rho$ | density |
| $\rho_r(\theta)$ | probe resistance as a function of $\theta$ |
| $\phi$ | rarefied effects parameter, see eqs. (11) and (12) |
| $\chi^2$ | goodness of fit parameter for linear least square fits of results to eq. (3) or eq. (29) |
| $\psi$ | hot-wire response parameter defined as in eq. (28) |

Subscripts

| | |
|---|---|
| a | corrected for sensor finite aspect ratio (if necessary), "classical" rarefied gas effects, and accommodation effects |
| Al | aluminum |
| c | conductive heat transfer, see eq. (14), or Nu corrected for sensor finite aspect ratio and "classical" rarefied gas effects |
| com | computed |
| h | convective heat transfer |
| i | incident on surface, see eq. (7) |
| j | joulean resistive heating |
| m | measured (uncorrected); such as $Nu_m$ |
| m | property determined at mean of sensor, s, and ambient temperatures, $\infty$; such as $T_m$, $\nu_n$, etc. |

| | |
|---|---|
| pt | platinum |
| qt | quartz |
| r | reflected from surface, see eq. (7) |
| s | sensor |
| x | gas under investigation |
| $\infty$ | ambient, such as $T_\infty$ |
| | or corrected for end conduction loss, as in $Nu_\infty$, i.e. $\frac{\ell}{D} \to \infty$ |
| 1 | gas 1 |
| 2 | gas 2 |

Table 1. Values found by Collis and Williams [15] for use in eq. (4)

| | $0.02 < Re < 44$ | $44 < Re < 140$ |
|---|---|---|
| n | 0.45 | 0.51 |
| A | 0.24 | 0 |
| B | 0.56 | 0.48 |
| a | - 0.17 | - 0.17 |

Table 2. Suppliers and purities of gases used in this work

| Gas | Supplier | Purity |
|---|---|---|
| Air | Air Products | Dry |
| $N_2$ | In house | > 99.5% |
| He | Air Products | > 99.995% |
| $CH_4$ | Matheson | > 98% |
| Ar | Air Products | > 99.998% |
| $CO_2$ | Roberts Oxygen | > 99.9% |
| $C_3H_8$ | Matheson | > 99% |
| $CF_4$ | Dupont | > 99.7% |
| $SF_6$ | Matheson | > 99.8% |
| $CF_3Br$ | Dupont | > 99.7% |

Table 3. Sources for the properties of gases used in this investigation

| Gas | k | μ | $C_p$ |
|---|---|---|---|
| Air | [45] | [46] | [47] |
| $N_2$ | [45] | [46] | [47] |
| He | [45] | [46] | [47] |
| $CH_4$ | [45] | [46] | [47] |
| Ar | [45] | [46] | [47] |
| $CO_2$ | [45] | [46] | [47] |
| $C_3H_8$ | [48] | [46] | [47] |
| $CF_4$ | [49] | [50] | [49] |
| $CF_3Br$ | [49] | [49] | [49] |
| $SF_6$ | [51] | [50] | [52] |

Table 4. Hot-wire and film properties used for calculations

| | D(cm) | ℓ(cm) | $R_s(\Omega)$ | $T_s(K)$ | $T_m(K)$ | $\alpha_\rho$ $(K^{-1})$ | $k_s(cal/s \cdot cm^2 \cdot k)$ |
|---|---|---|---|---|---|---|---|
| Wire | 0.0004 | 0.125 | 12.02 | 569 | 431 | 0.00303 | 0.33 |
| Film | 0.0051 | 0.10 | 9.60 | 650 | 472 | 0.00232 | 0.0075 |

Table 5. Values of $n_o$ resulting from fits of $E^2 = A' + B'U^n$ are listed for the hot-wire measurements made with different gases. Values of A' and B' are reported for n = 0.43. Also included are selected slopes and intercepts resulting from least square fit of $Nu_m$ and $Nu_a$ to eq. (3) with n = 0.43. These sets of data correspond to those seen in the various figures. The Re ranges over which the various measurements were made are also listed.

| Gas | $n_o$ | A' | B' | Re Range | $A_m$ | $B_m$ | $A_\infty$ | $B_\infty$ |
|---|---|---|---|---|---|---|---|---|
| Air | 0.43 | 3.749 | 0.355 | 0.09-1.4 | | | | |
| | 0.42 | 3.716 | 0.340 | 0.12-1.3 | 0.427 | 0.664 | 0.258 | 0.617 |
| | 0.43 | 3.716 | 0.336 | 0.16-1.2 | | | | |
| | 0.45 | 3.768 | 0.339 | 0.23-1.2 | | | | |
| | 0.43 | 3.742 | 0.339 | 0.18-1.2 | | | | |
| | 0.43 | 3.723 | 0.339 | 0.19-1.2 | | | | |
| $CH_4$ | 0.44 | 5.667 | 0.494 | 0.21-1.1 | 0.423 | 0.663 | 0.301 | 0.624 |
| | 0.43 | 5.667 | 0.488 | 0.17-1.1 | | | | |
| | 0.43 | 5.651 | 0.497 | 0.19-1.1 | | | | |
| Ar | 0.41 | 2.852 | 0.240 | 0.12-1.4 | 0.487 | 0.671 | 0.250 | 0.622 |
| | 0.42 | 2.865 | 0.241 | 0.12-1.4 | | | | |
| $C_3H_8$ | 0.44 | 4.058 | 0.658 | 1.28-1.8 | | | | |
| | 0.43 | 4.051 | 0.658 | 1.27-1.8 | 0.492 | 0.825 | 0.292 | 0.743 |
| | 0.43 | 4.051 | 0.655 | 1.27-1.8 | | | | |
| $CO_2$ | 0.42 | 3.180 | 0.370 | 0.21-2.4 | 0.478 | 0.741 | 0.263 | 0.691 |
| | 0.43 | 3.167 | 0.368 | 0.23-2.2 | | | | |
| | 0.43 | 3.206 | 0.369 | 0.24-2.2 | | | | |
| | 0.44 | 3.184 | 0.366 | 0.27-2.2 | | | | |
| | 0.44 | 3.200 | 0.365 | 0.26-2.2 | | | | |
| He | 0.26 | 14.92 | 0.431 | 0.18-0.7 | 0.323 | 0.372 | 0.275 | 0.356 |
| | 0.29 | 15.06 | 0.423 | 0.10-0.8 | | | | |
| $SF_6$ | 0.42 | 2.575 | 0.517 | 1.3-5.5 | | | | |
| | 0.41 | 2.656 | 0.519 | 1.6-6.1 | 0.489 | 0.765 | 0.229 | 0.717 |
| $CF_3Br$ | 0.42 | 2.212 | 0.382 | 0.94-5.1 | | | | |
| | 0.42 | 2.192 | 0.380 | 1.3-6.2 | 0.538 | 0.744 | 0.213 | 0.719 |
| $CF_4$ | 0.42 | 2.987 | 0.431 | 0.50-4.0 | 0.470 | 0.711 | 0.246 | 0.665 |

Table 6. Values of $n_o$ are listed which result when the hot-wire data for the different gases are fit to eq. (3). Values of $A_c$, $B_c$, $A_a$ and $B_a$ are reported using $n = 0.45$ in eq. (3). The last two columns list the values of A and B which result when $A_a$ and $B_a$ are modified using the $(K_A)_x$ and $(K_B)_x$ values as defined by eqs. (41) and (42), respectively.

| Gas | $n_o$ | $A_c$ | $B_c$ | $n_o$ | $A_a$ | $B_a$ | $A_a-(K_A)_x$ | $B_a/(K_B)_x$ |
|---|---|---|---|---|---|---|---|---|
| Air | 0.44 | 0.272 | 0.650 | 0.44 | 0.272 | 0.650 | 0.272 | 0.650 |
| $CH_4$ | 0.46 | 0.318 | 0.635 | 0.47 | 0.312 | 0.679 | 0.282 | 0.640 |
| Ar | 0.44 | 0.261 | 0.660 | 0.44 | 0.261 | 0.660 | 0.274 | 0.644 |
| $C_3H_8$ | 0.45 | 0.322 | 0.725 | 0.45 | 0.322 | 0.725 | 0.274 | 0.651 |
| $CO_2$ | 0.44 | 0.282 | 0.698 | 0.44 | 0.282 | 0.698 | 0.272 | 0.643 |
| He | 0.35 | 0.289 | 0.410 | 0.45 | 0.281 | 0.630 | 0.284 | 0.646 |
| $SF_6$ | 0.43 | 0.264 | 0.695 | 0.43 | 0.264 | 0.695 | 0.256 | 0.640 |
| $CF_3Br$ | 0.43 | 0.252 | 0.690 | 0.43 | 0.252 | 0.690 | 0.244 | 0.654 |
| $CF_4$ | 0.44 | 0.270 | 0.659 | 0.44 | 0.270 | 0.659 | 0.269 | 0.636 |

Table 7. This table lists results for the hot-film calibration in flows of different gases. Values of $n_o$ for fits of the data to eq. (29) are listed along with the corresponding values of A' and B' found for n = 0.45. The Re range covered by each set of measurements is also included. The last four columns contain selected $A_m$, $B_m$, $A_c$ and $B_c$ values which result from fits of the data in terms of $\overline{Nu}_m$ and $\overline{Nu}_c$ to eq. (3) with n = 0.45.

| Gas | $n_o$ | A' | B' | Re Range | $A_m$ | $B_m$ | $A_c$ | $B_c$ |
|---|---|---|---|---|---|---|---|---|
| Air | 0.44 | 12.04 | 1.387 | 1.3-13.5 | | | | |
| | 0.45 | 11.82 | 1.398 | 1.6-13.4 | | | | |
| | 0.45 | 11.69 | 1.392 | 1.6-12.5 | 1.089 | 0.854 | 0.434 | 0.807 |
| $CH_4$ | 0.42 | 17.36 | 2.284 | 2.6-12.9 | | | | |
| | 0.44 | 17.15 | 2.251 | 2.1-11.2 | 0.963 | 0.892 | 0.529 | 0.847 |
| Ar | 0.45 | 9.91 | 0.981 | 1.4-14.8 | 1.362 | 0.860 | 0.416 | 0.814 |
| $C_3H_8$ | 0.37 | 14.99 | 2.833 | 7.0-42.8 | | | | |
| | 0.38 | 14.46 | 2.816 | 4.3-43.3 | 1.247 | 0.962 | 0.592 | 0.911 |
| | 0.39 | 14.50 | 2.859 | 4.0-42.8 | | | | |
| $CO_2$ | 0.41 | 11.00 | 1.547 | 1.5-25.0 | | | | |
| | 0.41 | 11.00 | 1.551 | 1.9-23.8 | 1.272 | 0.926 | 0.457 | 0.872 |
| He | 0.39 | 40.34 | 2.550 | 1.0-2.5 | 0.694 | 0.730 | 0.506 | 0.738 |
| $SF_6$ | 0.37 | 10.68 | 2.083 | 14.4-40.2 | | | | |
| | 0.35 | 10.15 | 2.086 | 7.9-38.4 | 1.447 | 0.899 | 0.448 | 0.843 |
| $CF_3Br$ | 0.38 | 8.91 | 1.568 | 8.2-34.0 | 1.734 | 0.935 | 0.414 | 0.875 |

Table 8. Values of C and n' reported by Hilpert [16] for use in eq. (46)

| | $1 < Re < 4$ | $4 < Re < 40$ | $40 < Re < 400$ |
|---|---|---|---|
| C | 0.891 | 0.821 | 0.615 |
| n' | 0.330 | 0.385 | 0.466 |

## FIGURE CAPTIONS

Figure 1. The response of the hot-wire to varying velocities of an air flow is plotted as E(volts) versus U(cm/s). The solid curve is that predicted based on a least squares curve fit of the experimental data to eq. (29). A value of n = 0.43 has been used.

Figure 2. Values of $\chi^2$ (defined by eq. (36)) are plotted as a function of the value of n used to fit the experimental results of fig. 1 to eq. (29).

Figure 3. Representative data are shown for the response of the hot-wire to flows of eight different gases. The experimental results are plotted as $E^2(\text{volts}^2)$ versus $U^{0.43}(\text{cm/s})^{0.43}$. Solid lines correspond to least squares curve fits of the data to eq. (29) with n = 0.43.

Figure 4. Representative values of measured Nusselt number ($Nu_m$) calculated using eq. (37) are plotted as a function of $Re^{0.43}$. Results for nine different gases are included. With the exception of the helium results, the data used to calculate $Nu_m$ are those shown in fig. 3.

Figure 5. The results shown in fig. 4 have been corrected for the finite aspect ratio of the hot-wire. The resulting Nusselt numbers ($Nu_\infty$) are plotted as function of $Re^{0.43}$.

Figure 6. The results shown in fig. 5 have been corrected for "classical" rarefied gas effects. The resulting Nusselt number ($Nu_c$) corresponds to that expected for an infinite hot-wire placed in a continuum gas. Accommodation effects are assumed to be negligible. Values of $Nu_c$ are plotted as a function of $Re^{0.45}$.

Figure 7. Representative data are shown for the response of a hot-film to flows of seven different gases. The experimental results are plotted as $E^2(volts^2)$ versus $U^{0.45}(cm/s)^{0.45}$. Solid lines correspond to linear least squares curve fits of the data to eq. (29) with n = 0.45. Note the curvature in the plots for $SF_6$, $CF_3Br$, and $C_3H_8$. The curvature indicates that 0.45 is not the best value for n for fitting data of these gases to eq. (3).

Figure 8. Representative values of measured Nusselt numbers ($Nu_m$) for the response of the hot-film in different gases are plotted as a function of $Re^{0.45}$. The values of $Nu_m$ correspond to the experimental data shown in fig. 7 plus a data set recorded for flows of helium gas.

Figure 9. Hot-film results are plotted as $Nu_m$ versus $Re^{0.45}$ for $C_3H_8$, $SF_6$, and $CF_3Br$. These results span the Re range (Re $\approx$ 44) where the onset of vortex shedding from the heated cylinder is known to commence. This flow transition results in the markedly different heat transfer behavior observed in the high and low Re regions.

Figure 10. Values of $Nu_m$ versus $Re^{0.45}$ are plotted for $C_3H_8$ ($\Delta$), $SF_6$ ($\square$), and $CF_3Br$ ($\diamond$) over the Re range where the onset of vortex shedding from cylinders is known to occur. The measurements show a clear hysteresis in the data depending on whether the gas flow velocity is increased to the measurement value (denoted by filled symbols) or decreased to the measurement value (denoted by open symbols). For reasons of clarity, $Nu_m$ values for $SF_6$ have been offset downward by 0.188 and those for $CF_3Br$ have been offset upward by 0.063.

Figure 11. Values of $Nu_c$ versus $Re^{0.45}$ are shown for the hot-film. The results given in fig. 8 have been corrected for finite aspect ratio and rarefied gas effects to give the data shown here.

Figure 12. The parameters $A_c$ ($\Delta$) and $B_c$ (0) which result from fits of the hot-wire data for nine different gases to eq. (3) are plotted on a log-log plot as a function of Pr. Note that the value of $B_c$ for helium is not included on the plot. This figure shows that there is no apparent dependence of these parameters on Pr.

Figure 13. The parameters $A_c$ ($\Delta$) and $B_c$ (0) found for the hot-wire measurements made in nine different gases are shown on a log-log plot as a function of $(\mu_m)_x$. Note that $B_c$ for helium has been omitted. This plot indicates a dependence of $A_c$ on $(\mu_m)_x$. The straight line is the result of a linear least squares curve fit of $\log(A_c)$ versus $\log(\mu_m)_x$. Results of this fit are used to give eq. (40). The filled symbols correspond to values of $A_a$ and $B_a$ calculated for helium and methane.

Figure 14. The parameters $A_c$ ($\Delta$) and $B_c$ (0) found for the hot-wire measurements made in nine different gases are shown on a log-log plot as a function of $(\nu_m/\nu_\infty)_x$. Note that $B_c$ for helium has been omitted. This plot indicates a dependence of $B_c$ on $(\nu_m/\nu_\infty)_x$. The straight line is the result of a linear least squares curve fit of $\log(B_c)$ versus $\log(\nu_m/\nu_\infty)_x$. Results of this fit are used to give eq. (39). The filled symbols correspond to values of $A_a$ and $B_a$ calculated for helium and methane.

Figure 15. The correlation of the experimental results which is obtained when the values of $Nu_c$ for the hot-wire in different gases are corrected for variations in $(\nu_m/\nu_\infty)$ and $\mu_m$ is shown. Values of $Nu_c-(K_A)_x$ are plotted as a function of $Re^{0.45}(K_B)_x$. $(K_A)_x$ and $(K_B)_x$ are given by eqs. (40) and (39), respectively. With the exception of the results for helium, an excellent correlation of the data is obtained.

Figure 16. This correlation of experimental results is the same as that given in fig. 15 with the exception that the helium and methane results have been corrected for accommodation effects. The correlation of results for measurements made in all nine gases is now found to be excellent.

Figure 17. Values of $Nu_c$ measured for the hot-wire are multiplied by $(K_\nu)_x$ (as given by eq. (43)) and plotted as a function of $Re^{0.45}$. The results for helium have not been corrected for accommodation effects.

Figure 18. Values of $Nu_c$ measured for the hot-wire are multiplied by $(K_k)_x$ (as given by eq. (44)) and plotted as a function of $Re^{0.45}$. The results for helium have not been corrected for accommodation effects.

Figure 19. Values for $Nu_c-(K_A)_x$ versus $Re^{0.45}(K_B)_x$ are plotted for the eight different gases investigated with the hot-film. Expressions for $(K_B)_x$ and $(K_A)_x$ are the same as those used for the hot-wire (i.e., eqs. (41) and (42)).

Figure 20. Correlations reported by Andrews et al. [14], Collis and Williams [15], and Fingerson and Ahmed [42] are employed to give the solid lines shown (A, C, and D; respectively) as Nu versus $Re^{0.45}$ for the hot-wire placed in a flow of air. $T_m$ is assumed to be 431 K and $T_\infty$ is assumed to be room temperature. The correlation which has been obtained in this work (eq. (45)) is also included in the plot (line B). The dashed line is the result which is found if the correlation of Andrews et al. [14] is modified to reflect more recent literature measurements of the thermal conductivity of air than that used in [14] (see the discussion in the text).

Figure 21. Correlations reported by Andrews et al. [14], Collis and Williams [15], and Fingerson and Ahmed [42] are employed to give the solid lines shown (A, C, and D; respectively) as Nu versus $Re^{0.45}$ for the hot-film placed in a flow of air. $T_m$ is assumed to be 472 K and $T_\infty$ is assumed to be room temperature. The correlation which has been obtained in this work for the hot film is also included on the plot (line B). The dashed line is the result which is found if the correlation of Andrews et al. [14] is modified to reflect more recent literature measurements of air conductivity than that used in [14] (see the discussion in the text).

FIGURE 1: Typical Hot-Wire Response
Air. Line: Eq. (29) n=0.43

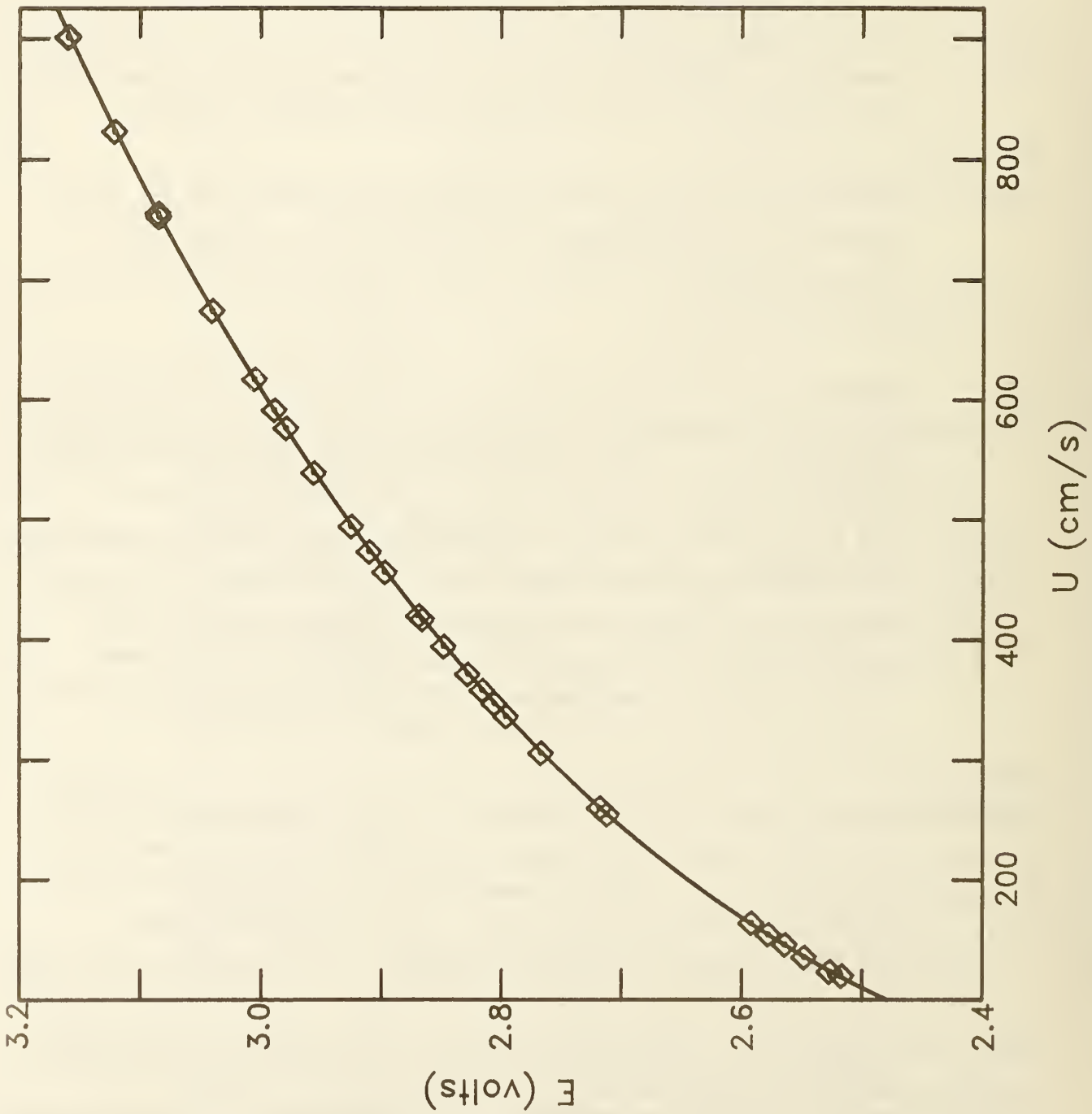

FIGURE 2: Sensitivity Analysis for n

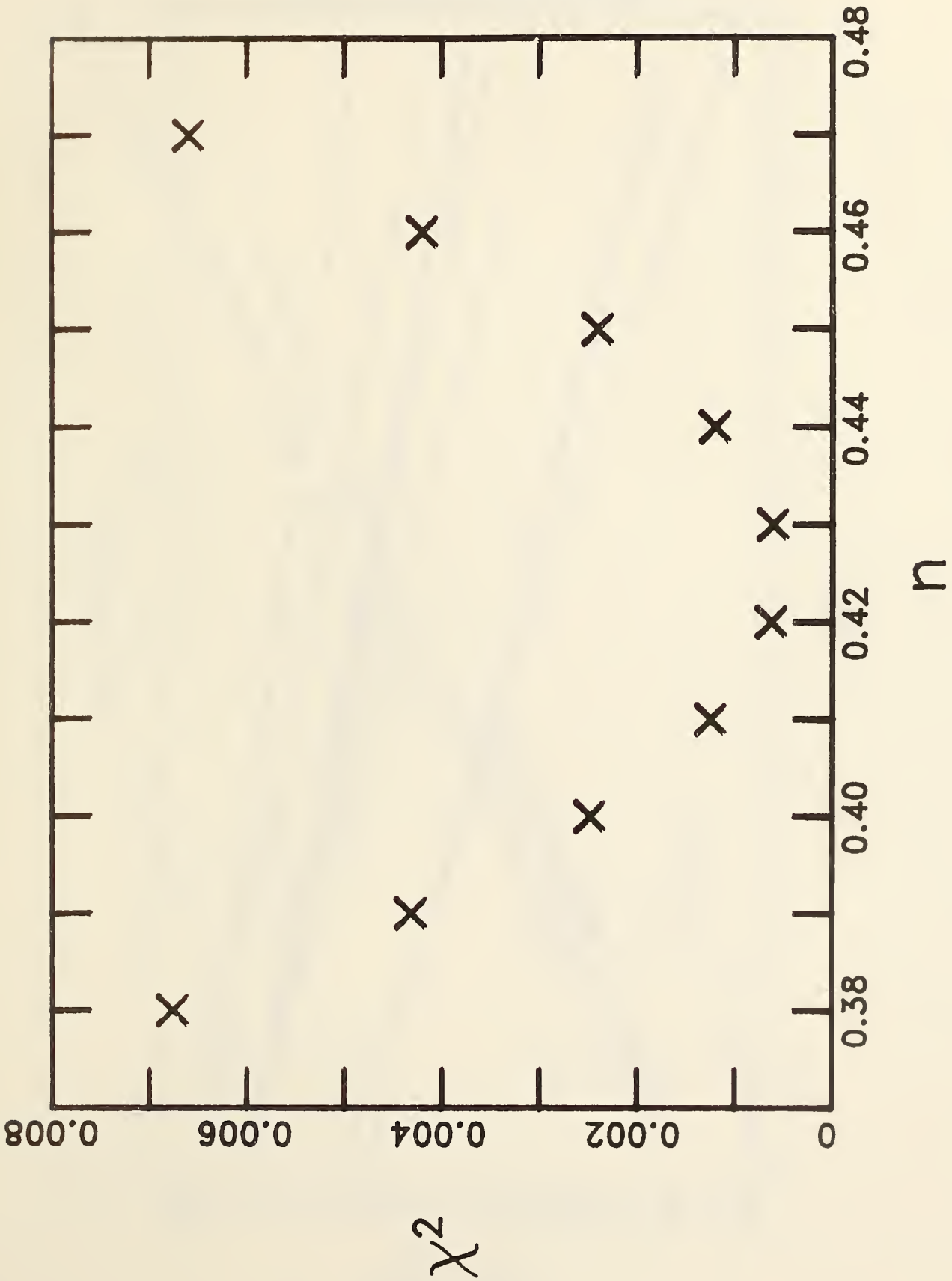

FIGURE 3: Hot-Wire Response for Eight Gases
Lines: Eq. (29)

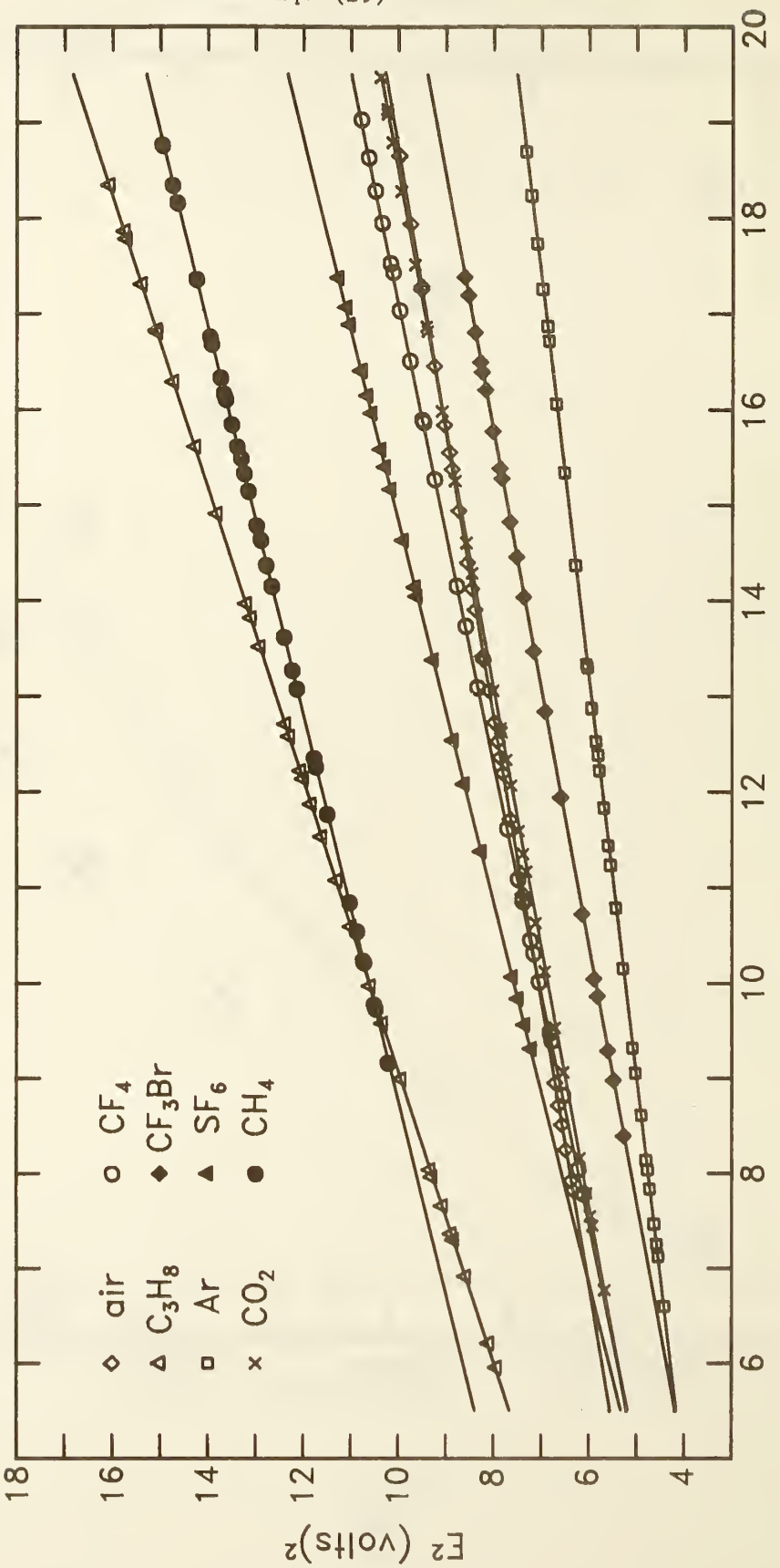

FIGURE 4: Measured Nusselt Number vs.
Reynolds Number to the 0.43 power

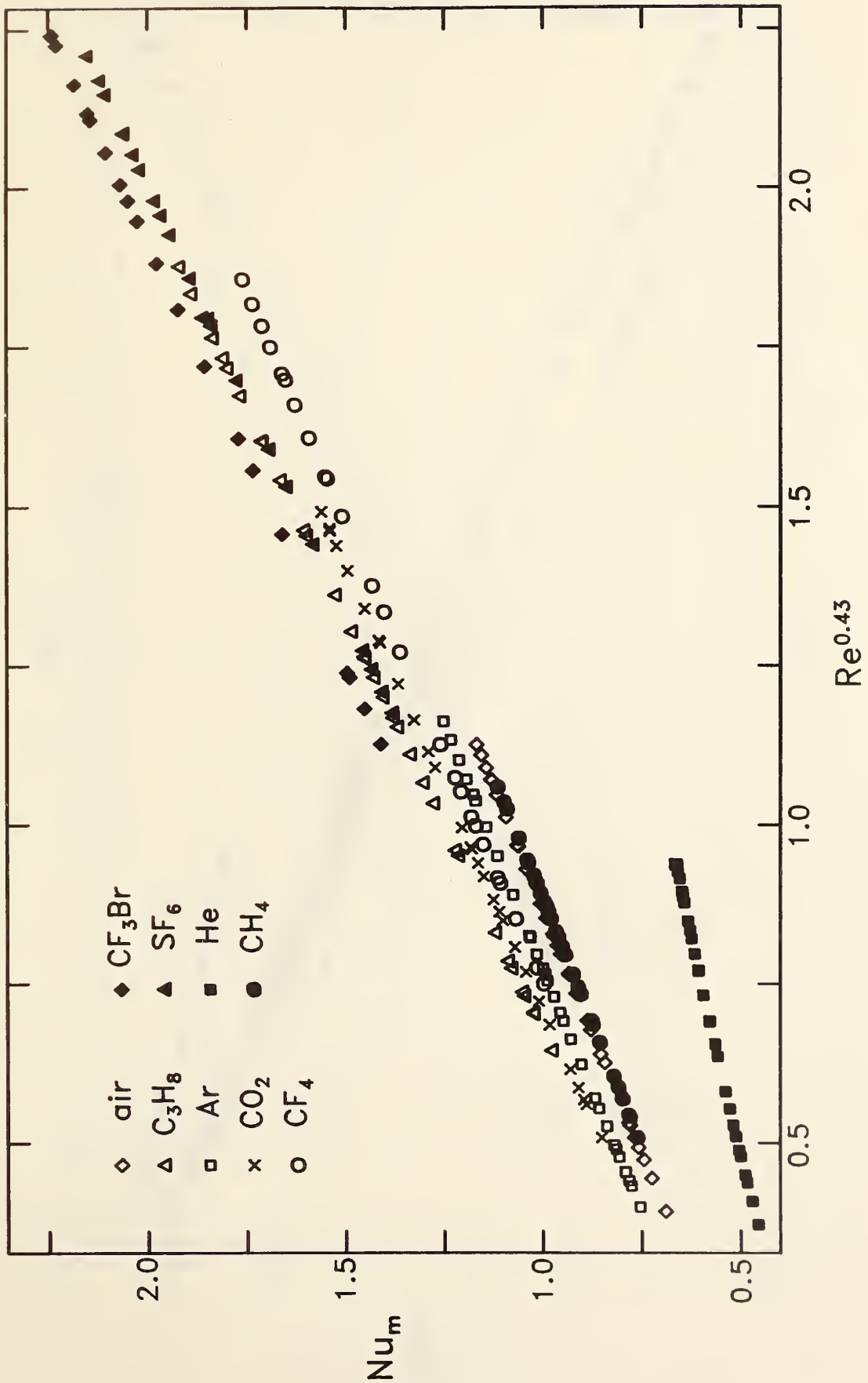

FIGURE 5: Nusselt Number Corrected for End Conduction Losses

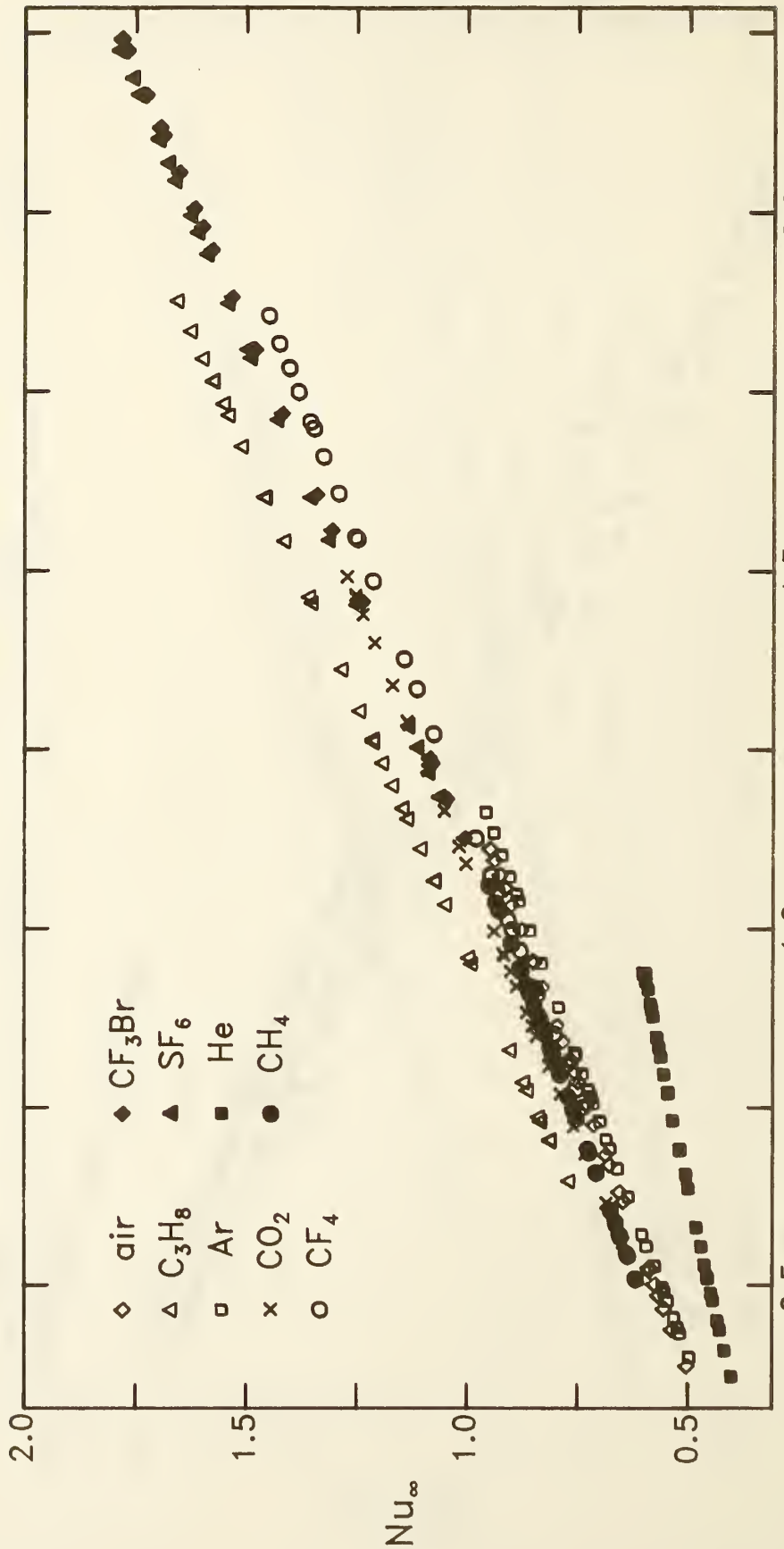

FIGURE 6: Nusselt Number Corrected for "Classical" Rarified Gas Effects and Finite Aspect Ratio

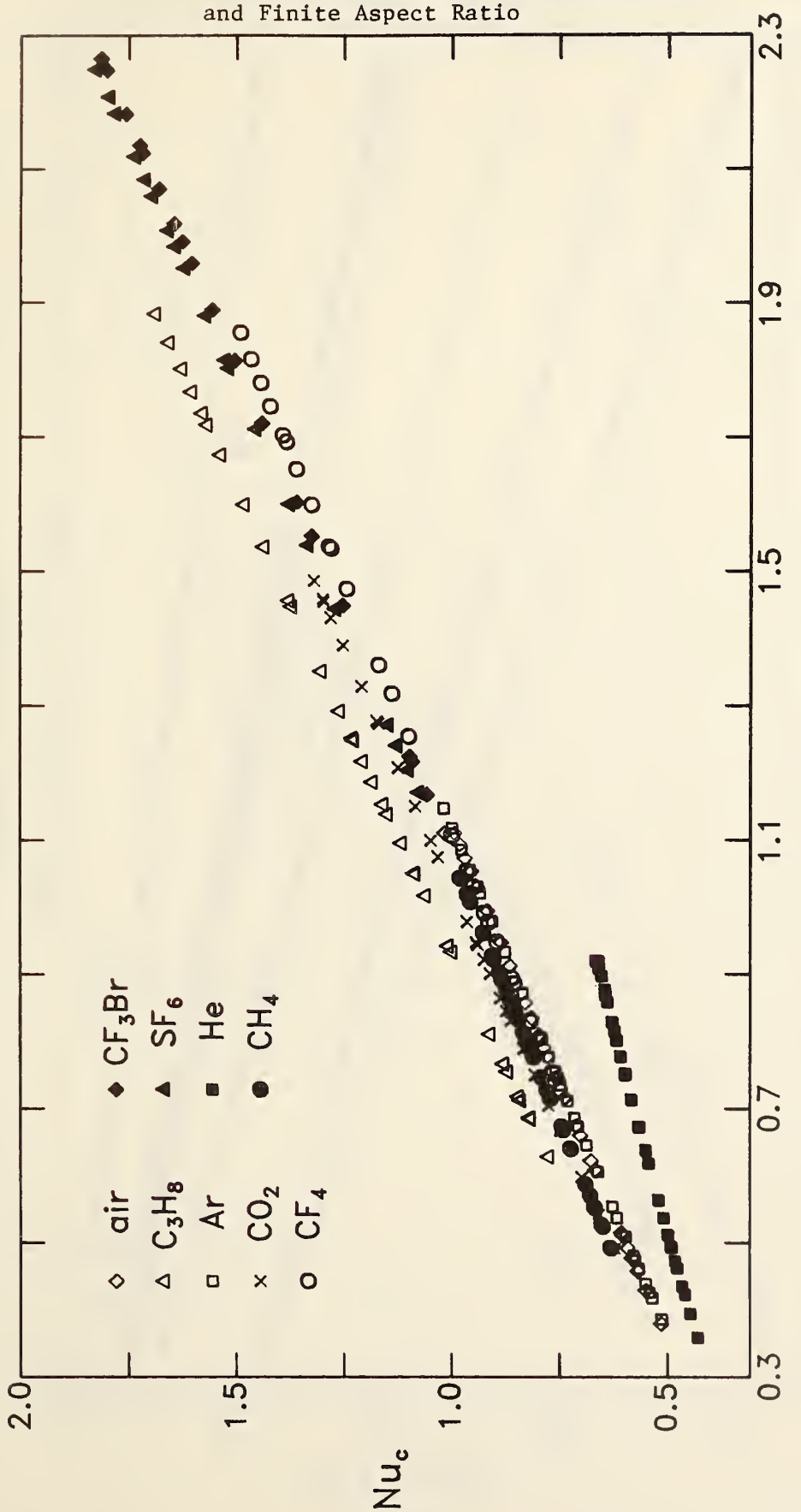

FIGURE 7: Typical Hot-Film Response.
Lines: Eq. (29) n=0.45

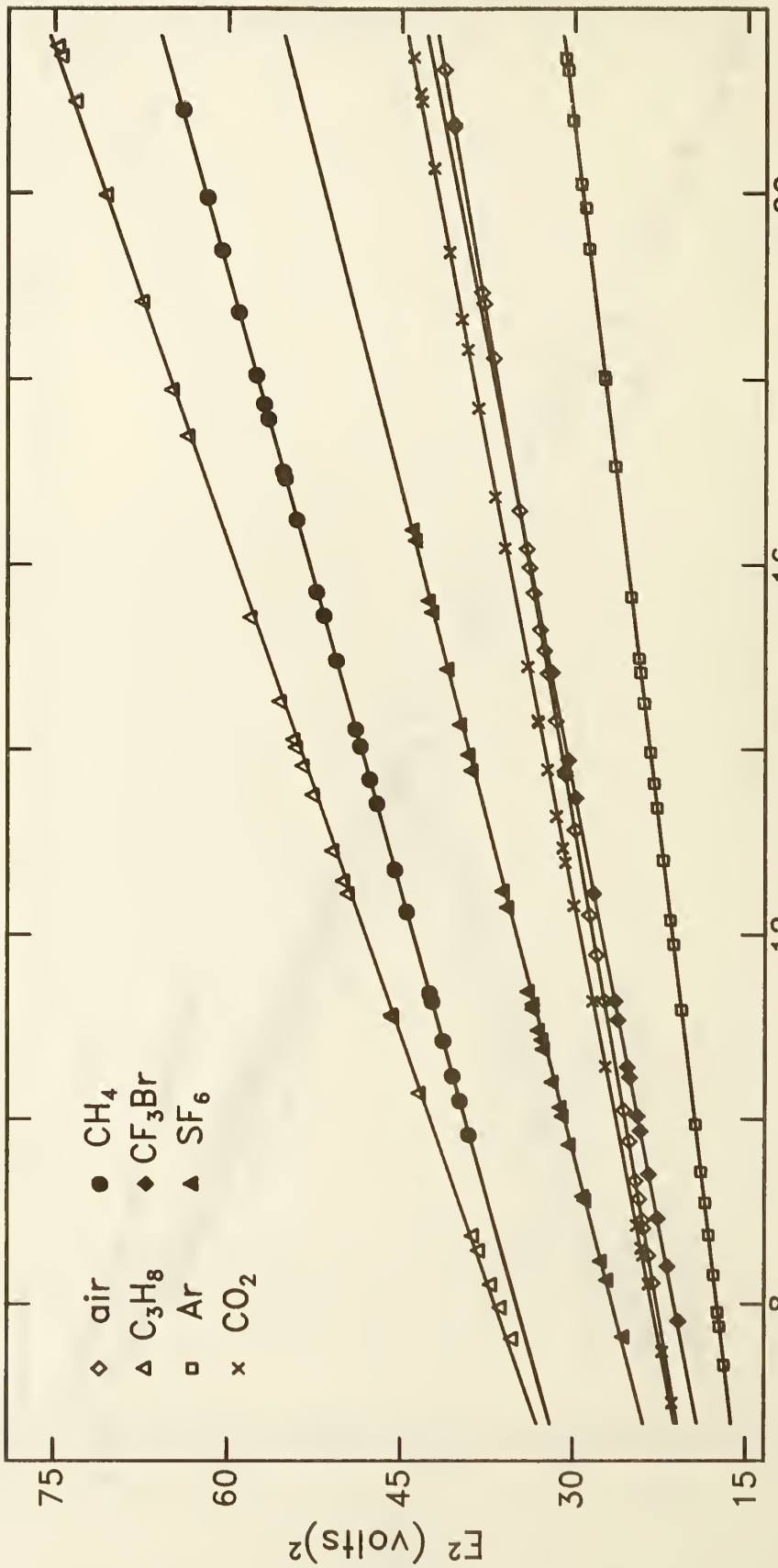

FIGURE 8: Measured Nusselt Number for Hot-Film

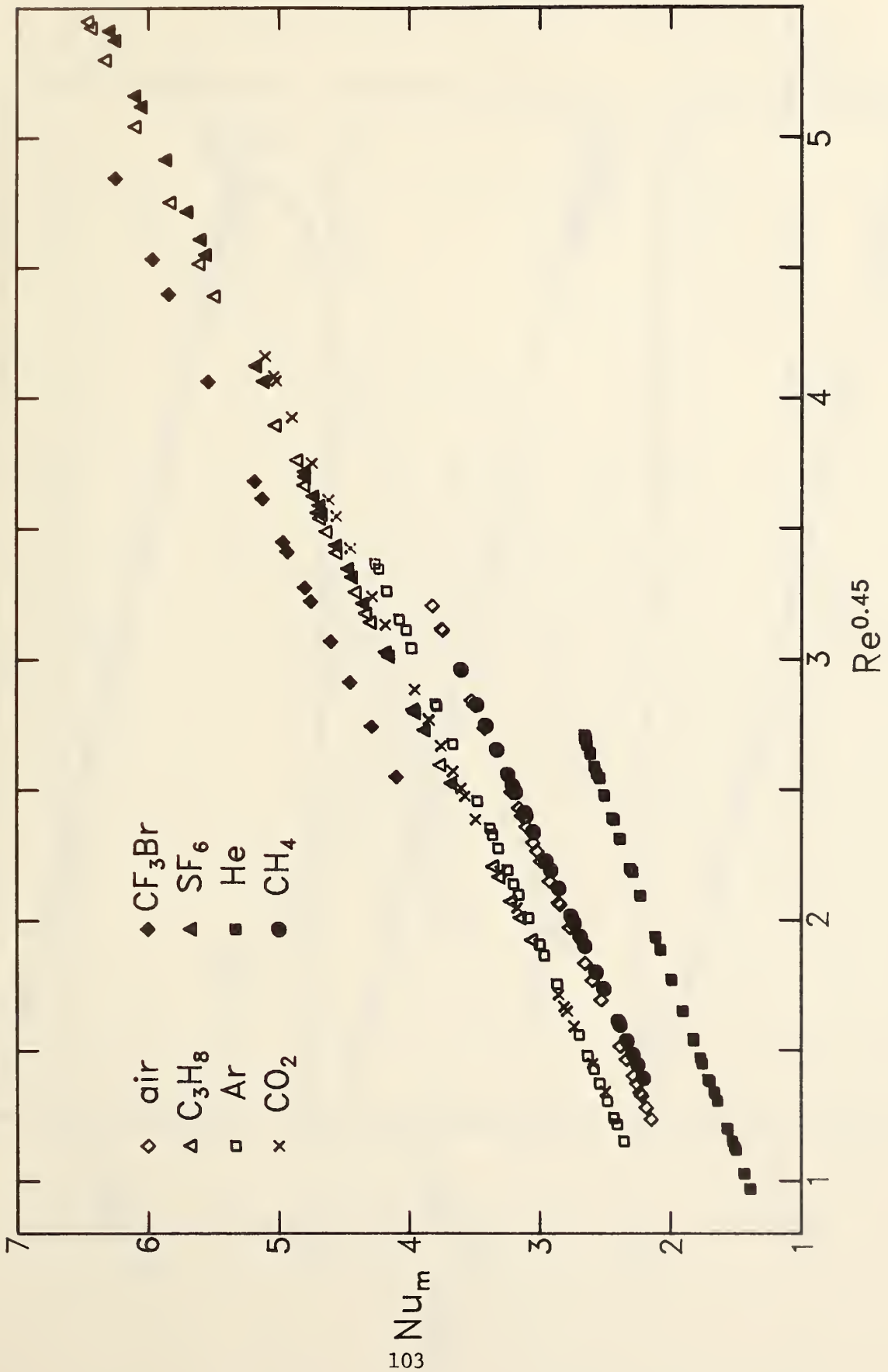

FIGURE 9: Response of Film at Onset of Vortex Shedding

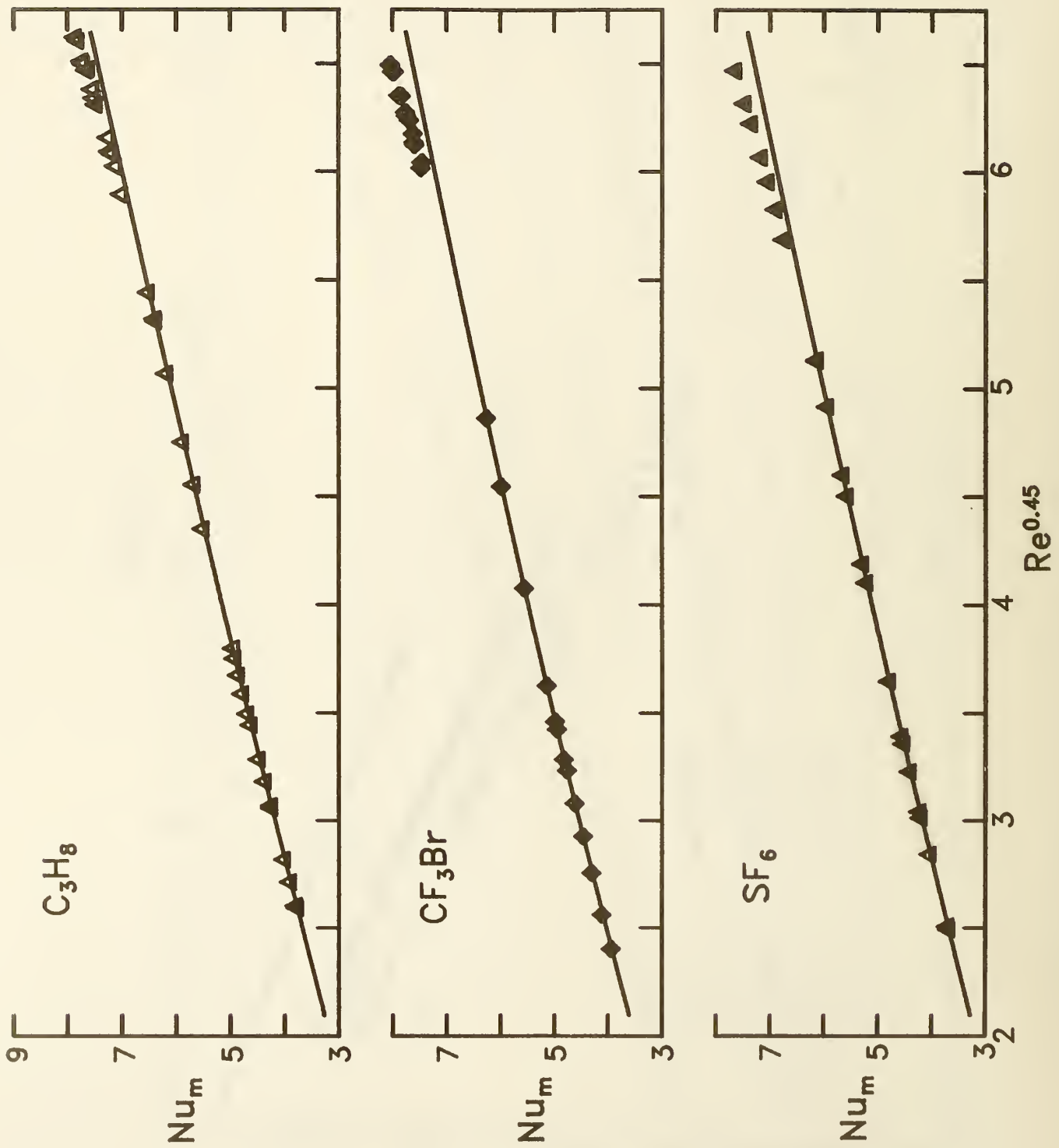

FIGURE 10: Hysteresis Near Flow Transition
(Re ~ 44)

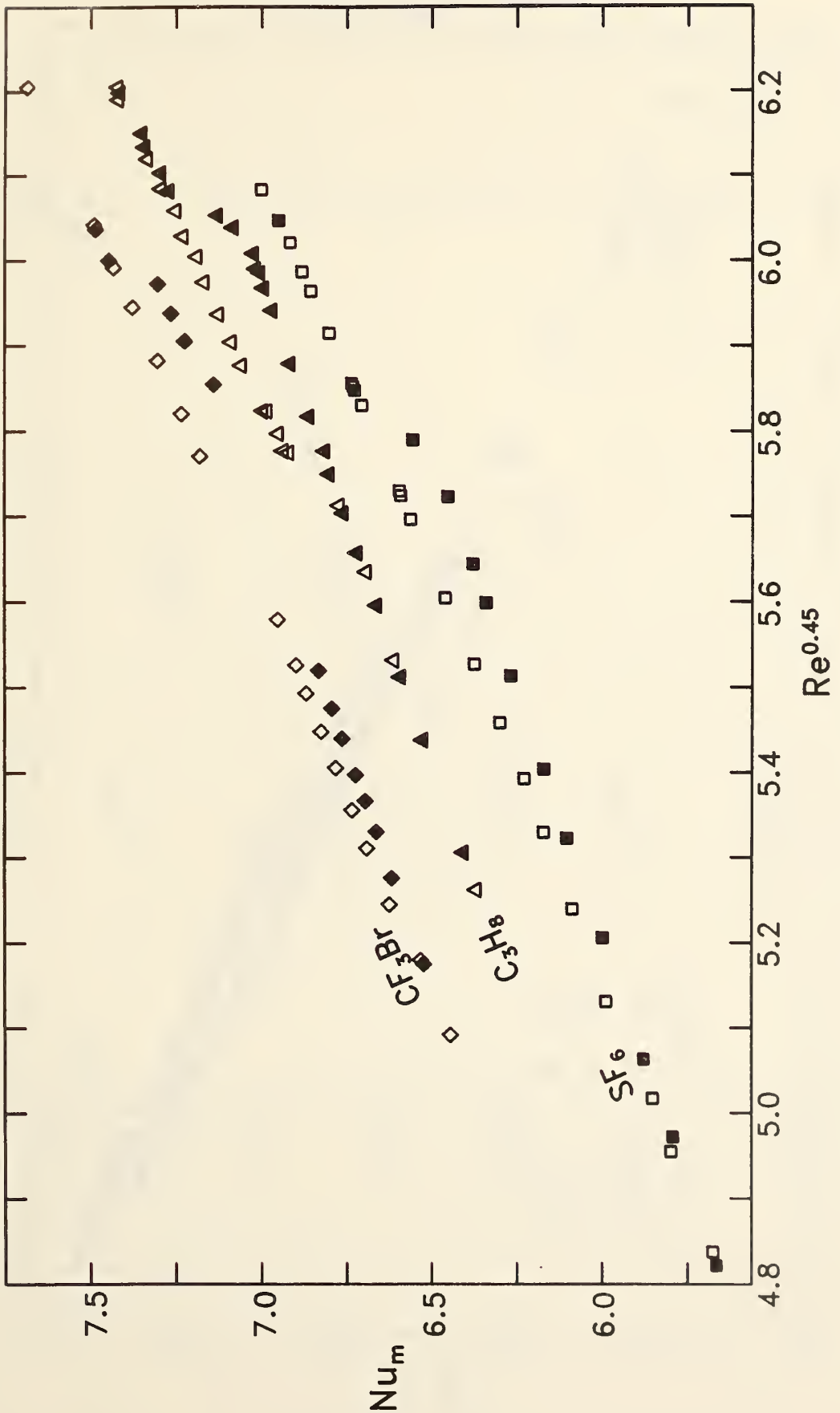

FIGURE 11: Corrected Nusselt Number for Hot Film

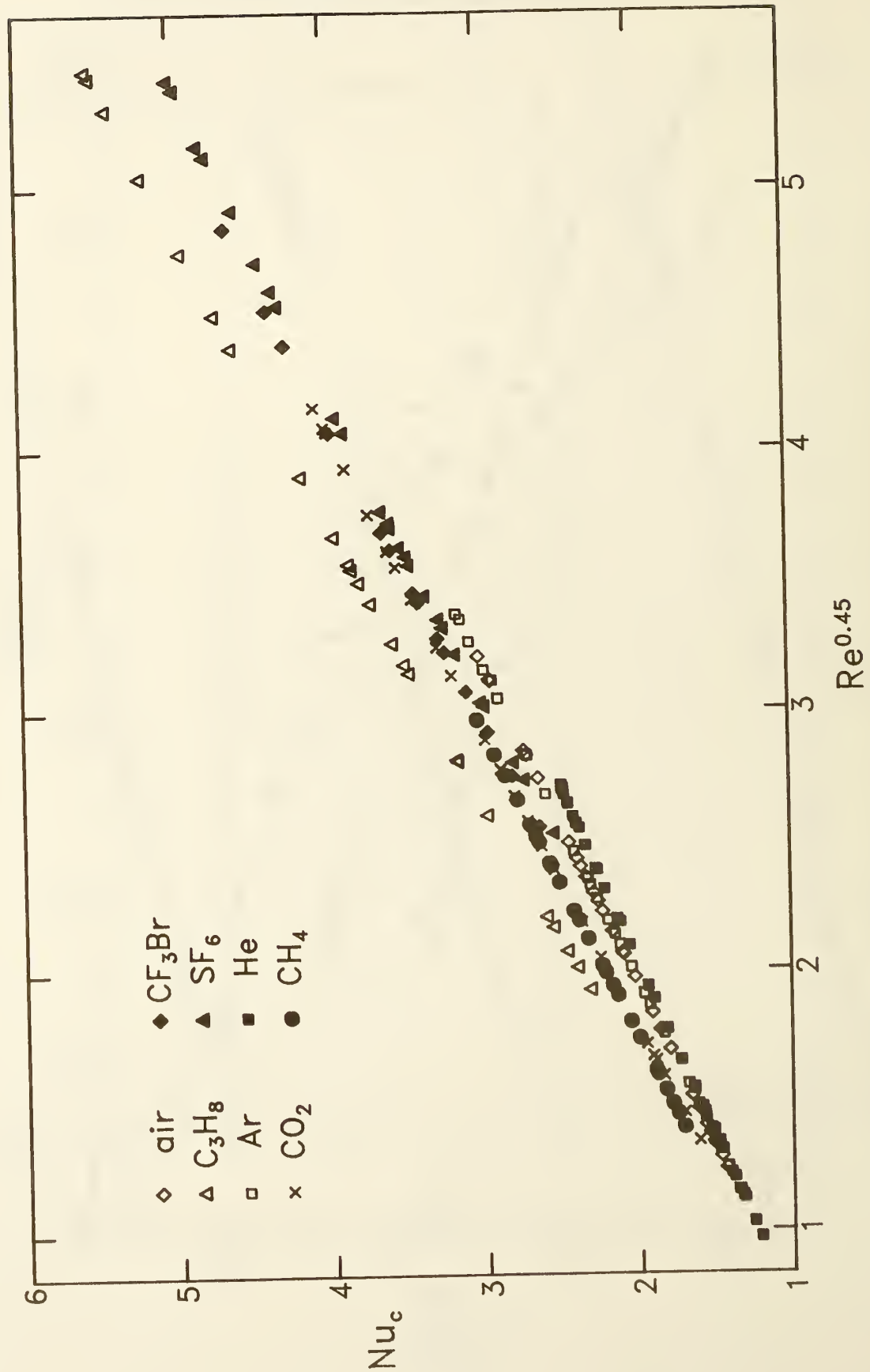

FIGURE 12: Failure of Correlation with
Prandtl Number

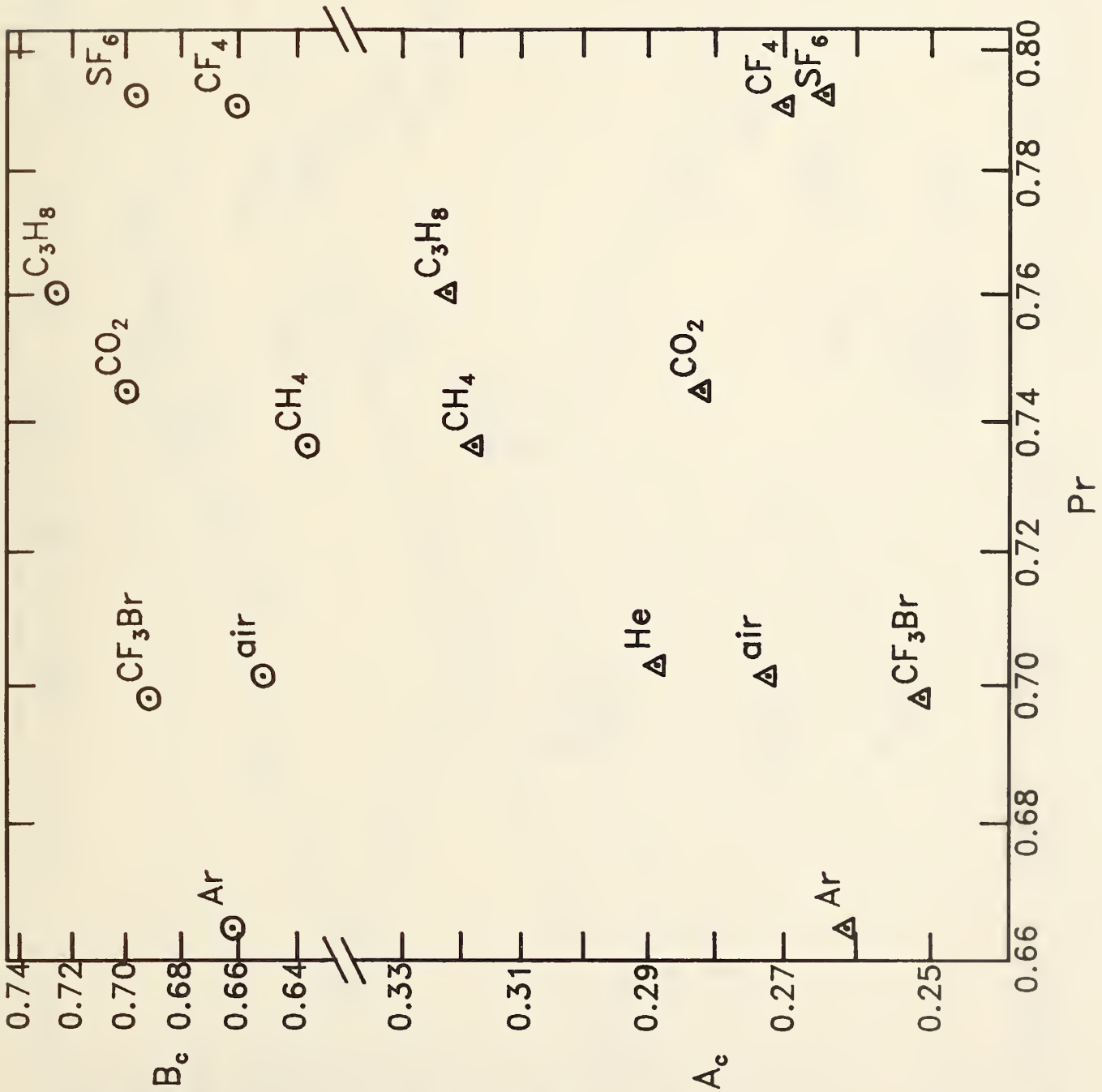

FIGURE 13: Correlation of Intercept with Viscosity (Hot-Wire)

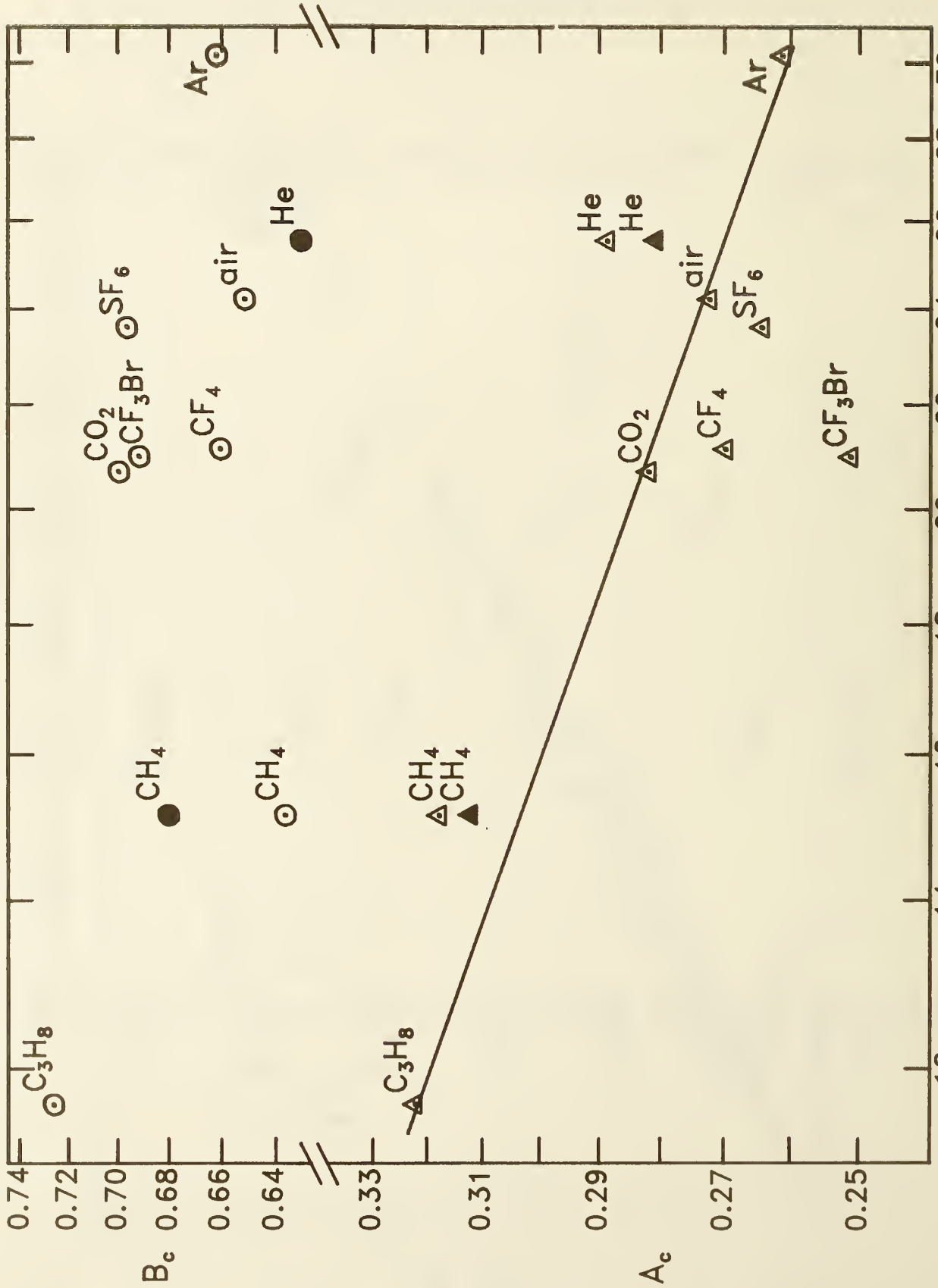

FIGURE 14: Correlation of Slope with Ratio
of Kinematic Viscosities.
(Hot-Wire)

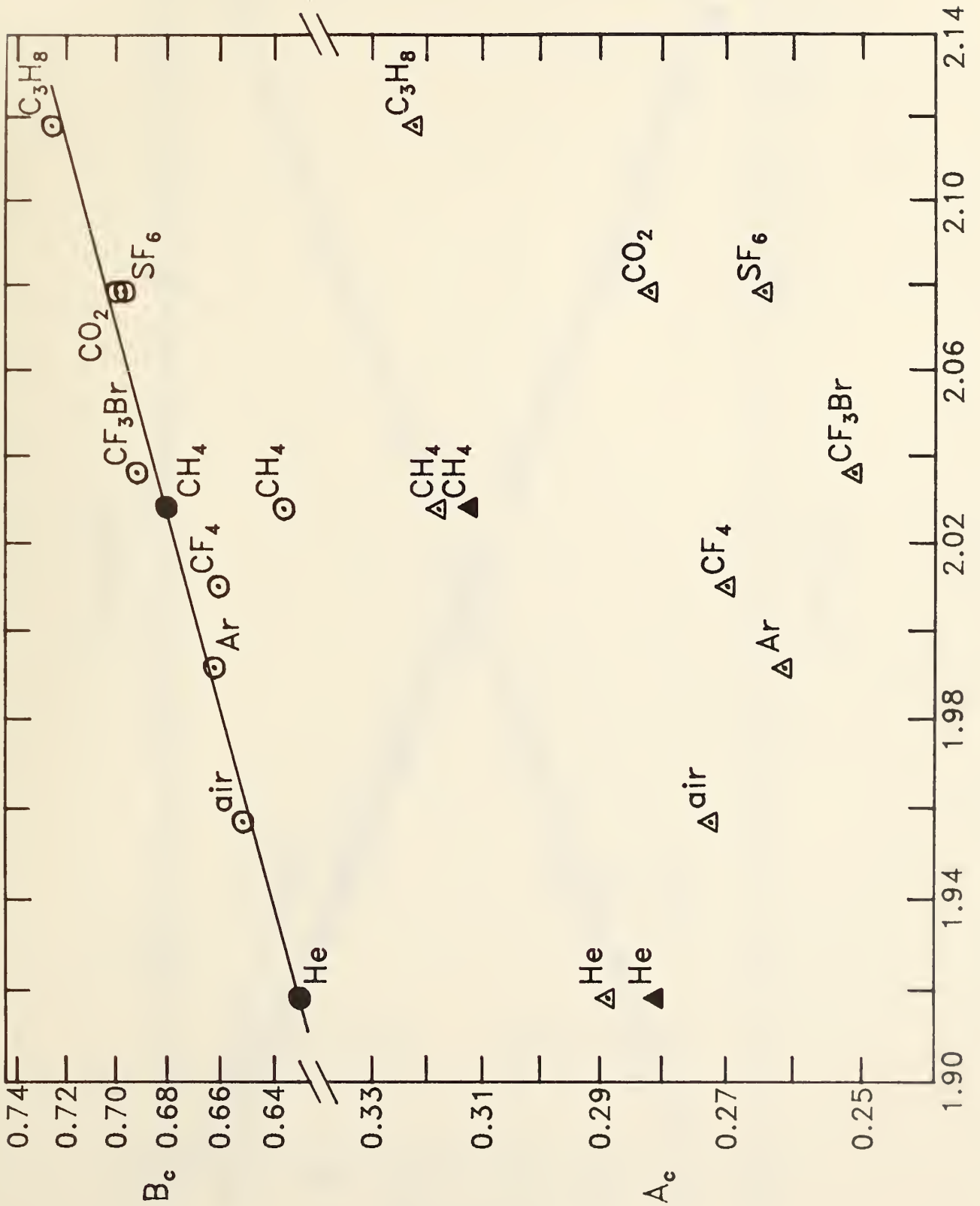

FIGURE 15: Hot-Wire Results Incorporating All Corrections Except Thermal Accommodation Effects

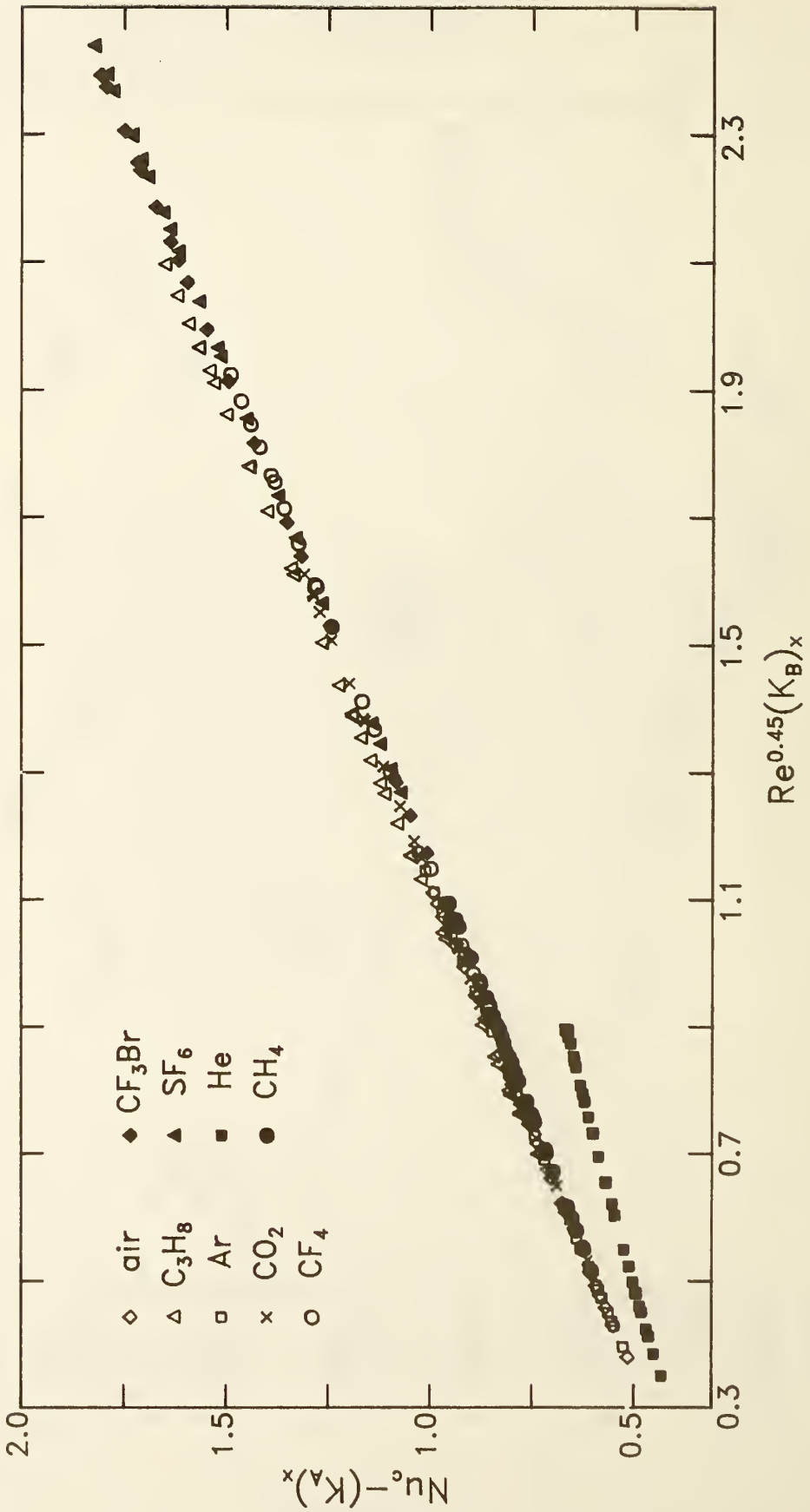

FIGURE 16: Hot-Wire Results INcluding Accommodation Corrections to He and $CH_4$

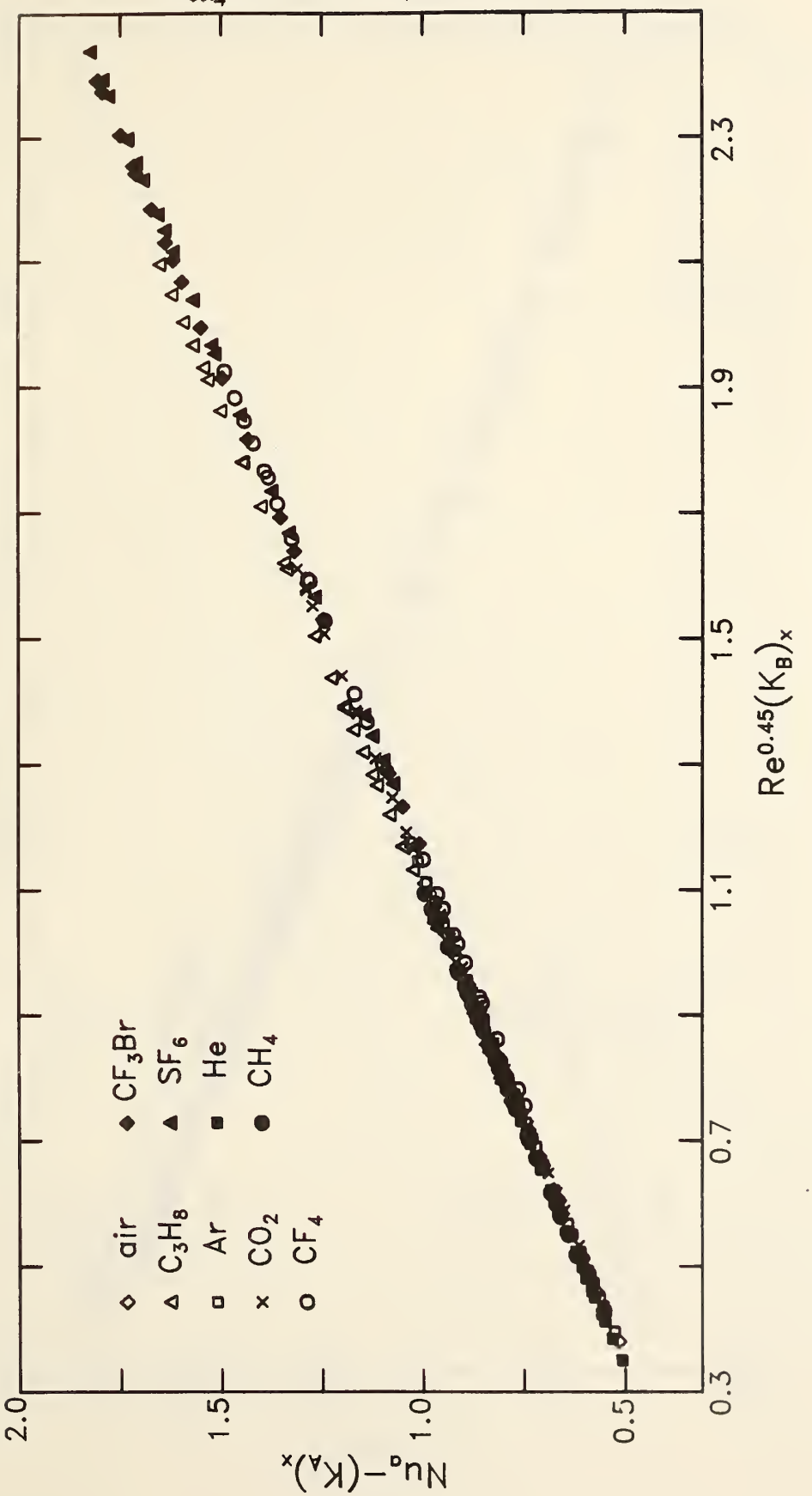

FIGURE 17: Simple Kinematic Viscosity
Correlation (no Accommodation)

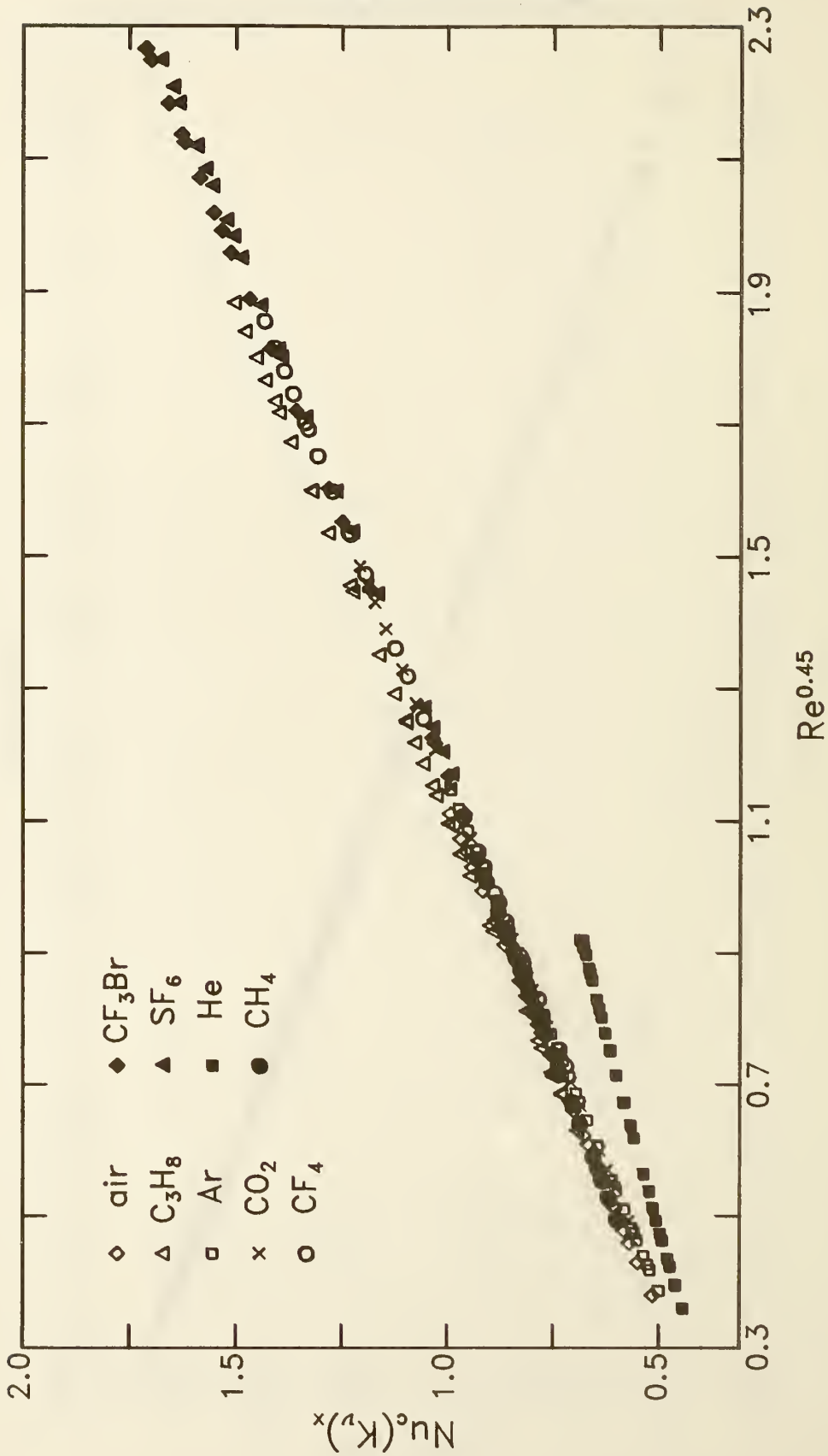

FIGURE 18: Simple Thermal Conductivity
Correlation (no Accommodation)

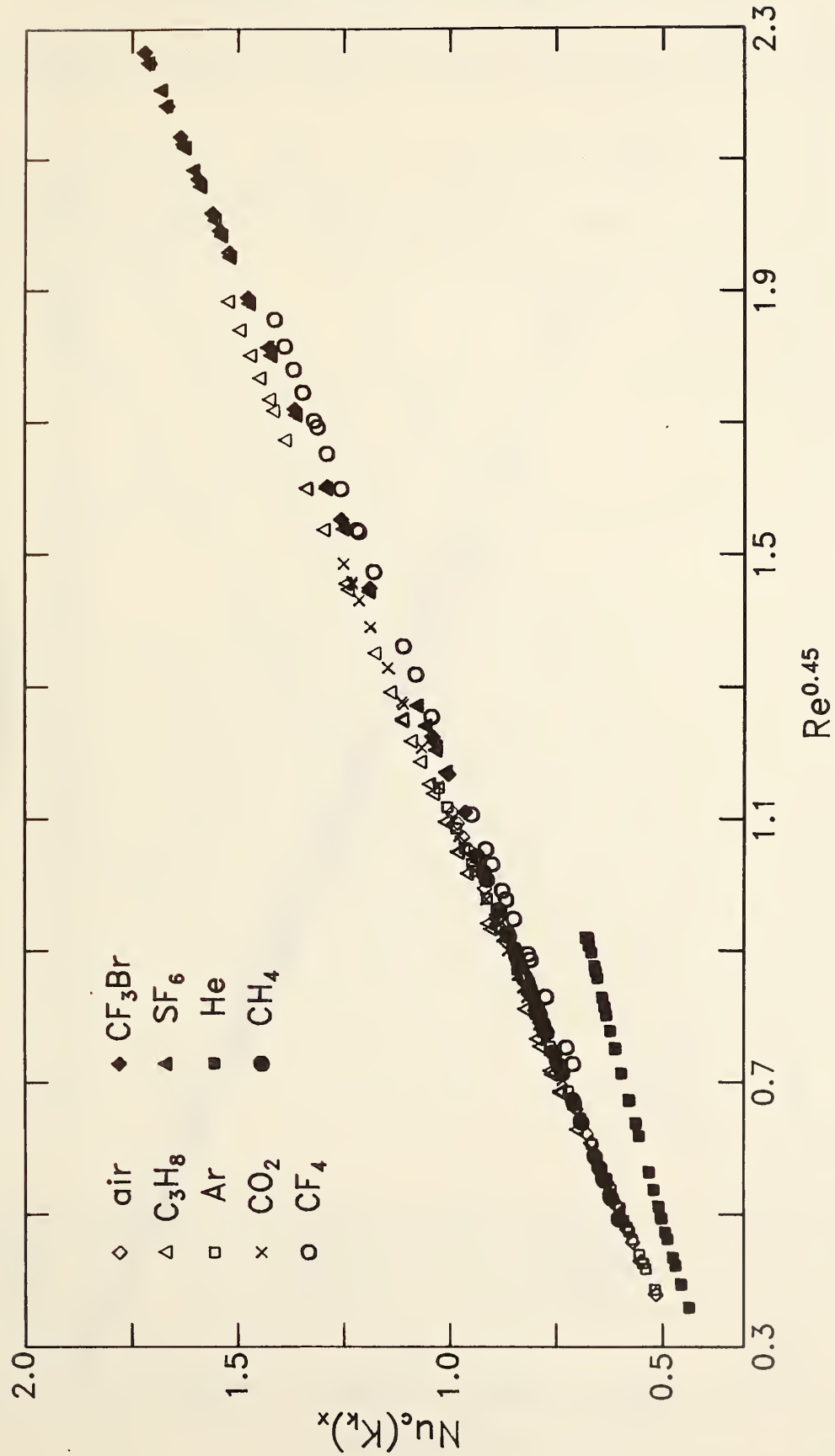

FIGURE 19: Hot-Film Results with All Corrections

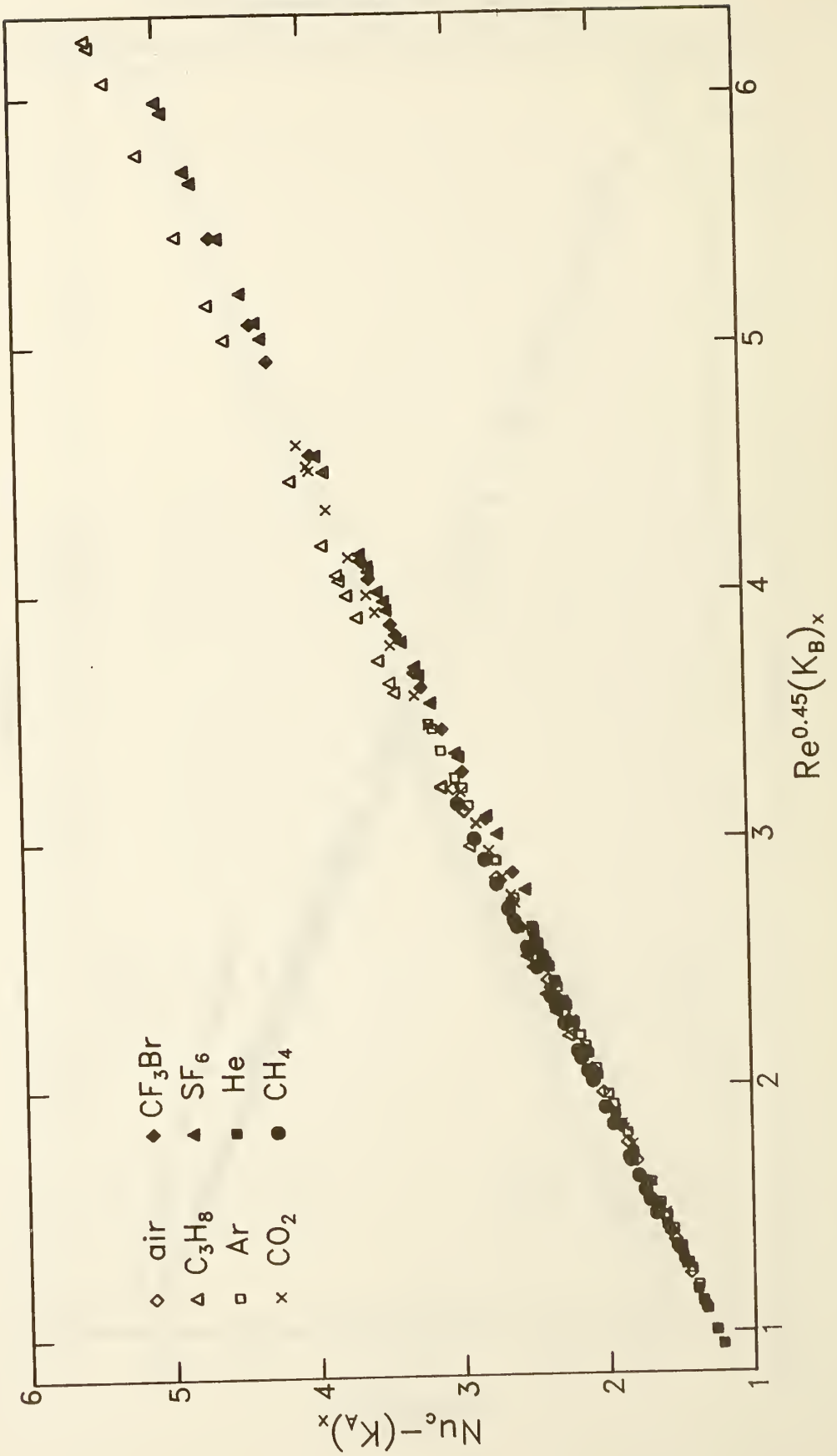

FIGURE 20: Hot-Wire. Comparison to Literature

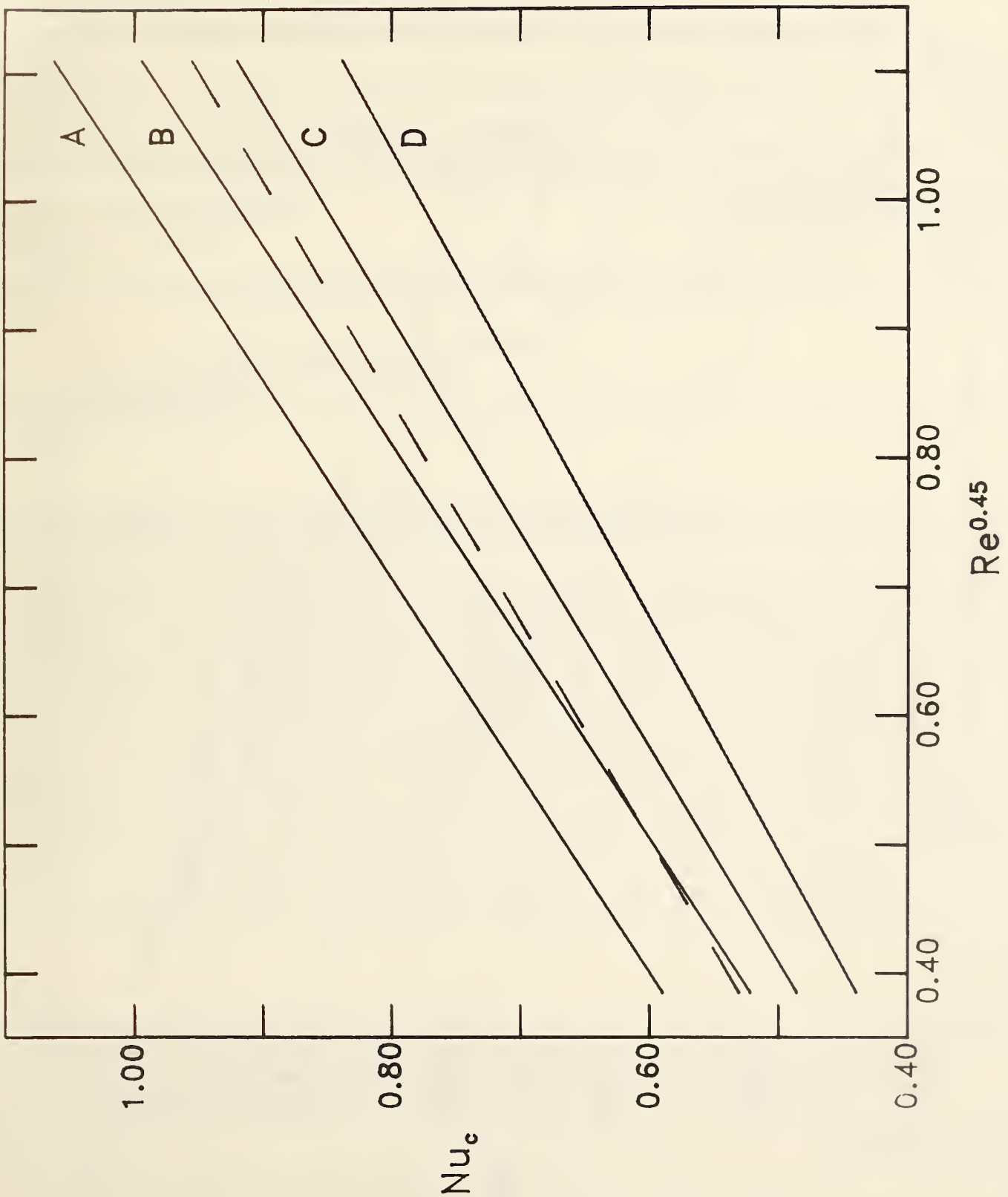

FIGURE 21: Hot-Film. Comparison to Literature

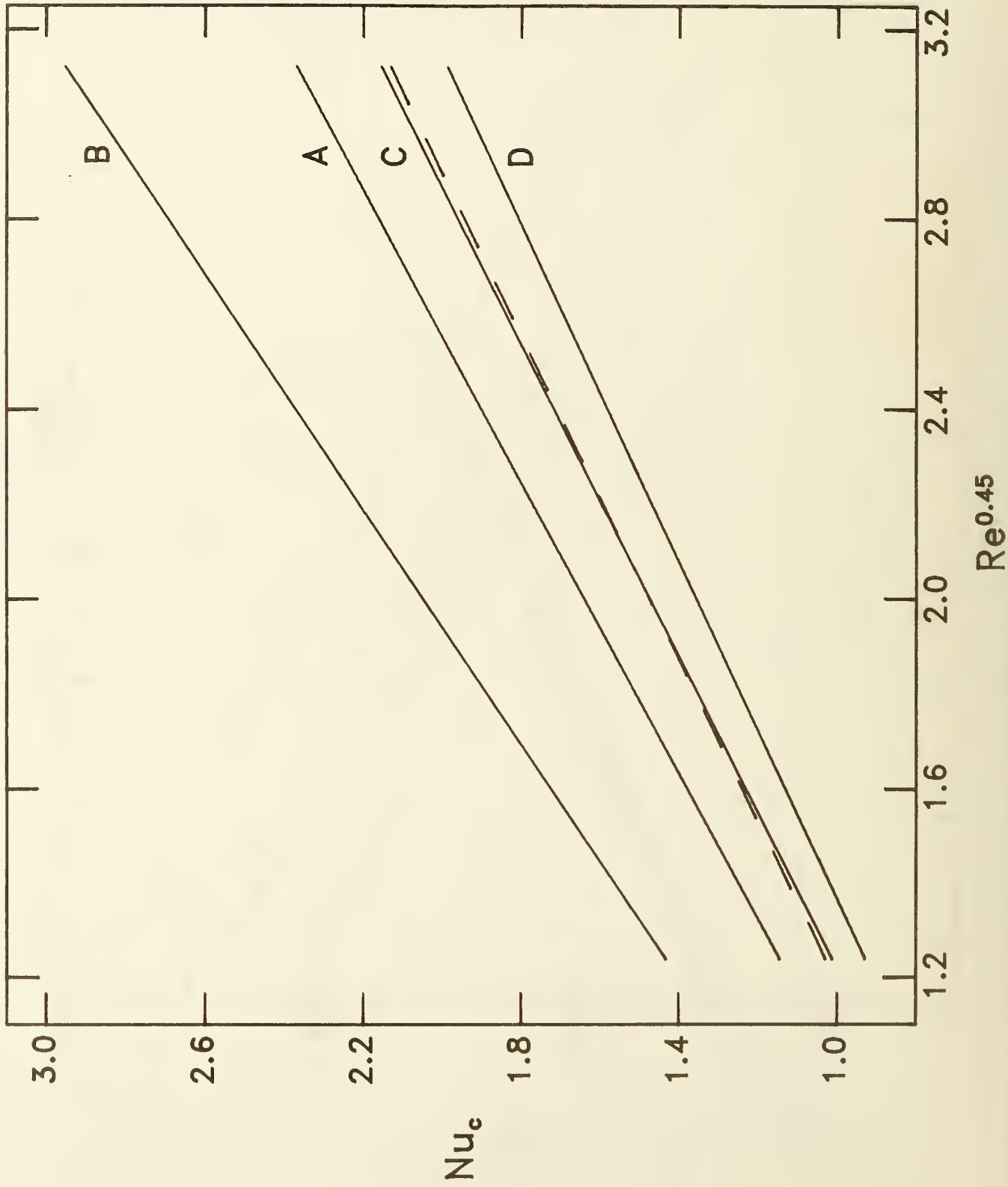

NBS-114A (REV. 2-8C)

| U.S. DEPT. OF COMM. BIBLIOGRAPHIC DATA SHEET (See Instructions) | 1. PUBLICATION OR REPORT NO. NBSIR-85/3203 | 2. Performing Organ. Report No. | 3. Publication Date July 1985 |
|---|---|---|---|

4. TITLE AND SUBTITLE

Response Behavior of Hot-Wires and Films to Flows of Different Gases

5. AUTHOR(S)

William M. Pitts and Bernard J. McCaffrey

6. PERFORMING ORGANIZATION (If joint or other than NBS, see instructions)

NATIONAL BUREAU OF STANDARDS
DEPARTMENT OF COMMERCE
WASHINGTON, D.C. 20234

7. Contract/Grant No.

AFOSR-ISSA-00005

8. Type of Report & Period Covered

9. SPONSORING ORGANIZATION NAME AND COMPLETE ADDRESS (Street, City, State, ZIP)

Air Force Office of Scientific Research
Air Force Systems Command, USAF
Washington, DC

10. SUPPLEMENTARY NOTES

☐ Document describes a computer program; SF-185, FIPS Software Summary, is attached.

11. ABSTRACT (A 200-word or less factual summary of most significant information. If document includes a significant bibliography or literature survey, mention it here)

Measurements of the voltage output for hot-wire and film anemometers placed in flows of nine different gases have been made as a function of flow velocity. It has been possible to correlate the measurements quite accurately by treating the data in terms of suitably defined Reynolds and Nusselt numbers. In order to obtain these correlations it has been necessary to consider and correct for the effects of probe end conduction losses, temperature dependencies of gas molecular properties, flow slip at the probe surfaces, and gas accommodation. With the exception of the results for helium (for which accommodation effects are strong), the most important correction is shown to be that for the different temperature dependencies of the gas molecular properties. This finding is contrasted with previous studies which have assumed that the largest effect among different gases was due to variations in the Prandtl number. The importance of the nature of the flow over the cylindrical devices to the heat transfer behavior is described. A previously unreported hysteresis in the heat transfer behavior for RE 44 has been characterized and attributed to the presence or absence of eddy shedding from the heated cylinder.

12. KEY WORDS (Six to twelve entries; alphabetical order; capitalize only proper names; and separate key words by semicolons)

Accommodation coefficients; convection; cylindrical bodies; heat transfer; hot wire anemometry; molecular effects; reynolds Number; Vortex Shedding.

13. AVAILABILITY

☒ Unlimited

☐ For Official Distribution. Do Not Release to NTIS

☒ Order From Superintendent of Documents, U.S. Government Printing Office, Washington, D.C. 20402.

☒ Order From National Technical Information Service (NTIS), Springfield, VA. 22161

14. NO. OF PRINTED PAGES

123

15. Price

$13.00

USCOMM-DC 6043-P80